UiT The Arctic University of Norway

Faculty of Biosciences, Fisheries, and Economics

γδ T cells in Atlantic salmon: Insight into the tissue distribution and gene usage of distinct TRG genes using molecular analysis

Andrea Luka

Master's thesis in akvamedisin BIO-3955 (60stp)

May 2024

Forord

Denne masteroppgaven symboliserer slutten på akvamedisinstudiet, utført ved Fakultet for biovitenskap, fiskeri og økonomi ved Norges Fiskerihøgskole, Universitet i Tromsø (UiT).

Jeg vil begynne med å rette en stor takk til min veileder Eva-Stina Edholm, som for første gang introduserte meg immunologifaget samt dette spennende prosjektet. Tusen takk for alt du har lært meg, dine motiverende ord, ditt smittende humør, og for din tålmodighet når ting har vært utfordrende. Du har vært en fantastisk veileder, og master-året ville aldri vært det samme uten deg.

Takk til Linn Greiner-Tollersrud, Guro Strandskog og Atefeh Kianian for opplæring og god hjelp på lab.

Videre vil jeg også rette en stor takk til gode kollegaer på Stingray, som har tatt seg tid til å hjelpe meg med oppgaven underveis, og som har lagt til rette for at jeg har kunnet kombinere jobb med studier best mulig.

Takk til klassen for fem fine år i nord, og for alle de fine stundene vi har delt i lag. En spesiell takk til Viktoria, Adele, Kristin, og Kristine for en uforglemmelig studietid og for vennskap jeg skal ta med meg livet ut.

Jeg vil også takke Mamma, Pappa, og Eivind for alt dere har lært meg, og for at dere alltid stiller opp og støtter meg. Helt til slutt vil jeg takke samboeren min Tinius for at du er den du er, og for alt vi får oppleve sammen. Jeg er heldig som har dere.

Tromsø, 14.05.2024.

Andrea Luka

Abstract

Salmon farming is among the fastest growing food production in the world, and what was once a luxury food is now among the most popular fish species in Europe and Asia. With the rapid growth and increasing demand, the salmon industry is, in addition to other factors, highly dependent on vaccines to ensure a sustainable practice. It is therefore important to fully understand the mechanisms of the adaptive immune responses against pathogens. The adaptive immune system in jawed vertebrates consists of both B- and T cells, and the focus in this study has been on a specific populations of T cells, namely γδ T cells. Previous mapping of the TRG-loci revealed 7 constants (C) regions, where TRGC1, TRGC2, TRGC3 and TRGC5 is functionally expressed in the tissue. To study the expression and distribution of TRG in Atlantic salmon, the basal expression of TRGC genes in different tissues was measured with qPCR analysis. Spleen and head kidney leukocytes (SPLs and HKLs) had the overall highest expression of all TRGC genes, along with peripheral blood leukocytes (PBLs). Following stimulation with a T cell mitogen, upregulation of TRG was observed in several tissues, and the results also showed great expression variation between the different TRGC genes. The highest expressed TRGC gene expression was TRGC3, and the lowest expressed TRGC gene was TRGC2. In addition, PrimeFlow RNA assay was for the first time conducted with Atlantic salmon cells, by utilizing IgM, TRD and TRG specific probes. Consistent with qPCR analysis, PrimeFlow analysis revealed the highest expression of TRG in SPLs. The flow cytometry analysis revealed successful staining with probes, as well as surprising results, including the detection of a high intensity staining IgM positive subpopulation.

Abbreviations

APCs	Antigen presenting cells
APC	Allophycocyanin
BCR	B cell receptor
bDNA	Branched DNA
CCL	Chemokine ligand
CD	Cluster of Differentiation
cDNA	Complementary DNA
CDR	Complementarity-determining region
CMS	Cardiomyopathy syndrome
Con A	Concanavalin A
CTL	Cytotoxic T cell
D	Diversity
degGSP	Degenerate gene specific primer
DN	Double negative
dNTPs	Deoxyribonucleotide triphosphates
DP	Double positive
dsDNA	Double stranded DNA
DTT	Dithiothreitol
EDTA	Ethylenediaminetetraacetic acid
EF1α	Elongation factor 1 alpha
ETP	Early T cell Progenitor
FITC	Fluorescein isothiocyanate
FSC	Forward scatter
GALT	Gut-associated lymphoid tissue
gDNA	Genomic DNA
GIALT	Gill-associated lymphoid tissue
GMO	Genomic modified organisms
GSP	Gene specific primer
HEV	High endothelial venules
HKLs	Head kidney leukocytes
HSMI	Heart and skeletal muscle inflammation
IELs	Intraepithelial lymphocytes
IFN	Interferon
IgM	Immunoglobulin M
IHC	Immunohistochemistry
IIGP	Interferon-gamma-inducible GTPase
IL	Interleukin
ILT	Interbranchial lymphoid tissue
ImAEs	Immune-mediated adverse events
J	Joining
MALTs	Mucosal-associated lymphoid tissues

MHC	Major histocompatibility complex
NaCl	Natrium chloride
NK cells	Natural killer cells
NKG2D	Natural killer group 2D
PBLs	Peripheral blood leukocytes
PBS	Phosphate Buffered saline
qPCR	Quantitative polymerase chain reaction
RACE	Rapid Amplification of cDNA Ends
RAG	Recombination activating gene
RT-PCR	Reverse transcription polymerase chain reaction
Sasa	Salmo salar
SPLs	Spleen leukocytes
SSC	Side scatter
TCR	T cell receptor
TdT	Terminal deoxyribonucleotidyl transferase
Th	T helper cell
TRA	T cell receptor alpha
TRB	T cell receptor beta
TRD	T cell receptor delta
TRG	T cell receptor gamma
USP	Universal primer
V	Variable
VHSV	Viral hemorrhagic septicemia virus

Table of contents

Introduction

In this introduction, I will first discuss the relevance of this project in the context of current and potential challenges facing the aquaculture industry. I will then provide an overview of key immunological concepts, with a focus on T-cell immunity and characteristics of γδ T cells. The main objectives of this study are presented at the end of the introduction.

1.1 Project relevance

As many as 783 million people faced chronic hunger in 2023, and more than 345 million people are experiencing acute levels of food insecurity. This is more than twice the amount reported in 2020 (World Food Programme, 2024). Thus, it has never been more important to invest in solutions that have the potential to provide sustainable food security. Since its origins in the 1970s, when nylon trawl nets were hung from wooden or polyethylene pipe structures in Norway and Scotland for Atlantic salmon farming, cage fish farming has evolved into a significant global industry (Sievers et al., 2021). Today, aquaculture is the fastest growing food supply sector in the world, significantly contributing to global, regional, and local food security (Directorate-General for Maritime Affairs and Fisheries, 2021; Seafish, 2023). Aquaculture not only meets the growing demand for seafood, it also alleviates the pressure on wild fish populations, and aid in protecting the marine ecosystems (Gentry et al., 2017). For instance, by minimizing bycatch [1], sustainable aquaculture plays a crucial role in preserving marine biodiversity (Office of Aquaculture, 2020).

In 2023, approximately 94.5 million tons of fish from Aquaculture were produced globally, which is an increase of 1,2% from the previous year (FAO, 2023). A total of 1,8 million tons came from Norway. The seafood industry is the second largest contributor to Norway`s economy, following the oil and gas sector (Norwegian seafood council, 2024). As part of a Norwegian Seafood Research Fund (FHF) funded collaborative research initiative, an extensive analysis assessing the comprehensive economic impact of the Norwegian seafood sector was recently conducted. The finding highlights the pivotal role the seafood sector has as one of the primary industries in Norway (Johnsen et al., 2022). Notably in 2021, the industry generated more than 106 000 jobs, representing an impressive increase of around 13 000 jobs compared

[1] Bycatch: Bycatch is the unintentional capture of non-target species during fishing

to the preceding year. Additionally, the seafood industry contributed significantly to the economy by generating a net value added of 172 billion NOK in 2023, which compared to 2022 is an increase of 20.7 billion NOK or 14 percent (Norwegian seafood council, 2024). This economic growth stems from both the direct impact within the industry and the indirect effects extending through the supply chain (Johnsen et al., 2022).

While aquaculture has numerous benefits, the industry is facing major problems and challenges. One main obstacle is the high mortality of farmed fish which results in annual deaths of tens of millions of fish across the world. In Norway, a total of 37.7 million Atlantic salmon and 4.9 million rainbow trout (*Oncorhyncus mykiss*) died in the pre-smolt stage in 2023. Additionally, 62.8 million (16.7%) Atlantic salmon and 2.5 million (14%) rainbow trout died during the sea phase of production, according to the Fiskehelserapporten 2023 (Sommerset et al., 2024). This marks the highest mortality both in number and percentage ever recorded for Atlantic salmon in the sea phase. There are various reasons for this high mortality, and three health challenges stood out: injuries during delousing operations, complex gill diseases, and winter sores. Moreover, a 2022 survey conducted by inspectors from the Norwegian Food Safety Authority revealed that two viral diseases, Heart and Skeletal Muscle Inflammation (HCMI) and Cardiomyopathy syndrome (CMS), are among the most significant health concerns in the salmon farming industry (Sommerset et al., 2024)

Another big challenge is global warming, and two of the most visible and consequential outcomes are the rise in sea levels and the warming of ocean waters (Paw & Thia-Eng, 1991). This is altering marine ecosystems and weather patterns and as such can disrupt fisheries, which would affect global seafood supplies and food security (Barange et al., 2018). The rise in temperature in the north can create a more favorable environment for various pathogens, such as bacteria, viruses, and parasites, which potentially can expose the fish to new disease risks (Duchenne-Moutien & Neetoo, 2021). Additionally, warmer waters can potentially induce a change in the metabolic and reproductive rates of many pathogens, which can lead to a higher infection rate among farmed fish. The fish might experience more stress, due to the temperature change, which can contribute to weaken the immune response (Nardocci et al., 2014). Collectively, these impacts will make the fish more susceptible to infections and disease outbreaks, which can cause significant losses.

Compared to wild stocks, farmed fish are more susceptible to infections and diseases as their natural life cycle is manipulated to shorten the production time, affecting their physiology

(Cascarano et al., 2021; Conte, 2004). In the wild, fish are exposed to pathogens throughout their entire life cycle, which presumably strengthens their immune systems (Esteban et al., 2013). In contrast, farmed fish are artificially smoltified in land-based tanks, making them arguably less prepared for the transition to the sea. Additionally, various stressful operations such as delousing, handling, and transport can potentially weaken their immune responses (Bortoletti et al., 2023). Vaccination of farmed fish is the fundamental preventive measure against the spread of diseases in Norway (Sommerset et al., 2024). Efficient fish vaccines are essential for several reasons, including safeguarding food security, reducing antibiotic use, ensuring economic sustainability, and mitigating environmental impact (Dadar et al., 2017; Khan et al., 2011). However, while effective vaccines exist for various bacterial diseases, anti-viral vaccines have overall not shown the same level of efficacy (Munang'andua et al., 2012; Røsaeg et al., 2021). This need underpins the necessity for a more in depth understanding of fish anti-viral immunity, in particular with regards to cell-mediated immunity and T cell responses that are essential in combating viral pathogens. Here, despite our current understanding of fish-cell-mediated immunity (Bela-ong et al., 2023; Cao et al., 2023; Tafalla et al., 2016; Wan et al., 2017) there is still much to learn.

1.2 Fish vaccination strategies: An overview of current challenges, and promising approaches

Vaccination relies on the formation of immunological memory. Protection against a specific pathogen is developed by exposing individuals to non-pathogenic variants or components of a given pathogen providing the host with an opportunity to develop an immune response without the risk of disease (Murphy et al., 2012). Currently, most fish vaccines used for preventing specific bacterial infections are formulated using inactivated bacteria or bacterial components. These vaccines primarily activate B-cells and are in other words focusing on activating humoral immunity. The decline of antibiotic use within the Norwegian fish farming industry over the past 30 years is a testament to the success of these vaccines in terms of combating bacterial infections (Sommerset et al., 2023). However, viral vaccines, formulated in a similar manner as bacterial vaccines, have been less successful in preventing and mitigating fish viral disease outbreaks in the field (Miccoli et al., 2021). Thus, inactivated vaccines are in general less efficient against viral infections and diseases caused by intracellular bacteria. One reason for this lack of efficacy is likely that they are ineffective in activating the cellular response. Viruses

are intracellular pathogens, able to hide within host cells. This means they can evade antibodies and other humoral defense mechanisms, and it is therefore crucial to activate the cell-mediated immune system, specifically CD8 cytotoxic T-cells, to successfully fight viral infections (Somamoto et al., 2013; Yamaguchi et al., 2019).

The first successful use of fish vaccines reported was oral vaccination against *Aeromonas salmonicida* in cutthroat trout (*Oncorhynchus clarkii*), and the first commercially licensed fish vaccine targeted enteric redmouth disease, utilizing a killed *Yersinia ruckeri* vaccine delivered through immersion in 1976 (Vinitnantharat et al., 2007). Today, the most common inactivated vaccine for Atlantic salmon in Norway is ALPHA JECT micro 7, a seven-component vaccine that includes *Vibrio salmonicida* (Coldwater vibrosis), *Listonella anguillarum* serotypes O1 and O2a (Vibriosis), *Aeromonas salmonicida* (Furuncolosis), *Moritella viscosa* (Winter ulcer), IPNV (infectious pancreatic necrosis virus serotype Sp 0), and ISAV (infectious salmon anemia virus) (Gudding & Goodrich, 2014; PHARMAQ, 2020). Currently, there are different kinds of fish vaccines in use globally, including inactivated vaccines, live attenuated vaccines and DNA vaccines. Inactivated vaccines are derived from disease-causing microbes that are made non-infectious through physical, chemical, or radiation processes, while preserving their antigenicity. They are generally considered safe but may induce weaker or shorter-lived immunity in fish due to challenges in activating cellular immunity. Inactivated vaccines however, have downsides, such as immunosuppressive passenger antigens, toxic reactions from adjuvants, reduced immunogenicity, and systemic reactions. (Ma et al., 2019; Pasquale et al., 2015; Tlaxca et al., 2015).

Live attenuated vaccines are created from viruses or bacteria with reduced virulence toward the target fish species. They are often highly immunogenic[2], as they can enter the host, stimulating robust cellular responses associated with both innate and adaptive immunity. However, the safety of attenuated live vaccines is a major concern. There is a need to address potential risks, such as reversion to virulence, residual virulence, or virulence in immunocompromised individuals. Additionally, contamination with unwanted organisms can impact vaccine efficacy and the licensing process for live vaccines. In the USA, three modified live aquaculture vaccines are currently licensed. These encompass an *Arthrobacter* vaccine against bacterial kidney disease (BKD) for salmonids, an *E. ictalurii* vaccine against enteric septicemia of catfish

[2] Immunogenic: The ability to provoke an immune response.

(ESC), and a *Flavobacterium columnare* vaccine against columnaris in catfishes (*Siluriformes)(Klesius & Pridgeon, 2014).* Considering that attenuated live vaccines created through molecular biology methods are considered genetically modified organisms (GMOs), they also need to be approved in accordance with the Gene Technology Act. In Norway, the use of GMOs in food or feed products is currently not allowed, and these types of vaccines are therefore not being used in Norwegian fish farms (Berg et al., 2006)

The principle behind a DNA vaccination is to allow antigens to be produced within the cells of the vaccinated individual. This is achieved by cloning genes from the pathogenic organism behind a strong promoter[3] in a plasmid[4] vector, which is then intramuscularly injected. Particularly for intracellular pathogens, such as viruses and bacteria that live inside host cells, there have been high expectations for this type of vaccine. The advantage of this method is that the desired protein(s) are expressed within the cells, thus stimulating the immune system in a manner similar to a natural infection. DNA vaccines can strongly activate both cellular and humoral immunity and are often more effective in protecting against viral infections (Berg et al., 2006; Kurath, 2008; Ma et al., 2019). In theory, DNA vaccines may be able to activate both B and T cells, which will create a much broader protection against both bacteria and viruses. In 2017, the European Medicines Agency approved Clynav, which is the first DNA vaccine approved for use in animals. Clynav consists of a recombinant DNA plasmid that encodes proteins from salmonid alphavirus subtype 3 (SAV-3). This DNA vaccine is designed to combat pancreatic disease in salmon caused by SAV-3, which primarily has been identified in Norway (Legemiddelverket, 2017)

1.3 Innate and adaptive immunity – A brief overview

Traditionally, host defenses can be categorized into two main categories: innate immunity, which offers immediate protection against microbial incursions, and adaptive immunity, a slower-developing system that delivers highly specialized defense mechanisms in response to infections. Innate immunity is often referred to as the first line of defense, and it is provided by epithelial barriers of the skin and mucosal tissues, cellular components, and natural

[3] Promoter: A DNA sequences that define where transcription of a gene by RNA polymerase begins.

[4] Plasmid: A small, circular DNA molecule in bacteria, carrying genes for specific functions.

antimicrobial agents inherent to these tissues. These elements collectively function to block the entry and replication of microbes (Janeway & Medzhitov, 2002). While innate immunity acts as a rapid, first-line defense against invading pathogens, the adaptive immune system offers a more specialized response, with a slower onset. Adaptive immunity is characterized by its capacity to recognize and develop memory towards specific antigens[5]. The recognition is facilitated by specific receptors present on the surface of immune cells known as T lymphocytes (T cells) and B lymphocytes (B cells). These specialized cells are essential for the immune system's ability to provide long-lasting protection against previously encountered pathogens, enabling the immune system to respond more effectively upon re-exposure, leading to faster and more targeted immune responses. The specific receptors, namely T cell receptors (TCRs) and B cell receptors (BCRs), are generated through a process of genetic rearrangement, resulting in a huge randomly generated repertoire of antigen-specific receptors within the immune system. When an infectious agent breaches the initial barriers of innate immunity and persists in the body, the adaptive immune system gets activated. First, dendritic cells[6], a "bridge" between the innate and adaptive immune systems, capture and process antigens from the invading pathogen. They then present these antigens to T cells, initiating a cascade of immune responses (Bonilla & Oettgen, 2010).

Innate immunity is evolutionary conserved and found, in some variation, in all living organisms. However, adaptive immunity (BCR, TCRs and MHC) is only found in jawed vertebrates. The TCR of a given T-cell can be one of two types, either αβ or γδ. The majority of T cells, called conventional T cells, express αβ TCRs, and they play a crucial role in the adaptive immune response, and for recognizing peptide antigens (Heath, 1998). There are two primary subsets of conventional T cells: cytotoxic T cells (CD8+) and helper T cells (CD4+). Cytotoxic T cells specialize in identifying and eliminating infected host cells and preventing the further spread of infection. Helper T cells can differentiate into various subtypes, such as Th1, Th2, Th3 (treg), Th17, or TFH, and each of these subtypes releases a unique set of

[5] Antigen: An antigen is a substance that triggers the production of antibodies, which can be recognized by the immune system.

[6] Dendritic cells: Immune cell that helps initiating and regulating immune responses by presenting antigens to other immune cells.

cytokines[7] that directs the immune response towards specific pathways. This is important for the activation and differentiation of various immune cells, including B cells and macrophages[8]. In addition, a unique subset of unconventional T cells (γδ T cells), can recognize various peptide and non-peptide antigens by using a heterodimeric receptor consisting of a TCR γ - and a TCR δ chain. While the conventional T cells depend on MHC molecules to present peptides for recognition, γδ T cells can detect antigens in an MHC unrestricted manner (Chien & Konigshofer, 2007). While immune cells are typically categorized as adaptive or innate, γδ T cells exhibit properties of both. Despite their capacity to generate unique TCRs, many γδ T cells express TCRs with limited diversity. Innate-like γδ T cells, also known as "natural" γδ T cells, acquire their effector functions early in thymic development, eliminating the need for clonal expansion[9] or differentiation from a naïve cell for their effector responses (Parker & Ciofani, 2020).

In summary, innate immunity constitutes an intrinsic defense mechanism within the body, to protect against microbial threats, while the adaptive immune system is a more specialized and adaptable defense mechanism. The adaptive immune system is slower to respond compared to innate immunity, and it offers the remarkable ability to recognize, remember, and specifically target pathogens, resulting in the formation of long-lasting immunity and protection against recurrent infections.

1.4 T cell development and distribution

Both B and T cells develop from bone marrow stem cells, however while B cells develop and mature in the bone marrow, T cells mature in the thymus. The diverse T cell lineages in the thymus will emerge from double-negative CD4− CD8− (DN) thymocytes, distinguished by the expression of either an αβ TCR or a γδ TCR. DN pro T cells, characterized by CD44, CD117

[7] Cytokine: Cytokines are small, secreted proteins that are released by a cell to regulate the function of another cell.

[8] Macrophages: A white blood cell that surrounds and kills microorganisms, removes dead cells, and stimulates other immune cells.

[9] Clonal expansion: A process of rapid cell division resulting in the multiplication of genetically identical cell clones from a single cell.

(c-kit), and CD25 expression, transition through early thymocyte progenitor cells (ETP/DN1), DN2, DN3, and DN4 cell stages (Parker & Ciofani, 2020). TRB, TRD, and TRG gene rearrangement begins in DN2 cells and ends in DN3 cells, coinciding with the divergence of αβ or γδ lineages. The DN3 stage acts as a critical checkpoint where productive rearrangement signals rescue the cells from apoptosis[10], leading to αβ or γδ lineage differentiation. β-selected cells (i.e cells that express a functionally rearranged TRB receptor on the cell surface) progress to the CD4+CD8+ double-positive (DP) stage, culminating in mature CD4+ or CD8+ single-positive αβ T cells. In contrast, γδ T cells follow γδ selection, bypassing the DP stage, and rather most γδ T cells remain as DN cells (Parker & Ciofani, 2020).

In the early thymocyte stages, Pro- T cells or double negative cells (CD4-CD8-), lacking TCRs on their surface expand in number under the influence of IL-17 (Interleukin 17) produced in the thymus (Abbas et al., 2019). The Pro T cells then undergo a process known as β-selection or TCRβ gene recombination, where rearrangement and expression of the β-chain of the TCR take place. If this step is successful, it will lead to the formation and surface expression of a pre-TCR complex consisting of a rearranged β-chain associated with an invariant pre-T α-chain encoded by an unrearranged gene (Fehling et al., 1995). The pre-T cells will now enter the double-positive (CD4+CD8+) stage and express both the CD4 and the CD8 co-receptors along with the pre-TCR. They will now rearrange and start expressing the α-chain of the TCR, and a functional TCR will be formed. The next step is positive and negative selection. At this stage the TCR expressed on an immature T cell will interact with thymic epithelial cells that presents self-peptides bound to Major Histocompatibility Complex (MHC)[11] class I and class II molecules. TCRs that bind to self-MHC molecules with moderate affinity are selected to become single-positive (CD4+ or CD8+) T cells, and this is called positive selection (Klein et al., 2014). This type of selection drives the migration from the cortex to the medulla, and the T cells will exit the thymus as mature, naïve T cells expressing either CD4 or CD8 co-receptors. On the other hand, if the TCR of a developing T cell interacts too strongly with a peptide-MHC ligand, it will result in apoptosis. This is called negative selection, and serves to eliminate T

[10] Apoptosis: Programmed cell death.

[11] Major Histocompatibility Complex: A group of genes that code for proteins on the surfaces of cells, helping the immune system to recognize foreign substances.

cells that may be self-reactive, contributing to the development of a predominantly self-tolerant repertoire of peripheral T cells (Klein et al., 2014).

In mammals naïve T cells migrate to lymphoid tissue by crossing the walls of specialized venules known as high endothelial venules (HEV). The migration of näive T cells follows a continuous cycle, moving from the bloodstream to lymphoid organs and back, engaging with numerous antigen-presenting cells (APCs) within lymphoid tissues daily. Some of the naive T cells also migrate to the spleen, participating in immune responses, particularly against blood-borne pathogens. Additionally, mucosal-associated lymphoid tissues, including the tonsils and Peyer's patches attract naive T cells, contributing to immune surveillance in mucosal surfaces.

The majority of T cells within the human body are situated in lymphoid tissues, like the bone marrow, spleen, tonsils, and within the estimated 500-700 lymph nodes. Additionally, substantial T cell populations are present in mucosal sites such as the lungs, small and large intestines, as well as the skin. Approximately 2–3% of the total T cell complement is found in human peripheral blood (Clark, 2010; Ganusov & De Boer, 2007; Kumar et al., 2018).

1.5 T cell development and distribution in fish

1.5.1 Thymus

T cells in fish develop in the thymus, just like in mammals, and it is a primary lymphoid organ. One important difference between fish and mammals is the location of the thymus. In fish, the thymus is located beneath the gill chamber epithelium, where it is covered by mucosal epithelium (figure 1 & figure 2A), while in mammals it is located in the anterior portion of the chest cavity (Chilmonczyk, 1983). In mammals, the thymus has a clearly defined cortex and medulla structure that creates specialized immune zones, vital for T cell development. Within the cortex, T cells undergo proliferation, recombination and positive selection, while in the medulla, T cells undergo negative selection, where the T cells that don’t pass the selection undergo apoptosis (negative selection). In a review on the evolution of adaptive immunity published in 2018, Flajnik summarized that in gnathostomes[12], including teleosts (bony fish),

[12] Gnathostomes: Jawed vertebrates.

the thymic organization typically resembles the classic cortex/medulla structure seen in mammals. In zebrafish regionalization of cortex and medulla was established using in situ hybridization for the recombination activating gene-1 (RAG-1) (Lam et al., 2002). RAG-1 is only expressed in developing lymphocytes and primarily found in T cells located within the cortex. However, unlike zebrafish, where the distinction between cortex and medulla is clear, the salmonid thymic organization is not yet firmly established and the distinction between medulla and cortex has proven to be challenging in salmonids (Flajnik, 2018).

In 1983, Chilmonczyk suggested that the trout thymus could be divided into five zones including an outer capsular zone (C), a subcapsular zone (SZ), an inner zone (IZ), an outer zone (OZ), and finally, the pharyngeal epithelium (PE). This classification was based on histogenesis[13] of early thymic rudiment and structural investigations performed on various salmonids (Chilmonczyk, 1983). Outside the thymus, T cells are primarily found in the head kidney and spleen where they constitute a significant proportion of the lymphocyte population. In addition, T cells have been shown to accumulate in mucosal tissues (gill, intestine) and in the newly discovered bursa (Løken et al., 2020). Unlike mammals, fish lack traditional tonsils, and the presence of T cells in specialized lymphoid structures, such as the Interbranchial Lymphoid Tissue (ILT), is postulated to play a crucial role in their immune system (Haugarvoll et al., 2008). These unique structures differ from the thymus in some aspects, as discussed in detail below, and are integral components of the fish's immune response.

Figure 1. White arrow showing the location of the thymus in rainbow trout (Oncorhynchus mykiss) (Barraza et al., 2020)

[13] Histogenesis: Differentiation of cells into specialized tissues and organs during growth.

1.5.2 Spleen

In mammals, the spleen is a dynamic organ located in the abdominal cavity, capable of expanding and contracting. This flexibility allows the spleen to serve as a reservoir, facilitating the recruitment of circulating cells during times of stress. Fish also exhibit this phenomenon. The spleen in fish is recognized for its variable size in response to various infections, and like the kidney, the spleen plays a crucial role in filtering blood and removing damaged blood cells (Lewis et al., 2019). Notably, adaptive immune responses in the spleen are generated, concentrating the antigens for interactions between T cells, B cells and antigen presenting cells (APCs) (Flajnik, 2018). In fish, the filtration of blood through the spleen emerges as a particularly vital immune mechanism, due to the absence of lymph nodes and potentially lymphatic vessels (Flajnik, 2018). In mammals, the white pulp can be parted into layers based on the presence of various leukocytes, including distinct T-cell subpopulations, B cells, plasma cells[14], and macrophages (Cesta, 2006). In fish, comparable studies have not been conducted to date. Nevertheless, research has demonstrated the existence of MHC class II-positive cells, likely macrophages, and T cells in the white pulp (Koppang et al., 2010; Koppang et al., 2003). However, detailed studies regarding the specific distribution of T cells within this compartment is currently lacking.

1.5.3 Interbranchial lymphoid tissue (ILT)

A special lymphoid structure near the end of the Atlantic salmon`s interbranchial septum (figure 2E) (Haugarvoll et al., 2008), which connects the proximal third of the primary lamellae was reported in 2008. This lymphoid tissue was later named interbranchial lymphoid tissue (ILT). The ILT is found in several species including Atlantic salmon (*Salmo salar*), rainbow trout (*Oncorhynchus mykiss*), zebrafish (*Danio rerio*), Siberian sturgeon (*Acipenser baerii*), and bonefish (*Albula vulpes*), and it develops in an area where the outer and inner layers of the throat meet (Haugarvoll et al., 2008; Liang et al., 2022).

In larvae, with a well-developed thymus, this structure is not visible. Dalum et al. (2016) performed a study where they investigated the development of the ILT during different life

[14] Plasma cell: Immune cell that makes large amounts of a specific antibody.

stages in relation to the thymus and its position in the gills. While ILT volume is closely related to the growth of gills rather than the thymus, its emergence appears linked to increased antigen exposure during respiratory and feeding transitions (Dalum et al., 2016). Despite similarities to tonsils in higher vertebrates, the ILT is not a primary lymphoid tissue-associated transcripts, which means that T cells must come from extrabranchial sites at a certain time point. Additionally, there has not been found any relationship between the ILT and the thymus, evaluated from the degree of T cell proliferation and differences between levels of transcripts. In addition, the ILT outgrows the size of the thymus with age, and it appear after the yolk-sac stage (Dalum et al., 2016).

The ILT primarily consists of lymphocytes, with a predominant population of T cells and MHC class II-expressing cells. Immunohistochemistry (IHC)[15] detected the presence of MHC class II+ cells, while laser capture micro-dissection and subsequent reverse transcription polymerase chain reaction (RT-PCR) analysis indicated the expression of T-cell receptor transcripts in the examined tissue, suggesting the presence of T cells (Haugarvoll et al., 2008). The ILT can be divided into a proximal and a distal part, but unlike the thymus, the ILT lacks blood vessels and innervation. This raises questions about how such a cell-rich structure can exist without vascularization. Bjørgen et al. (2019) suggested that the ILT should be considered as a lymphoid organ on its own rather than part of the gill-associated lymphoid tissue (GIALT). This is because they found expression of cytokine CCL19 in the ILT, which is known for its participation in the activation of T-cells. In mammals, expression of CCL19 is restricted to primary and secondary lymphoid organs. Aas et al. (2014) however, did not detect RAG-1 or RAG-2 expression in the ILT samples. Dalum et al. (2016) reached a similar conclusion through another morphological and transcriptional study, including an analysis of RAG expression. This study showed no functional relationship between the thymus and the ILT, but did show T-cell proliferation within certain regions of the ILT. Moreover, there is currently no evidence that cells within the ILT exhibit antigen uptake and processing as observed in mucosal-associated lymphoid tissues (MALTs), which is expected for a secondary lymphoid organ.

[15] Immunohistochemistry: A laboratory method that uses antibodies to detect antigens (markers) in tissue samples.

1.5.4 Bursa

In birds, the bursa of Fabricius serves as a primary organ for B-cell maturation and is also associated with gut-related lymphoid tissue (Løken et al., 2020). Studies of this structure have been crucial to the understanding of the adaptive system of vertebrates, and until recently the organ was thought to be exclusive to birds. Mammals do not have a bursa of Fabricius, but they have tonsils which are thought to be analogous[16] (Løken et al., 2020). In fish, there aren't traditional tonsils like in mammals. Løken et al. (2020) discovered that the cloacal bursa in salmon transforms into a lymphoid tissue, resembling the bursa of Fabricius found in birds (figure 2F). The presence of intraepithelial lymphocytes and the expression of the cytokine CCL19 indicate lymphoid organ functions. However, in the same study no genetic rearrangement was detected within salmon bursal lymphocytes, which indicates that it lacks the functions needed to be classified as a primary lymphoid organ. However, other abilities such as capturing various antigens and the presence of APCs imply secondary lymphoid organ functions. Løken et al. (2020) also discovered that a large majority of the bursal lymphocytes were immunopositive for the T-cell marker CD3, and that both γδ and αβ T cells were present. In contrast to the bursa of Fabricius in birds, which is dominated by B cells, T cells is the major infiltrating lymphocyte in the salmon bursa.

1.5.5 Intestine

The fish intestine contains various T-cell subpopulations, primarily CD3+/CD8+, that are distributed along the intestinal tract. In sea bass (*Dicentrarchus labrax)*, the intestine harbors the highest amount of T cells in the body (Picchietti et al., 2011). The intestinal CD3+ T cells in the epithelium/lamina propria express both TRA/TRB and TRD/TRG genes indicating that both conventional and unconventional T cells are present in this tissue. Notably, the RAG-1 gene is also expressed in the intestine (Picchietti et al., 2011). In addition, spontaneous somatic rearrangement of V(D)J combinations (explained in detail under "The T cell receptor") in both TRB and TRG occurs in the absence of antigen stimulation, which indicates that the intestine of teleosts functions as a true primary lymphoid tissue for T cells (Picchietti et al., 2011). In

[16] Analogous: Similar features to another thing and therefore comparable. Example: The lens eyes of vertebrates and cephalopods.

humans and mice, a population of lymphocytes known as intraepithelial lymphocytes (IELs) play a vital role in immunity to substances encountered through the oral route. IELs consist mainly of CD3+ T lymphocytes expressing either γδ TCR or αβ TCR and are mostly CD8+CD4− lymphocytes. In contrast to mammals, teleost fish lack specialized structures like Peyer's patches in their gut-associated lymphoid tissue (GALT), but IELs are observed in the mucosa of various fish species, containing mainly T cells. The exact function of the fish IELs is still not known, but studies in rainbow trout suggest a diverse population of αβ T cells in the gut epithelium (Bernard et al., 2006; Picchietti et al., 2011).

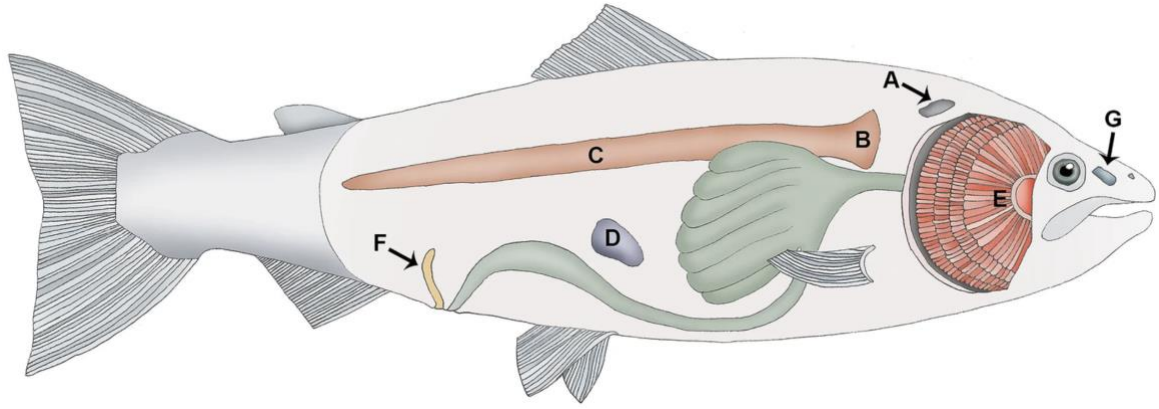

Figure 2. Anatomy of teleost fish immune structures and organs. **A** Thymus, **B** Head kidney, **C** Trunk kidney, **D** Spleen, **E** Gills with interbranchial lymphoid tissue, **F** Salmonid bursa, **G** Olfactory organ with the nasopharynx-associated lymphoid tissue (NALT) (Bjørgen & Koppang, 2021).

1.6 The T cell receptor

The formation of functional genes that encode B and T antigen receptors is mediated by somatic recombination. This is a genetic process that is responsible for generating the diverse repertoire of antigen receptors, namely BCRs and TCRs, which are crucial for recognizing and responding to a wide range of pathogens and antigens (Netea et al., 2019). It is like mixing and matching puzzle pieces to create unique keys for the immune system. All of these puzzle pieces come in different shapes and sizes, and they all represent a “key” called an antibody or TCR. The body will randomly select a distinct set of few puzzle pieces and put them together in a special way, which will create a unique key. The immune system has a diverse collection of these keys, which fit specific pathogens and antigens. Thus, when a pathogen enters the body, the immune system will look for the “right” key to recognize it and respond.

In T cells, the generation of a TCR involves the rearrangement of gene segments encoding the variable regions of TCRα- and β-chains (and γ and δ for γδ T cells). These gene segments include multiple variable (V) gene segments, numbering about 30 to 45 in humans, and one or a few constant region (C) genes. The α-chain consists of V and joining (J) segments, in contrast the β-chain consists of a V, J and diversity (D) segments. In humans the TRA gene cluster is found on chromosome 14 and consists of about 70 to 80 Vα gene segments. Each of these Vα gene segments consist of an exon[17] that encodes for a leader sequence (L) an intronic region and an exon encoding for the variable gene. Until this day, it is not entirely clear how many of these Vα gene segments are functional. Located next to the Vα gene segments there is a cluster of 61 Jα gene segments. Following the Jα gene segments is a single Cα gene, which has separate exons encoding for the constants and hinge domains. In addition, the Cα gene segment also has an additional exon that codes for the transmembrane and cytoplasmic regions. For the TRB gene cluster, which is located on chromosome 7, the gene arrangement is different. It includes a cluster of 52 functional Vβ gene segments, which are located far from two separate clusters, each containing a single Dβ gene segment. Each of these Dβ gene segments are together with six or seven Jβ gene segments and one Cβ gene, where each Cβ gene has separate exons that code for the constant domain, hinge, transmembrane region, and cytoplasmic region (Janeway et al., 2001).

During somatic recombination, the V, D and J gene segments are randomly selected and combined (figure 3). This is a tightly controlled sequential process that begins with one J segment combining with one D segment, followed by a recombination of the DJ segment to a V segment resulting in a diverse set of antigen receptor genes. The specificity of the antigen receptor is determined by the particular V(D)J combination, and when an antigen matches the binding site of a T cells TCR it triggers an immune response. The somatic recombination of V, D and J gene segments is mediated by a lymphoid-specific enzyme called the VDJ recombinase, and additional enzymes. The VDJ recombinase consists of the recombination-activating gene 1 and 2 (RAG-1 and RAG-2) proteins, which recognizes DNA sequences that flank all the antigen receptor V, D and J gene segments. The recombinase brings TCR gene segments close together and cleaves the DNA at specific sites. A DNA ligase will then repair the DNA breaks, which will produce a full-length recombined V(D)J exon without any intervening DNA

[17] Exon: A region of the genome that ends up within an mRNA molecule.

sequences. Adding to the antigen receptor diversity is the use of different combinations of V, D and J gene segments in different clones of lymphocytes (combinatorial diversity), and even more by the changes in nucleotide sequences (called junctional diversity) (Janeway et al., 2001; Krangel, 2009).

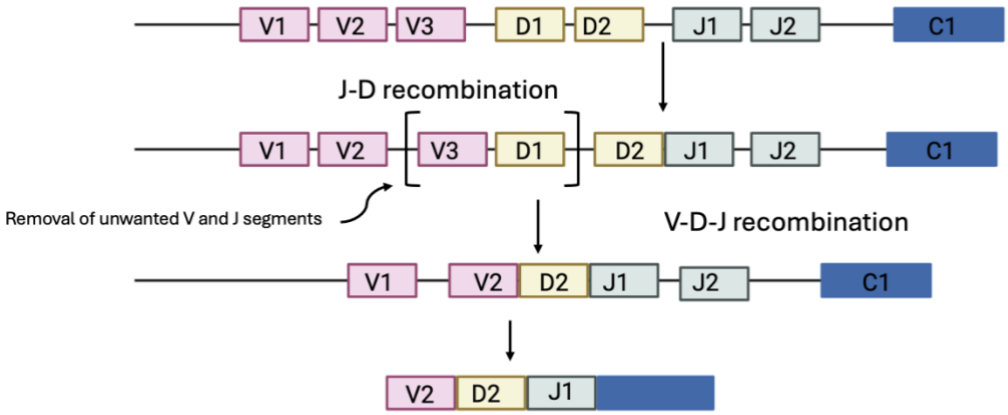

Figure 3. Illustration of VDJ rearrangement, which occurs in the TRB- and TRD chain. Variable (V) gene segments are shown as pink, Diversity (D) gene segments as yellow, Junctional (J) gene segments as green, and constant gene segments as blue. Step one shows the J-D recombination, with the removal of unwanted V- and J segments. Step 2 shows the JD to V recombination, and the last step shows transcription and splicing (Illustration: Andrea Luka).

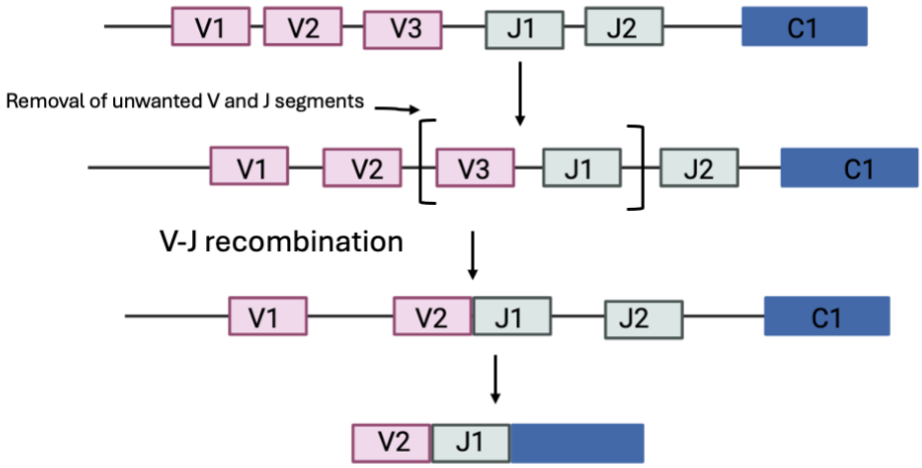

Figure 4. Illustration of VJ rearrangement, which happens in the TRA- and TRG chain. Variable (V) gene segments are shown as pink, Junctional (J) gene segments as green, and constant gene segments as blue. Step one

shows the V-D recombination, with the removal of unwanted V- and J segments. Step 2 shows transcription and splicing (Illustration: Andrea Luka).

Junctional diversity is almost unlimited, and it is primarily three mechanisms that create this diversity. The first one is when exonucleases remove nucleotides from V, D and J segments at the site of recombination. The second one is when a lymphocyte-specific enzyme, TdT (terminal deoxyribonucleotidyl transferase) catalyzes random addition of new nucleotides to the junctions between V and D segments and D and J segments (N nucleotides). The third mechanism of junctional diversity is during an intermediate stage in the process of V(D) J recombination, the two broken strands of the DNA at each end of the cut DNA form hairpin loops. The repair process begins with the loops being cut and formation of an overhanging DNA sequence. Then these overhangs need to be filled in with new nucleotides, called P-nucleotides, which creates even more variability at the sites of recombination. The most variable region of the TCR is called the CDR3 region, this region is composed of amino acids encoded by V, D and J gene segments as well as n and p nucleotides (Janeway et al., 2001; Krangel, 2009).

There are important differences when it comes to the organization of the TRG and TRD loci, although the organization resembles that of the TRA and TRB loci (figure 5). A main difference is that the gene segments encoding for the delta chain are located within the alpha chain locus, typically between the Vα and the Jα gene segments. Because of this, when the alpha chain genes rearrange, the delta chain genes will be lost. The human TRG locus is quite similar to the TRB locus. Both have two C genes, and each C gene has its own set of J gene segments. In mice, the TRG locus is more complex, including three functional clusters of TRG gene segments. Each of these clusters has its own V and J gene segments, along with a C gene. Thus, TRG genes are organized in individual cassettes, each consisting of V J and C genes. When rearrangement occurs at the TRG and TRD gene regions, it proceeds like it does for the other T-cell receptor genes. A key difference is TRD rearrangement, where multiple D segments can be used in the same gene generating for example a VDDJ gene. This increases the variability of the δ-chain because extra bits of genetic material (N-region nucleotides) can be added at the junction between the gene segments, making the δ-chain more unique (Janeway et al., 2001; Krangel, 2009).

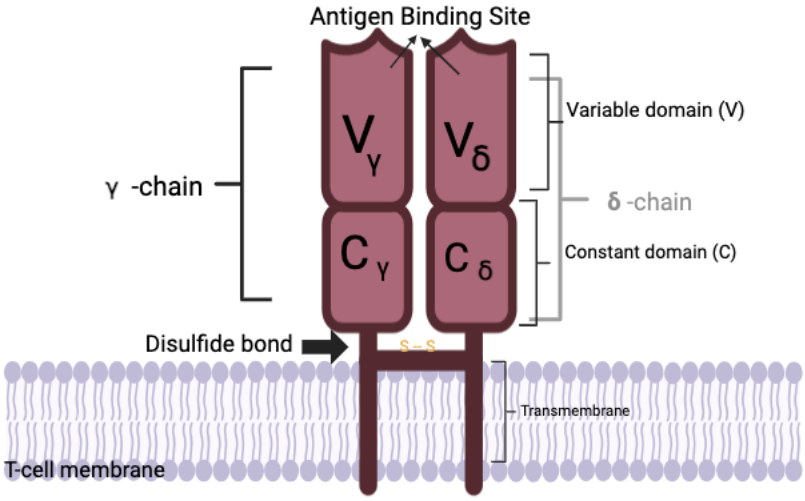

Figure 5. Illustration of γδ T cell receptor, showing the antigen binding site, and both the γ and δ chain with respective variable and constant domain (Illustration: Andrea Luka).

1.7 Conventional T cells

T cells are the principal actors of cell-mediated immunity, and with their antigen-specific heterodimeric receptors (TCRs) they can recognize an almost unlimited number of foreign antigens. TCRs are expressed on the cell surface membrane, and T cells are classified based on which TCRs are expressed. There are two major subpopulations of T cells, and the most abundant are the αβ T cells (conventional T cells) which represent the majority of T-cells found in lymphoid tissues, peripheral blood, and various tissues throughout the body. The receptor expressed on conventional T cells consist of a disulfide-linked heterodimer consisting of α and β chains expressed as a complex with multiple invariant CD3 chains. The αβ T cells are primarily involved in recognizing peptide antigens presented to the TCRs in the context of MHC molecules expressed on the surface of cells. (Antonacci et al., 2020; Lefranc, 2014)

αβ T cells include three functionally distinct subtypes with well-characterized functions including cytotoxic activity (CTLs), helper functions (Th), and regulatory functions. All these functions are essential to the adaptive immune response. Cytotoxic T cells (CTLs) are CD8+ T lymphocytes that have the capacity to kill cells harboring intracellular microbes and tumor cells. T helper cells (Th) are CD4+ T cells that help B lymphocytes to produce antibodies and help phagocytes, such as macrophages to destroy microbes (Lefranc, 2014). Th cells will also help activation of CTLs to kill infected target cells. CTLs express the co-receptor CD8 on the surface

membrane, and therefore will bind to MHC class I molecules. Th cells on the other hand express the co-receptor CD4, and therefore binds to MHC class II molecules. Regulatory T cells are also CD4+ T cells, but they belong to a special subset that helps prevent or limit immune responses. (Abbas et al., 2019)

1.8 Conventional T cells in fish

When it comes to fish, all four TCR chains have been identified, and the existence of two major T cell populations, categorized αβ or γδ based on their expressed T cell receptors is a characteristic common to all jawed vertebrates (Yazawa et al., 2008). Moreover, in many teleost species, including Atlantic salmon and rainbow trout, both CD8 α and CD8 β genes have been characterized (Hansen & Strassburger, 2000). Hansen and Strassburger (2000) has also suggested that the amount of CD8 expressing T cells is higher in the thymus, in contrast to the spleen, kidney and intestine. In addition to CD8, two types of CD4 molecules (CD4-1 and CD4-2) have been described in several teleost (Hordvik et al., 2004)

In addition to both CD8 and CD4, various cytokines, such as interleukin (IL)-2, IL-10, IL-12, IL-18, IFNα, IFNβ, and IL-17, which are known for their variable roles in proliferation, activation and differentiation of T cell subsets, have been identified in fish (Díaz-Rosales et al., 2009; Secombes, 2008). Studies indicate that fish, much like mammals, possess both cytotoxic T lymphocytes (CTLs) and T helper (Th) cells (Yamaguchi et al., 2019). Boudinot et al. (2001) conducted research into the direct αβ T cell response to viral hemorrhagic septicemia virus (VHSV), in Atlantic salmon. Using spectratyping[18] of the CD3 region of the TCRβ chain in rainbow trout, they revealed a diverse and polyclonal[19] repertoire of naïve T cells. Furthermore, their study identified CD3 region profiles of the same length for multiple Vβ 4J β1 expressing T cell clones in response to acute VHSV infection, indicating an expansion of these particular T cell clones during both the primary and secondary immune responses (Boudinot et al., 2001)

[18] Spectratyping: A method where antigen receptor length diversity is assessed as a surrogate for functional diversity.

[19] Polyclonal: Cells derived from two or more cells of different ancestry or genetic constitution.

Edholm et al. (2021) published an article mapping and characterizing the TRA/D locus in Atlantic salmon, as well as two strains of rainbow trout (Arlee and Swanson). Similar to other vertebrates, salmon have connected TRA and TRD genes conserved within a single locus. The study shows a comprehensive annotation of the TRA/TRD locus, which is an important step to define the expression pattern of TCR isotypes among salmonids. In the study, in salmon, 128 TRA J genes were identified within the TRA/TRD locus (Edholm et al., 2021). The majority of the genes were also found as corresponding genes in rainbow trout. Although the organization of the TRA/TRD locus is similar in both, there is a significant difference in the number of TRA/D V genes. Rainbow trout, specifically the Arlee strain, only have 163 TRA/D V genes, while Atlantic salmon has 239 TRA V genes. This difference is due to a higher number of non-functional pseudogenes in Atlantic salmon. An analysis of the functional TRV suggested that there are 25 subgroups, defined as having over 75% nucleotide identity common in both species. The only difference was one unique subgroup in rainbow trout, that was not found in salmon (Edholm et al., 2021). This supports the theory of the conservation of TRA/TRD repertoire across different salmonid species (Edholm et al., 2021).

1.9 γδ T cells

In addition to conventional T-cells there are functionally distinct γδ T cells. These cells are typically less abundant, but have a broader antigen recognition spectrum, and are primarily found in mucosal tissues such as the skin and gut mucosa. In humans and mice, γδ T cells make up 1-10% of all circulating T cells, and since they are abundant in mucosa and epithelial tissue it has been speculated that they play an important role in early immune responses (Kalyan & Kabelitz, 2013). In contrast, in species such as chickens, sheep, cattle and pigs, they make up between 15-60% of all the T cells in the peripheral blood (Ciccarese et al., 1997; Sowder et al., 1988). γδ T cells are often referred to as CD4 and CD8 double negative cells, and thus express neither the CD8 nor the CD4 co-receptor. Key to γδ T cells is that they can recognize both peptide and non-peptide antigens in an MHC independent manner. γδ T cells attack target cells directly through cytotoxic activity or indirectly through the activation of other immune cells (Bonneville et al., 2010).

Human γδ T cells share some of the same characteristics with conventional T cells, natural killer cells (NK cells) and APCs, suggesting they have a critical role in the first lines of host

immune defense. However, the exact function and phenotype[20] within tissue are still not well understood. In humans, there are two main subsets of γδ T cells identified by their Vδ chain. Vδ1 T cells are prevalent in the peripheral tissues and in the thymus, where they recognize stress-related antigens (Hayday, 2009). On the other hand, Vδ2 T cells, which constitute the majority of blood γδ T cells, recognize primarily phosphoantigens (phosphorylated non-peptidic molecules) (Lawand et al., 2017; Vantourout & Hayday, 2013). Both subsets of γδ T cells exhibit a cytotoxic potential through both their TCR and NKG2D receptors (natural killer group 2D) which is mediated by the release of soluble mediators such as granzyme B and perforin. In addition, human γδ T cells induce NK cell-mediated cytotoxicity and killing of tumors, by manipulating the CD137 pathway (Maniar et al., 2010). All of this tells us that the functions of γδ T cells are very varied and diverse.

1.10 γδ T cells in fish

While TRG and TRD genes have been found in a number of different teleost species (Castro et al., 2011), functional studies are scarce. In 2017, Wan et al. (2017) published a study on the characterization of γδ T cells from zebrafish and most of the current functional knowledge regarding γδ T cells in fish is derived from this study. The study showed the γδ T cells accounted for 7.7-20.5% of the total lymphocytes in spleen, head kidney, peripheral blood, skin, gill and intestine tissue. In addition, Wan et al. (2017) also conducted an in vitro assay to determine if zebrafish γδ T cells could function as antigen-presenting cells (APCs) capable of triggering adaptive immunity. This was done by examining the presence of specific APC markers, including MHC-II, CD80/86, and CD83, which are crucial for presenting antigens and providing signals for CD4+ T cell activation. They then sorted the activated γδ T cells from fish stimulated with the antigen Keyhole limpet hemocyanin (KLH) and used RT-PCR and double-immunofluorescence staining to analyze the results. The results revealed clear expression of MHC-II, CD80/86, and CD83 on the surfaces of the activated γδ T cells. Moreover, this expression was significantly upregulated in response to antigen stimulation. These findings suggest that zebrafish γδ T cells may exhibit the functional characteristics of

[20] Phenotype: Characteristics or traits in an individual based on the expression of their genes.

APCs. Other findings also suggest that they play a critical role in antigen-specific IgZ [21]production in intestinal mucus (Wan et al., 2017).

Compared to zebrafish, there are currently no functional studies regarding γδ T cells in salmonids. Yazawa et al. (2008) published the first study on the characterization of the Atlantic salmon TCRγ locus. An Atlantic salmon CHORI-214 bacterial artificial chromosome (BAC) library was screened and sequenced, and two different BAC clones containing TRG loci were found (TRG 1 and TRG 2). Sequencing of the BAC contig showed that the TRG 1 contained a total of five constant (C) regions, five joining (J) segments, and 10 variable (V) segments. TRG 2 consisted of one C region, one J segment, and one V segment. Flanking the TRG 1genes was a gene similar to binding protein 1, and in the TRG 2 two interferon-gamma-inducible GTPase (IIGP) genes (IIGP1 and IIGP5), and a myosin-1 and chaperonin gene were identified. Figure 6 is from a more recent study (2022), carried out by Mari Jahren Herud, that illustrates the organization of the TRG-locus on chromosome ssa20. The results from this study, which was based on sequence analysis of a fully sequenced and annotated Atlantic salmon genome found a total of 7 C regions, 7 J segments, and 16 V segments, which is one previously unidentified C region, J - and V segment.

Both the IIGP1 and IIGP5 matches with previous findings by (Yazawa et al., 2008). Yazawa et al. (2008) found TRG localized on two loci. In contrast, Herud (2022) found all TRG genes localized on the same locus, but they were separated by a large gap (figure 6). Herud (2022) suggested that the V, D and J genes were divided into 7 cassettes, where a single cassette consisted of at least one of each gene. The fifth cassette differed from the others in that it lacked a V gene. In addition to this, Herud (2022) also identified four of the TRGV-genes as "partial", and three of them as pseudogenes[22]. Partial means that the sequence was incomplete, and that only a part of it was identified.

[21] IgZ: A immunoglobulin characterized by its involvement in mucosa-associated lymphoid tissues (MALTs) for mucosal defense against pathogen infection.

[22] Pseudogenes: Nonfunctional segments of DNA that resemble functional genes

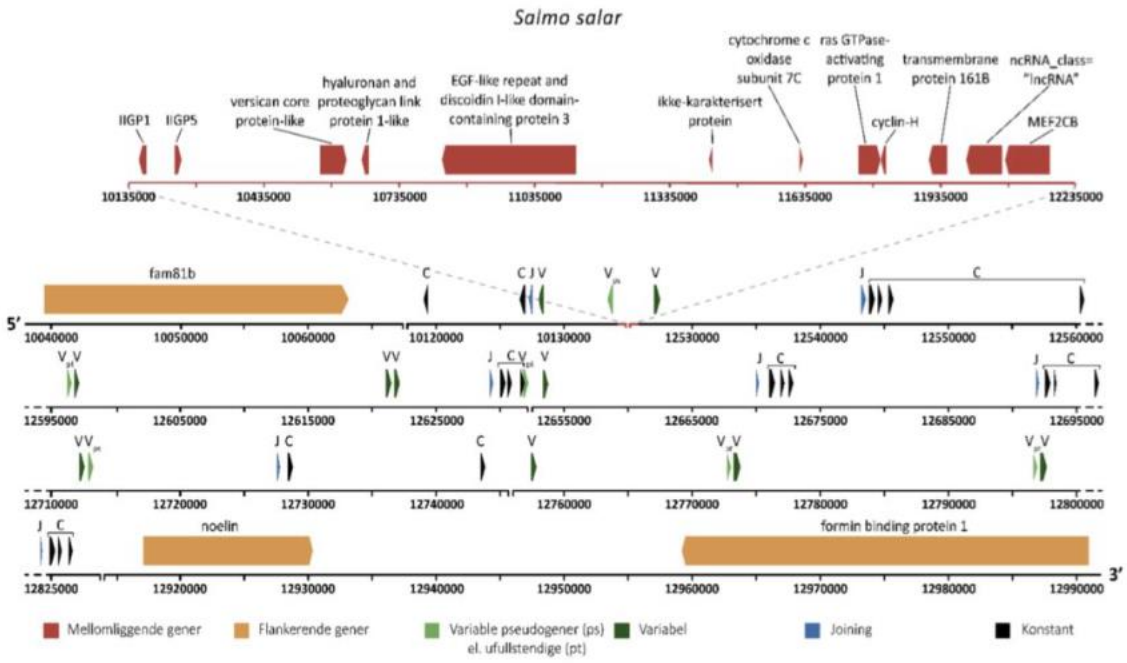

Figure 6. Results from Herud (2022), showing the organization of the TRG-loci in Atlantic Salmon. Constant genes are marked black, joining is blue, variable genes are dark green, variable pseudogenes are light green, flanking genes are red. The loci are orientated forward 5´- to 3´end.

1.11 Immune repertoire analysis

The immune repertoire encompasses all the unique genetic rearrangements of TCRs and BCRs within the adaptive immune system. When studying T cells and B cells separately, scientists often use the terms "TCR repertoire" and "BCR repertoire" (Thermo Fisher Scientific, 2024). T-cell and B-cell lymphocytes undergo a process similar to natural selection, where only those with the right antigen receptors are activated, forming clones during an immune response. Understanding the immune repertoire is vital for precision medicine and immunotherapy, enabling tailored treatments. Monitoring the immune repertoire can predict therapeutic outcomes, guide treatment effects, and address potential side effects like a weakened immune system. Immune-mediated adverse events (imAEs), limiting cancer treatment, can be predicted by monitoring the immune repertoire. Methods to monitor and boost immune repertoire recovery would be beneficial (Thermo Fisher Scientific, 2024). The human TCR repertoire, which comprises various TCRs, is crucial for the body's defense. Through genetic recombination involving insertion, deletion, and substitution, the limited set of genes encoding

the TCR has the potential to generate between 10^15 and 10^20 TCR clonotypes[23]. However, the real diversity of an individual's TCR repertoire is much narrower. With an estimated 10^13 cells in the human body, many clonotypes are prevalent due to strong selection forces, such as thymic education and antigen specificity (Laydon et al., 2015).

TCR sequencing methods can be divided into two categories: one involves bulk sequencing of immune cell populations, while the other focuses on single-cell analysis. Bulk sequencing is the preferred approach when the goal is to study TCR diversity and compare repertoires in larger collections. There are three distinct bulk sequencing techniques for generating library analyses of TCR chains, namely Multiplex PCR, target enrichment, and 5´RACE (Rosati et al., 2017). Target enrichment is a technique in next-generation sequencing (NGS) workflows. It helps exclude genomic DNA regions not relevant to a specific experiment. By focusing exclusively on particular areas, such as exons, it achieves more extensive DNA sequencing coverage in regions of interest or allows for increased sampling of individuals. This involves the use of oligonucleotides that are complementary to the sequence of interest (Kozarewa et al., 2015). These oligonucleotides will hybridize with the correct gDNA/cDNA sequences in the library before being captured using magnetic beads. Consequently, the sequences are prepared for further amplification before sequencing (Kozarewa et al., 2015). Multiplex PCR (Polymerase Chain Reaction) is a molecular biology technique that allows the simultaneous amplification of multiple DNA fragments in a single reaction. It is an extension of traditional PCR, which typically amplifies a single DNA target. In Multiplex PCR, a mixture of primers for known V-alleles is combined with primers for J-alleles or primers from the constant region of TCR α- and TCR β-chains, which results in a specific amplification of the CDR3 region from the TCR transcript (Petro et al., 2015)

Rapid Amplification of cDNA Ends (RACE) is a method used for obtaining complete RNA transcript sequences. RACE can provide the RNA transcript sequence from a known, short fragment within the transcript to either the 5' end (5' RACE-PCR) or the 3' end (3' RACE-PCR) of the RNA (Takara, 2024). When it comes to analysis of the results, it is either submitted by an external company specializing in repertoire analyses, or conducted in-house at a non-specialized laboratory, essentially doing it yourself. A common approach is to use a

[23] Clonotypes: Groups of identical T cells

commercially available kit to prepare the gene sequence library and then send it to a specialized company for "deep sequencing”.

1.12 Main research objectives

Previous studies have shown that in Atlantic salmon, out of seven TRGC genes, five TRGC genes are functionally expressed in healthy unchallenged adult Atlantic salmon. However, it is still clear if all five TRGC genes are equally expressed across tissues, and if there is a difference in function. Due to few antibodies available for Atlantic salmon, it is difficult to determine the percentage and cell distribution of specific cell populations, such as g/d T cells. PrimeFlow RNA assay, which combines branched-DNA technology with single-cell resolution of flow cytometry, expands the capability of flow cytometry by measuring RNA with target-specific probes. In this study, the main research objectives are to study the expression patterns and induction capabilities of different TRGC genes as well as determine the distribution of γδ-T cell subpopulations, using a combination of molecular approaches.

Sub-objectives:

- Optimization of PrimeFlow protocol for use in Atlantic salmon primary leucocyte populations
- Determine the percentage and distribution of γ and δ positive T-cells within various tissues of Atlantic salmon, using PrimeFlow.
- Contrast the basal expression of specific TRGC genes in various lymphoid and mucosal tissues of Atlantic salmon
- Study the functionality and expression levels of TRGC and TRDC genes in freshly isolated leucocytes from spleen, head kidney, and peripheral blood samples, and contrast these with cells that have been maintained in culture for up to 72 hours
- Study the fold change in expression of TRGC genes in response to stimulations with T cell mitogens, relative to basal expression levels, to assess the potential for T cell proliferation and/or activation

2 Material and methods

All kits, chemicals and reagents used in this study, in addition to producer and catalog number, is shown in table 3 & 4 (Appendix).

2.1 Experimental animals

For basal tissue expression, primary leukocyte isolation, and in vitro primary cell stimulations, tissues from healthy, unchallenged adult Atlantic salmon (Salmo salar) were used. Specifically, for PrimeFlow, fish weighing approximately 1.3 kg were utilized, while for primary cell stimulations and qPCR, fish weighing approximately 300 g were used. The fish were obtained from the Tromsø Aquaculture Research Station (Skarsfjordvegen 860, Kårvik, Troms, Norway). The roe originated from Aqua gen (Aqua Gen, Kyrksæterøra, Norway), and the fish were fed standard feed from Skretting (Skretting, Stavanger, Norway). The lighting regime consisted of six weeks of winter light (6 hours light, 18 hours dark), followed by six weeks of continuous 24-hour light. All the fish were lethally anesthetized with Benzoak Vet (ACD Pharmaceuticals AS, 519389) and the fish was placed on a wet paper towel to prevent it from slipping during the tissue isolation procedure. All tissue extractions were performed under semi-sterile conditions. Accordingly, 70% ethanol was prepared and used as disinfection solution to sterilize all surgical instruments, including scalpel, scissors, and surgical forceps. All animals were treated in accordance with relevant guidelines and regulations given by the Norwegian Animal Research Authority. The protocols used for live fish experiment were based on the Animal Welfare Act (Regjeringen, 2009)

2.2 Tissue isolation

The day before the experiment, 1,5ml microcentrifugation tubes were prepared, each containing 500µl of RNA Later (Invitrogen, AM7021) alongside the appropriate number of 50 ml Falcon tubes filled with 10 ml transport media (L15 media supplemented with 10% FBS, 2% heparin, and 10 U/ml penicillin, 10 µg/ml streptomycin), all stored at 4°C. Adult Atlantic salmon was used for all experiments. The initial step involved drawing blood from the caudal vein using a heparinized vacutainer tube (BD Vacutainer Heparin Tubes) equipped with a 21-gauge, 1.5-inch-long needle (BD Vacutainer Blood Collection Precision Glide Needle 21g x 1.5) to prevent

clotting, given that heparin functions as an anticoagulant. Subsequently, the blood, approximately 10 ml, was transferred into 50 ml Falcon tubes containing 20 ml of ice-cold transport medium. Before exposing the internal organs, the thymuses were collected. Using a sterile scalpel, each thymus, which is situated near the base of the gills within the gill cavity closely associated with the pharyngeal epithelium, was carefully scraped out. The thymuses were either placed in a tube with 500 ml RNA Later and put on ice for RNA isolation, or alternatively placed directly into transport media for primary thymocyte isolation.

Subsequently, a small portion of gill tissue from the second gill arch, was excised using a surgical scissor and transferred into a separate tube containing 500 µl RNA Later. Using a sterile surgical scalpel and forceps, a midline incision was made along the ventral surface of the fish from the throat area to the vent, and by gently opening the body cavity the internal organs were exposed. A small piece (0,5mm x 0,5mm), from spleen, liver, head-kidney, middle kidney, trunk kidney, heart tip, pancreas, stomach, upper- and lower intestine, and skin, was removed and placed in separate tubes with RNAlater. The rest of the spleen and head-kidney was placed in separate 50ml Falcon tubes with transport-medium and placed on ice for transport and further cell-isolation. All RNA Later-samples were kept on ice at room temperature during transport, then placed at 4°C for 24 hours. The following day, the samples were transferred to -20°C for long term storage and later use.

2.3 Primary cell isolation

Leukocytes from head-kidney (HKLs), spleen (SPLs), thymocytes and peripheral blood (PBLs) were isolated as outlined in figure 7. Head kidney, spleen and thymus tissue were homogenized by gently pushing it through a 100-µm cell strainer (Falcon) with a 10 ml syringe plunger, and all the cells were washed through the strainer using transport medium. Leucocytes were isolated from single cell suspension using percoll (GE Healthcare) gradients. Percoll gradients were prepared fresh the same day, beginning with the preparation of 90% percoll. This involved mixing 90ml of percoll stock (GE Healthcare) with 10 ml of 1.5M NaCL (3ml 5M NaCl +7ml dH_20), and 400 µl of Heparin (LEO Pharma, 585679), resulting in a 100ml of the solution. For the preparation of 100 ml 25% percoll, 28ml already prepared 90% percoll was gently mixed with 72 ml PBS (Phosphate Buffered saline, Invitrogen), and 288 µl Heparin. To prepare 100

ml of 54% percoll, 59ml of 90% percoll and 41ml of L15 (added 164 µl heparin and 820 µl FBS) was gently mixed.

Next, the gradients were layered by adding 10ml of 25% percoll to new 50ml Falcon-tubes. 8 ml of 54% percoll was carefully layered beneath the 25% percoll solution, pipetting through a Pasteur pipette. 10 ml of the single cell suspensions was carefully loaded on top of the 25%/ 54% gradients, slowly pipetting one drop at the time to prevent mixing. Both single cell suspensions from spleen and head kidney tissues were layered on 25% /54% percoll, while PBLs were layered on a single 54% percoll gradient. Cell suspensions obtained from thymus tissue were not separated based on percoll gradients but used straight after pushing through the cell strainer. The gradients were then centrifuged at 400 x g for 40 minutes at 4°C with the acceleration break was set at 4 using a centrifuge (Heraeus multifuge, Kendro Laboratory Products Heraeus D-37520). After centrifugation, the top part, consisting of debris and tissue, was removed and the cloudy band at the interface between the two gradients (see figure 7, part 3) was collected and transferred to a new 50 ml Falcon tube. Next, the cells were washed, by adding 40ml of transport medium and centrifugate for additionally 10 min at 600 x g at 4°C. After removing the supernatant, which is the liquid above the pellet, the cells were resuspended in 5ml of transport medium. 1,5ml Eppendorf tubes were marked and prepared with 10 µl of Trypan blue, which stains dead cells to quantify live cells, followed by 10 µl of cell suspension. After briefly mixing, a total of 10 µl cell suspension/trypan blue mix was transferred to a counting chamber (Countess Cell Counting Chamber Slides, Invitrogen, C10283). The counting chamber were then placed into the counter (Countess 3 Automated Cell Counter, Thermo Fischer Scientific), and the number and viability of cells were determined.

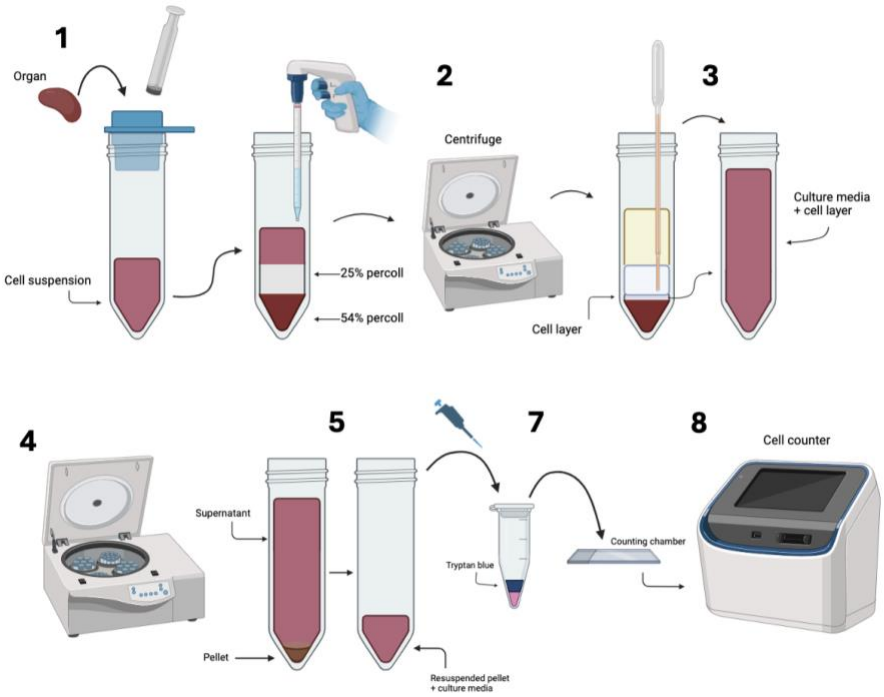

Figure 7. Illustration of primary cell isolation. 1. Cell straining, transferred to 25%/54% gradient, 2.Centrifugation, 3. Cell layer transferred to new tube with culture media, 4. Centrifugation, 5. Removal of supernatant, and resuspension in culture media, 6. Equal amounts of cell suspension and trypan blue mixed in separate Eppendorf tube, 8. Transferred to counting chamber and counted (Illustration: Andrea Luka).

2.4 Con-A stimulation and harvesting of cells

Primary leukocytes isolated from head kidney, spleen and peripheral blood were, as described above, counted and diluted to 4 million cells/ ml in culture media (L15-media supplemented with 8% FBS and 10 U/mL penicillin, 10 µg/mL streptomycin). A total of 4 million cells were seeded into each cell culture plate well (24-well plates). The cells were plated out in duplicates, including one control sample and one containing 2,5 µg/ml Concanavalin-A (Con-A, Sigma, C 7642). Con-A is a plant lectin, purified from jack beans, that binds to glycoproteins on the cell surface, making T cells proliferate. It can be used as an alternative T cell stimulus, and is often used as a surrogate for antigen-presenting cells in T cell stimulation experiments (Ando et al., 2014) Next, the 24-well plates were sealed and incubated at 16°C. At different time points post stimulation (24h, 72h and 7 days) cells in the wells were mixed by gently pipetting, collected into micro centrifugation tubes and spun down in a tabletop centrifuge at 800 x g for 5 minutes. The resulting pellet was resuspended in 350 µl RLT buffer (Qiagen, 79216) and stored at -20°C until use. The 24 and 72h samples were further processed.

2.5 RNA isolation

Total RNA was isolated from stimulated and control (unstimulated) SPLs, HKLs and PBLs following the RNeasy® Mini Kit Part 1 protocol (Qiagen, 74104). The process began by adding 7 µl of dithiothreitol (DTT) to each sample. DTT is a reducing agent, used to stabilize proteins and enzymes, to keeping monothiols in a reduced state. As such the addition of DTT helps to breaks disulfide bonds within or between proteins, which can help with protein denaturation, protein refolding, and protein purification. In this case it was added aid in the purification of the RNA (Thermo Fischer Scientific). After vortexing, 350 µl of 70% ethanol was added to each sample. Next, 700µl from each sample were transferred to RNeasy Mini spin columns which were placed in 2 ml collection tubes. The samples were centrifuged for 15 s at 12,000 x g, and the flow-through was discarded. Following this, 700 µl of Buffer RW1 was added, the samples were centrifuged for 15 s at 12,000 x g, and the flow-through was discarded. The next step included adding 500 µl of Buffer RPE to each sample, centrifuging for 15 s at 12,000 x g, and discarding the flow-through. This step was repeated twice, with the second round involving centrifugation for 2 minutes in order to remove any residual ethanol which is present in the RPE buffer. The RNeasy spin column was placed in a new collection tube, and 30 µl of RNase-free water was added directly to the spin column membrane. The samples were centrifuged for 1 min at 12,000 x g to elute the RNA. Samples were immediately placed at -80°C and they were stored until the cDNA preparation procedure began.

To quantify and qualify the RNA, a NanoDrop ND 1000 Spectrophotometer was used (Thermo Fisher Scientific). The Nanodrop ND 1000 Spectrophotometer is a laboratory instrument that allows for measurement of nucleic acid (DNA and RNA) and protein concentrations in biological samples. The instruments allow to determine the quality and concentration of the samples. After opening the sampling arm on the instrument, 1 µl of milliQ water was pipetted onto the lower measurement pedestal, the sampling arm was closed, and the “Blank button” on the computer was pressed. This was because an initial blank needed to be measured as a reference to normalize the samples against. The RNA from both stimulated and control HKLs, SPLs, and thymocytes was analyzed by measuring 1 µl from each sample. “RNA-40” was chosen as “Sample type”, and the sample concentration in ng/µl based on absorbance at 260nm was measured. In addition, the ratio of sample absorbance at 260 and 280nm (260/280) and at 260 and 230nm (260/230) was also measured. This was to assess the purity of the RNA.

2.6 cDNA preparation and synthesis

Reagents and volume used in cDNA synthesis is shown in table 5 (Appendix). Based on quantification results from Nano Drop, the amount of RNA to be transcribed into cDNA was determined. To maintain consistency across all samples, a total of 1 μg RNA per sample was chosen. Before starting the cDNA synthesis, the RNA was treated with DNase I to remove any residual genomic DNA (gDNA). This was done by adding 1 unit of DNase I (Thermo Scientific, EN0521) for each µg of RNA, and 1 µl 10x DNase reaction buffer to the RNA. Subsequently, RNase free water was added to reach a total volume of 10 µl for each sample. The samples were then incubated for 30 minutes at 37°C in a thermal cycler. After the incubation, 1 µl of 50 mM EDTA was added to each sample. EDTA chelate calcium and magnesium ions which indirectly will inactivate DNase I (Sigma-Aldrich, 2012). This step was followed by an additional incubation for 10 minutes at 65°C. Next, the DNase-treated RNA was reversed transcribed to cDNA using TaqMan reverse transcription reagents (Applied Biosystems).

Briefly, cDNA was synthesized by adding 10,4 µl of master mix consisting of 2 µl 10X RT Buffer, 1,4 µl 25mM MgCl2, 4 µl 10mM dNTP mix, 1 µl RNase Inhibitor, 1µl MultiScribe Reverse Transcriptase, and 1 µl Random Hexamers to each of the DNase treated RNA. Random hexamer are primers that are used for random priming of single-stranded RNA, by giving random coverage to all the regions of the RNA. This generates a type of cDNA pool that contains different lengths of cDNA (Meridian Bioscience). There are three steps in reverse transcription, primer annealing, DNA polymerization, and enzyme deactivation. Following incubation for 10 minutes at 25°C, 30 minutes at 37°C, and then 5 minutes at 95°C. In addition, 1-2 samples from each synthesis reaction chosen at random were added RNase-free water instead of MultiScribe Reverse Transcriptase to serve as negative controls allowing for the detection of genomic DNA contamination. After the cDNA synthesis, the samples were diluted 1:1 in ultrapure water and kept on –20 °C until qPCR-analysis.

2.7 Quantitative PCR and Transcript Analysis

Reagents and volume used in qPCR analysis is shown in table 6 (Appendix). SYBR-Green based quantitative PCR (qPCR) was performed, using the 7500 Fast Real- Time PCR system program (Applied Biosystems). SYBR Green, which is a fluorescent dye that bind double-stranded DNA was used in all reactions. In qPCR, it is used to determine how much DNA has

been amplified, by measuring the fluorescence at the end of each amplification cycle (Rodríguez et al., 2011). For the qPCR, every sample was tested in duplicates in 96-well Reaction Plates (MicroAmp Fast 96-well Reaction Plate (0.1mL) Life Technologies kat.nr. 4346907), and for the reaction 2,5 µl cDNA, 2,5 µl primermix (containing equal amounts of both forward and reverse primers), and 5 µl Fast SYBR Green Master mix (Applied Biosystems, 4385612) was used. This gave a total of 10 µl per sample, including the negative controls. All samples were run with melt curve analysis. SYBR Green dye non-specifically binds to double-stranded DNA (dsDNA), and to confirm that target-specific amplification occurred it is normal to do a melt curve analysis. This analysis takes place after the qPCR, and if non-specific binding occurs between SYBR Green and dsDNA, the melt curve shows two peaks instead of one. This is a good way to detect contamination and genomic DNA in the sample. The negative control is important to test for contaminating DNA, such as genomic DNA, that may interfere with the results. If PCR amplification is seen for the negative controls, it indicates the presence of contaminating genomic DNA.

The integrity and quality of each individual cDNA sample was first assessed using a housekeeping gene, in this case Elongation Factor 1α (EF1 α). Housekeeping genes represent genes ideally being stably expressed in all cells and conditions and are required for the cell to sustain life (Joshi et al., 2022). All the qPCR data were standardized relative to the same reference gene, and the expression of this gene should therefore not vary in the tissues under investigation. EF1 α is known to be relatively stable expressed, and Ingerslev et al. (2006) concluded with EF1 α being the most appropriate reference gene for Atlantic salmon compared to Beta-Actin gene and RPS20. For the main analyses we used four different Sasa-TRGC specific primers to detect TRGC1-, TRGC2-, TRGC3-, TRGC5- transcripts respectively, as well as primers specific for TRD-, and TRA-transcript. The concentration of specific amplified cDNA in each reaction is determined by the Ct-value. This number gives information about how many cycles it took to reach a set threshold (0,05). If the Ct-value is low it indicates that there is a high amount of cDNA in the sample, and if the Ct-value is high it indicates the opposite.

2.8 TRG-Primer design

All primers used in relative expression and Con A studies is shown in table 10 (Appendix). Previous studies have shown that there are 7 different TRGC regions (Herud, 2022), and in order to compare the relative expression of each one, before and after stimulations, specific primers were designed and tested. Each of these TRGC regions has an associated nucleotide sequence, and when designing TRGC primers, the similarity between the C region nucleotide sequences were examined. TRGC2_1 and TRGC2_2 exhibited a 97.6% similarity in nucleotide sequence, and therefore a shared primer was designed for these two (TRGC2). For TRGC1, TRGC3, and TRGC 5, the nucleotide sequences ranged between 70 to 80%, and one specific primer pair was designed for each. To be able to make direct comparative measurements with regards to transcription of the different C-regions it was important to measure primer efficacy, so that each primer pair has the same efficacy. Specific primer pairs targeting each Sasa-TRGC gene sequence were manually designed, and their amplification efficiency was evaluated by using a standard curve derived from serial dilutions of cDNA from salmon thymus. A universal approach to primer design was applied to all TRG genes. Forward primers were designed to match the 3'-end of respective C regions; TRGC1, TRGC2, TRGC3, and TRGC5. Reverse primers, were designed to match the connecting peptide. To ensure the comparability of PCR primer efficiency across various TRGC primers average Ct values obtained from a four-point dilution series were used to calculate the slope using the following formula:

Slope = (average Ct value / log DNA dilution)

Calculated efficiency with 90-110% as recommended minimum and maximum values respectively, using the following formula:

$$= (10^{-1/slope} - 1) \times 100$$

The efficiency of TRGC primers ranged from 99 to 106%, where each primer had a length of 24 base pairs and a GC content between 37 and 62%.

Table 1. Summary of calculated slopes and primer efficiency in percentage for TRGC primers.

	TRGC1	TRGC2	TRGC3	TRGC5
Slope	- 3,5	- 3,3	- 3,3	- 3,2
Primer efficiency (%)	99,8	100,7	100,5	106,9

2.9 Statistical analysis

The comparison of TRGC relative expression in various tissues relied on the Ct-values obtained from qPCR analysis. Given the genetic variability among the six fish tested, we employed a common reference gene, EF1 α, to ensure accurate comparisons. Before analyzing the target genes, EF1 α expression was assessed in all groups. All samples were run in duplicates, with the standard deviation of cycle threshold (Ct) values measured to ensure consistency and precision in the results. By calculating the delta Ct, representing the difference between the reference and target genes, we determined the relative expression levels. This normalization approach ensured consistent comparisons across all samples. The relative expression was calculated in Microsoft Excel.

$$X = ct\ value\ of\ a\ spesific\ primer$$

$$\Delta ct = \frac{ct\ x}{ct\ EF1a}$$

$$Relative\ expression = 2^{-\Delta ct}$$

After determining the relative expression, the fold change was calculated by comparing the mean control Ct-values for each fish in every group, with the corresponding values at different timepoints. Fold change was calculated for Con A-stimulated leukocytes at two time points (24h and 72h). This analysis helped identifying potential upregulation in various tissues following stimulation, and observations of differences between groups. The fold change was calculated in Microsoft Excel

Fold change = relative expression / mean (relative expression of control)

The statistical analysis and graphics were done in GraphPad Prism, and one-way ANOVA was used to estimate the differences between the groups.

2.10 SMARTer RACE 5`/3`

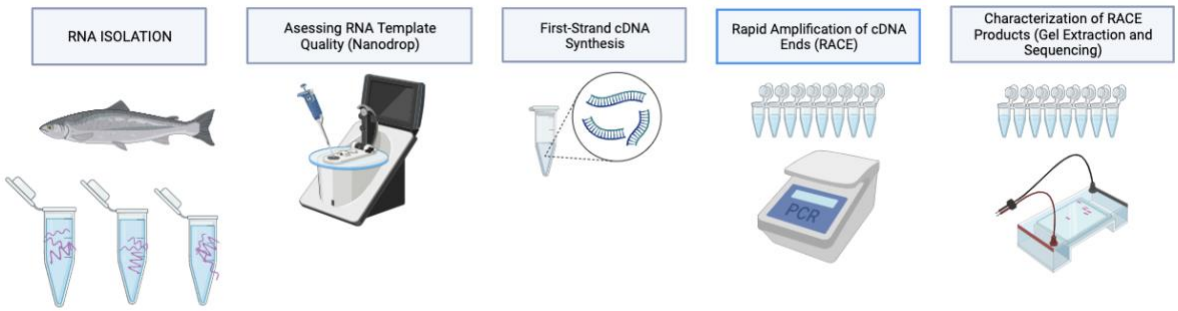

Figure 8. Illustration of SMARTer RACE 5´/3´ protocol (Illustration: Andrea Luka).

Rapid Amplification of cDNA Ends (RACE) as outlined in figure 8, is a method used to obtain the full-length sequences of RNA transcripts, by using a single gene specific primer. In this study we used the SMARTer RACE 5'/3' Kit (Takara Bio USA, Inc (kat.nr. 634860)) with the aim to amplify all possible VJ rearrangement associated with either TRGC1, TRGC2, TRGC3 or TRGC5. The main difference between first strand cDNA-synthesis (RACE) and normal cDNA synthesis is the addition of SMARTer II A Oligonucleotide. This is a known sequence that binds to the 5`end of the mRNA and is added prior to the cDNA synthesis. The 5`-CDS Primer A will then bind to the poly-A tail on the 3`end of the mRNA, and the complete mRNA with the SMARTer II A Oligonucleotide sequence will be transcribed. This will result in RACE ready cDNA. The main advantage of RACE is that due to the addition of the SMARTer II A Oligonucleotide, it only needs one gene specific primer, which allows for amplification of unknown transcripts in an unbiased manner as the second primer is designed to match the known sequence of the SMARTer II A Oligonucleotide.

For the SMARTer RACE protocol two GSPs (gene specific primers) were designed. These were named GSP1 (5`-GATTACGCCAAGCTTTGTCTCCAGCCAAACATAGCAGGGTG-3`) and GSP2 (5`-GATTACGCCAAGCTTCTGGGTAGACCGTCACTTTGGGTTT-3`). In addition, two corresponding degenerated GSPs, degGSP1

(5`GATTACGCCAAGCTTTGTCTCYAGCCARACATAGCAGGGTG-3`) and degGSP2 (5-`GATTACGCCAAGCTTCTGRGTASACCGTCACTTTGGGTTT-3`), were designed. The reason why degenerated primers are included, is to catch a broader range of genetic variants. Easier explained, when you want to amplify a specific gene there might be variations or differences in the gene sequence. In this case, there are some nucleotide differences between the different TRGC regions, and therefore, using only one specific primer might not amplify all genes. This is due to these genetic variations. By this means, degGSP1 codes for the same oligonucleotide sequence as GSP1, but some of the nucleotides are switched out with an Y. The Y codes for both C and T, which makes the primer cover a broader range of target sequences.

2.10.1 First-strand cDNA synthesis

Reagents and volume used in first-strand cDNA-synthesis is shown in table 8 (Appendix). The first step was the preparation of a buffer mix for the 5'-RACE-Ready cDNA synthesis. Enough buffer mix for 1 extra reaction was routinely prepared. Started off by measuring 36 µL of 5x First-Strand Buffer, putting it into a microcentrifugation tube. Next, 4.5 µL of DTT (Dithiothreitol) and 9 µL of dNTPs (deoxyribonucleotide triphosphates) were added to the same tube. After mixing, and a brief spin in a microcentrifuge, the Buffer Mix was set aside at room temperature for later use in the experiment.

In this experiment, RNA from three different fish was used, sourced from the skin, gills and intestine. 800ng of RNA was mixed with 1 µL of the 5'-CDS Primer A and individual volumes of sterile H2O were added to ensure a total volume of 11µL. The tubes were then mixed and given a brief spin in the microcentrifuge, before being incubated at 72°C for 3 minutes and cooled to 42°C for 2 minutes. While the tubes were incubating, the Buffer mix was prepared by adding 4,5 µL of RNase Inhibitor (40U/µl) and 2 µL SMARTScribe Reverse Transcriptase (100 U), followed by a brief mix. After the first incubation step, 1 µl of the SMARTer II A Oligonucleotide was added to each tube followed by 8 µl of the prepared Buffer mix to each tube, and the contents of the tubes were mixed by gently pipetting. Each cDNA synthesis reaction then had a total volume of 20 µl. After a quick spin to collect the contents at the bottom, tubes were incubated at 42°C for 90 minutes, followed by 70°C for 10 minutes. All the first-strand cDNA synthesis reaction products were then diluted by adding 20µl of Tricine-EDTA Buffer. 5'-RACE-Ready cDNA samples were then stored at –20°C until further use.

2.10.2 RACE

Reagents and volume used in the RACE reaction is shown in table 9 (Appendix). GSP primers were diluted to a 10 µM concentration. To make a working stock solution, 10 µL of each primer and 90 µL of PCR-grade H2O was mixed. After diluting the primers, they were mixed and put on ice. Next, enough PCR Master Mix was prepared for all the PCR reactions, plus one extra to ensure sufficient volume. Started off by mixing 139,5 µl PCR-grade H2O with 225µl 2x SeqAmp Buffer and 9 µl SeqAmp DNA polymerase, which gave a total volume of 41,5 µl for each PCR reaction.

RACE ready cDNA from the gills of four different fish was initial tested with GSP1 and degGSP1 primers, by adding 2,5 µl of cDNA from each fish to two different 0.5ml PCR-tubes. PCR tube 1-4 were added 1 µl of GSP1, while PCR tube 5-8 were added 1 µl of degGSP1. 41,5 µl prepared Master Mix were added to all the PCR tubes, as well as 5 µl of Universal Primer Short (UPM). After spinning down the PCR tubes in the centrifuge, the samples were then ready for thermal cycling (PCR). The following touchdown PCR program was used: 5 cycles: (94 ℃ 30sec, 72℃ 3min), 5 cycles: (94℃ 30 sec, 70℃ 30 sec, 72℃ 3 min), 25 cycles: (94℃ 30 sec, 68℃ 30 sec, 72℃ 3min). Touchdown PCR is used to reduce non-specific amplification. It begins with a high annealing temperature and gradually lowers it over PCR cycles until the desired annealing temperature is attained. When the program was finished, the PCR-reactions were incubated at 4℃ until the next day.

2.10.3 Gel electrophoresis

Gel electrophoresis is a way of separating DNA fragments of varying sizes, by applying an electric field to an agarose gel. After mixing the samples with a loading buffer containing dye, individual samples are loaded into wells in the gel. The charged molecules will migrate through the gel, and while the smaller molecules will travel faster, the larger molecules will stay closer to the well and travel at a slower pace. This is due to the resistance in the gel. Accumulated DNA fragments of a given size will form bands in the gel, which will be visible under UV light.

100ml of TAE Buffer, consisting of Tris, acetic acid, and EDTA, and 1g of Agarose powder (Termo Scientific) were added to an 300ml Erlenmeyer flask, and mixed together by swirling the flask. The solution was then microwaved for 2 minutes, until all the agarose was dissolved. Next, the solution was cooled down for about a minute followed by the addition of 10µl of

SYBR safe DNA gel stain (Gel red, Biotium, 41002). Gel trays were placed into a cassette, and a comb was placed into the top of the gel. A 9 well comb was chosen. Agarose solution was poured into the tray and left to solidify for about 20-25 minutes. Next, water was loaded on top of the gel, and TAE buffer was added on the outside of the trays.

45µl PCR product was added 5µl of purple loading dye in new PCR-tubes, pipetted to mix. The PCR-tubes were then centrifuged. After the comb in the gel tray was removed carefully, 10 µl of Gene ruler (DNA ladder) was loaded into the first of nine wells. The remaining 8 wells were loaded with 50 µl PCR products mixed with loading dye. After closing the gel chamber with a lid, the electrodes were attached to a power supply, generating an electric current that induced the migration of molecules within the gel. The electrophoresis was conducted at 100 volts for 35 minutes. After electrophoresis, the gel was exposed to UV light to check for visible bands.

2.11 PrimeFlow RNA Assay

Reagents used in PrimeFlow analysis is shown table 7. The PrimeFlow RNA Assasy is a technique based on Fluorescence in situ hybridization (FISH) that combines branched DNA (bDNA) signal amplification with flow cytometry. This method is designed for microscopic analysis of RNA in cells and tissue, and by using bDNA technology it is possible to amplify the reporter signal rather than the target sequence. The PrimeFlow RNA Assay workflow can be divided into four steps, as shown in figure 9. It begins with sample preparation, where cells are fixed and permeabilized. The next step is target hybridization, during which cells are incubated with gene-specific target probes. Following this, signal amplification takes place, involving hybridization with pre-amplifier and amplifier DNA. The final step includes adding fluorescent label probes and analyzing the cells using a flow cytometer.

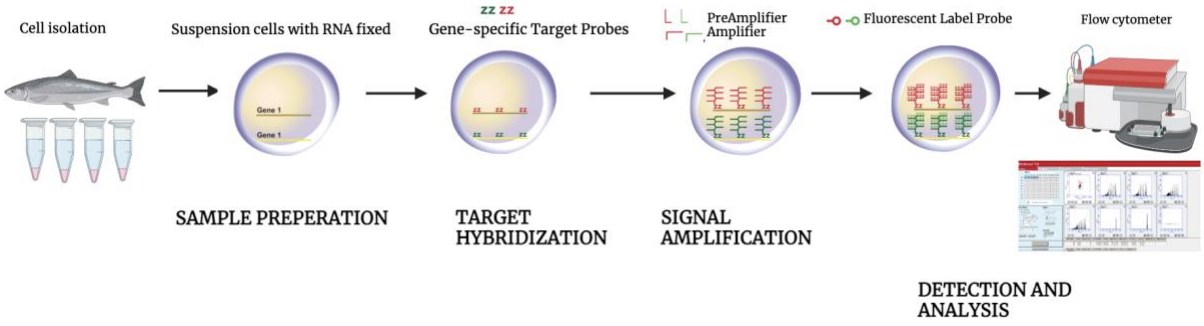

Figure 9. Illustration of PrimeFlow procedural steps (Illustration: Andrea Luka).

2.11.1 Probe design

The TRG loci comprise seven different C-regions (TRGC1, TRGC2_1, TRGC2_2, TRGC3, TRGC4, TRGC5, and TRGC6), while the TRD loci have only one TRDC-region. Amino acid sequences from the seven TRGC-regions were organized, segmented into exons, and similarities among sequences were identified by marking amino acids in different colors for visual clarity (shown in figure 20 and 21 in Appendix). Nucleotide composition comparisons were made for the different C-regions, followed by translation using the ExPasy translate tool to analyze both nucleotide and amino acid sequences. The most similar segments in the C-regions were retained, forming a template using Clustal Omega for alignment. Since unique sequence stretches in the seven nucleotide sequences of the C-regions were too short for making functional probes, they were combined into the same TRG cocktail. Consequently, our TRG probe was not specific to one C-region, but covered all seven TRGC-regions of the TRG. Additionally, a probe for the TRD was created, and since this receptor only had one C-region, the full nucleotide sequence was directly used as the template.

In addition to the TRG and TRD probes, we also included probes for EF1α and IgM. EF1α, a housekeeping gene that is postulated to be transcribed at comparable levels in most cells, was used as a control (Olsvik et al., 2005). IgM is highly expressed in B cells, and given that we are using lymphoid organs, positive binding to the IgM probe is expected (Van der Wal et al., 2021). A negative control was included to account for background fluorescence.

2.11.2 Cell fixation and permeabilization

The RNA Wash Buffer was pre-warmed to room temperature. Fixation buffer 1 was then prepared by combining equal parts of RNA Fixation Buffer 1A and RNA Fixation Buffer 1B. This mixture was prepared in bulk to accommodate all samples. 1 ml of the Fixation Buffer was added to each sample, the samples were then inverted and incubated for 30 minutes at 4℃. While incubating, RNA Permeabilization Buffer with RNase Inhibitors was prepared by diluting the RNA Permeabilization Buffer (10X) to 1X with RNase-free water and adding RNase Inhibitor (100X) at a 1/100 dilution. The samples were then centrifuged at 800 x g for 5 minutes, and the supernatant was carefully discarded. The residual pellet was subsequently gently resuspended, and 1 ml of RNA Permeabilization Buffer with RNase inhibitors was added to each sample. Following another centrifugation at 800 x g for 5 minutes, the supernatant was

again carefully discarded, and the pellet was gently resuspended. This process was repeated two more times, for a total of three wash steps. RNA Fixation Buffer 2 was prepared in bulk by combining 125 µl of RNA Fixation Buffer 2 (8X) with 875 µl of RNA Wash Buffer per sample. Carefully inverting to mix, 1 ml of this mixture was added to each sample. The samples were then incubated at 4℃ overnight.

2.11.3 Target probe hybridization

The RNA Wash Buffer was pre-warmed to room temperature, and the target probe along with positive control target probes specific to either elongation factor alpha or immunoglobulin M were thawed and brought to room temperature. The RNA Target probe diluent was pre-warmed to 40℃, and the target probes were subsequently diluted 1/20 in the RNA Target Probe diluent. To each sample, 1 ml of RNA Wash Buffer was added, followed by centrifugation at 800 x g for five minutes. After discarding the supernatant, 100 µl were retained. This washing step was performed twice.

Next, 100 µl of the diluted target probes were added to the samples, vortexed for thorough mixing, and then incubated for two hours at 40℃. After one hour, the samples were inverted. Following this, the samples underwent one wash with RNA Wash Buffer. Additionally, a solution of RNA Wash Buffer with RNase Inhibitor (100X) at a 1/100 dilution was prepared. 1 ml of this RNA Wash Buffer with RNase Inhibitor was added to each sample, followed by centrifugation at 800 x g for five minutes. The supernatant was discarded, leaving 100ul, and the remaining volume was gently vortexed. The samples were then incubated overnight at 4℃ in the dark.

2.11.4 Signal amplification

The samples and RNA Wash Buffer were pre-warmed to room temperature, while RNA PreAmp mix, RNA Amp Mix, and RNA Label Probe Diluent were pre-warmed to 40 ℃. Subsequently, 100 µl of RNA PreAmp Mix was added to each sample and the samples were incubated at 40 ℃ for 1.5 hours. The samples were then subjected to three rounds of washing, centrifugation, and resuspension, following the same procedure as earlier.

Next, 100 µl of RNA Amp mix was added to each sample, mixed by vortexing, and then incubated at 40 ℃ for 1.5 hours. After three washes with 1 ml RNA Wash buffer, involving centrifugation and resuspension, RNA Label Probes (100X) were diluted 1/100 in RNA Label Probe Diluent. This dilution was prepared in bulk, adding 100 µl directly into the cell suspension and briefly vortexing to mix. The samples were then incubated for another hour at 40 ℃.

Following this, the samples underwent two washes, and after the last centrifugation, the supernatant was discarded. Subsequently, 1 ml of Flow Cytometry Staining Buffer was added to each sample. The samples were inverted, centrifuged for 5 minutes at 800 x g, and after discarding the residual volume, approximately 200 µl remained. The samples were then analyzed by using a flow cytometer.

2.11.5 Flow cytometry analysis

Flow cytometry is a method used for the parametric analysis of single cells (Cram, 2002). The flow cytometer (BD Accuri C6 Plus, BD) analyzes particles or cells suspended in buffered salt-based solutions as they pass by lasers. Cells are assessed for visible light scatter, measured in both a forward direction (FSC) and at a 90° angle (SSC). FSC (forward scatter) reflects cell size, while SSC (side scatter) indicates cellular complexity (Cram, 2002). Additionally, fluorescence emitted from the cells is measured, aiding in the identification of different cell populations.

The first run served as the control sample, analyzing 35,000 events. This helped identify clear populations of interest through gating. A histogram was then created using only events within the designated region, and a gate was drawn to indicate positive cells for either FITC or APC. FITC and APC are fluorescent dyes, used to identify different cell populations. After gating the control sample, the sample with EF1 probe was checked under the same conditions. If the EF1 alpha peak shifted into the FITC-positive gate or showed multiple peaks, it indicated positive staining. Since EF1α is a housekeeping gene, supposed to be present in all cells, all the cells should be stained. The same process was repeated for samples with IgM and TRD probes. For the TRG probe, the dye was switched to APC. This procedure was first conducted on SPLs, followed by HKLs and PBLs.

Analysis was done using FlowJo (FlowJo Software, BD bioscience), which is a specific software package used for analyzing flow cytometry data. Using FlowJo, a graphical interface was used to draw a gate around the population of interest in the dot plots. In this research, the fluorescent dye fluorescein isothiocyanate (FITC), emitting green light, was utilized for the detection of EF1α, IgM- and δ positive T cells, while allophycocyanin (APC), emitting red light, was employed for the detection of γ positive T cells. Given its strong signal strength compared to FITC, APC was chosen to ensure accurate detection, particularly considering the uncertainty surrounding the expression levels of γ T cells. Before adding our probes, a negative control was employed to gate the leukocytes. This step helped to eliminate debris and minimize background that could potentially interfere with and influence the results. Following the gating of single cells, additional gates were set for FITC positive and APC-positive leukocytes. Leukocytes falling within these gates after adding the different probes, would be categorized as FITC or APC positive. For each tissue a universal gate was set for the negative (no probe) control. This gate was called "Gate 1" and all the probes were normalized to this specific gate. For Gate 1 the y and x axis were set as SSC and FSC. Next, the FSC was changed to FITC and a FITC+ gate was made, marking the area with no cells in the control samples. For the last gate the SSC was changed to histogram, and a line was drawn from the peak to the end of the x-axis. In this way, the FITC positive populations could be seen as a peak that moved into the positive gating area. Both the "Gate 1" and "FITC positive" gates were then marked and copied to the EF1α -, IgM-, and TRD- probe. After analyzing the results, the FITC positive gate was changed to an APC positive gate. This APC positive gate, in addition to Gate 1, was copied to the TRG probe.

3 Results

3.1 PrimeFlow RNA Assay

In lieu of either Atlantic salmon TRG or TRD specific antibodies, PrimeFlow RNA assay was employed to determine the percentage and distribution of γ and δ positive T-cells within isolated PBLs, HKLs, thymocytes and SPLs. A total of four separate experiments were conducted using four adult Atlantic salmon obtained from Tromsø aquaculture research facility at Kårvika. Following the Probe design protocol (see Probe design, Material and method), target specific probes for TRD and TRG were designed. The RNA targets within the cells were hybridized with target-specific probes, leading to amplification upon binding of the oligonucleotides to the RNA transcripts. Following amplification, cells were analyzed using flow cytometry.

In order to optimize the PrimeFlow protocol for use in salmonids, freshly isolated SPLs were stained with controle probes specific for EF1α. To determine the level of background fluorescence, negative control cells were treated identical, with the exception of target probe addition. The result is shown in figure 10A. Surprisingly there were two clearly defined EF1α populations; one positive, and one that did not stain above background. Next a probe specific for IgM was used, and as expected, using PrimeFlow, results that largely recapitulate those previously reported based on anti-IgM surface staining were seen (Van der Wal et al., 2021), demonstrating a population of IgM expressing cells representing about 20% of splenocytes (figure 10B). Notably, the use of IgM specific probes in PrimeFlow also identified a small population of high intense staining IgM positive cells. This implies that there is a subset of cells within the population that express high amounts of IgM mRNA, but they represent a small proportion of the total cell population being analyzed.

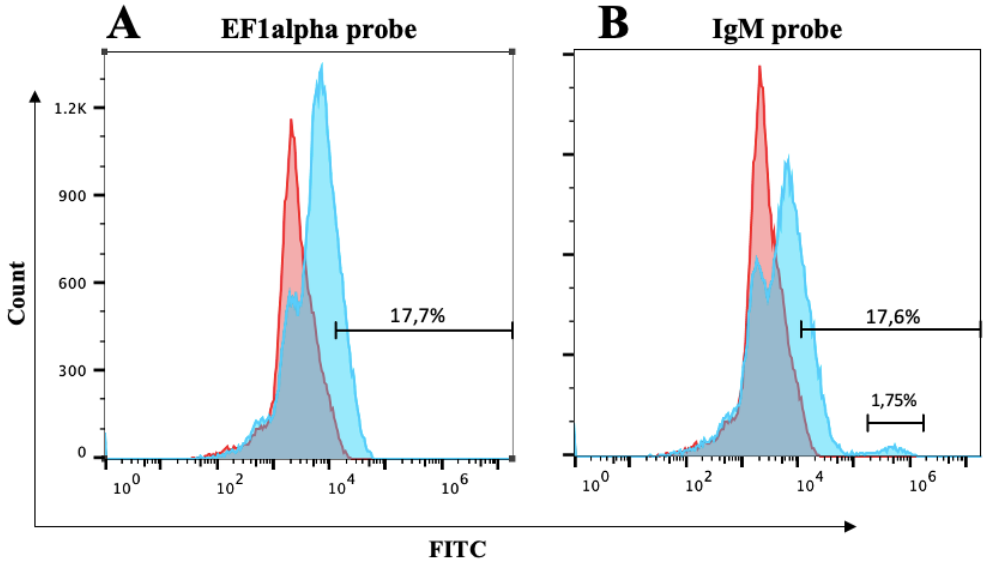

Figure 10: Flow cytometry analysis of (A) SPLs incubated with Elongation factor 1 alpha probe (blue histogram), compared to negative control (red histogram), and (B) SPLs incubated with IgM probe (blue histogram) compared to negative control (red histogram).

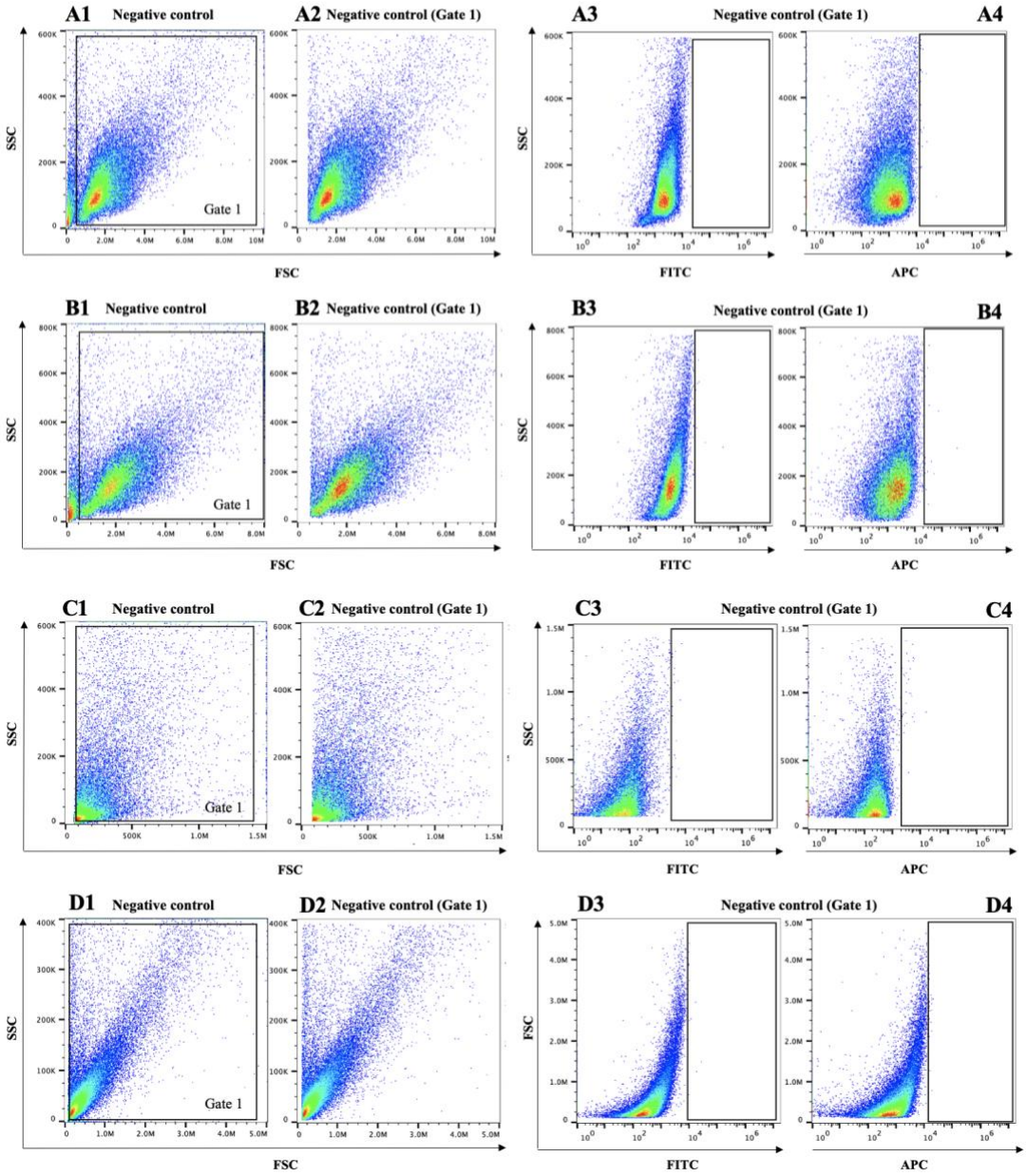

Figure 11: Flow cytometry analysis of SPLs, HKLs, and PBLS. Figure showing the gating of leukocytes, with FITC and APC gates. Results presented in dot plot, representing (A) SPLs with FITC gating (A3) and APC gating (A4). (B) HKLs with FITC gating (B3) and APC gating (B4). (C) Thymocytes with FITC gating (C3) and APC gating (C4). (D) PBLs with FITC gating (D3) and APC gating (D4).

Following the establishment of the staining protocol, additional cell populations were tested. Representative scatter plots and gating strategies for each population is shown in figure 11. Figure 12 shows the results from, SPLs, HKLs and PBLs. As illustrated in figure 12A, using the probe targeting EF1α, 17.2% of SPLs stained positive with the probe. Additionally, 20% of SPLs were positive for IgM, while only 1,3% TRD positive cells were identified. For the TRG probe 11,8% of the SPLs were APC positive indicating that these cells express TRG mRNA.

Comparably in HKLs (figure 12B), 55,8% of the cells stained positive for EF1α, 28,7% for IgM, and 1,29% for TRD. Similar to SPLs, 11,8 % of HKLs stained positive for TRG. Subsequently, both PBLs and thymocytes were analyzed alongside spleen and head kidney. For thymus, the cells did not survive the staining protocol (figure 11 C shows the scatter profiles), while for PBLs (figure 12C), 18,4% were positive for EF1α, 17,6% for IgM, and 7,02% for TRD. The expression of TRG positive PBLs were 14,8%.

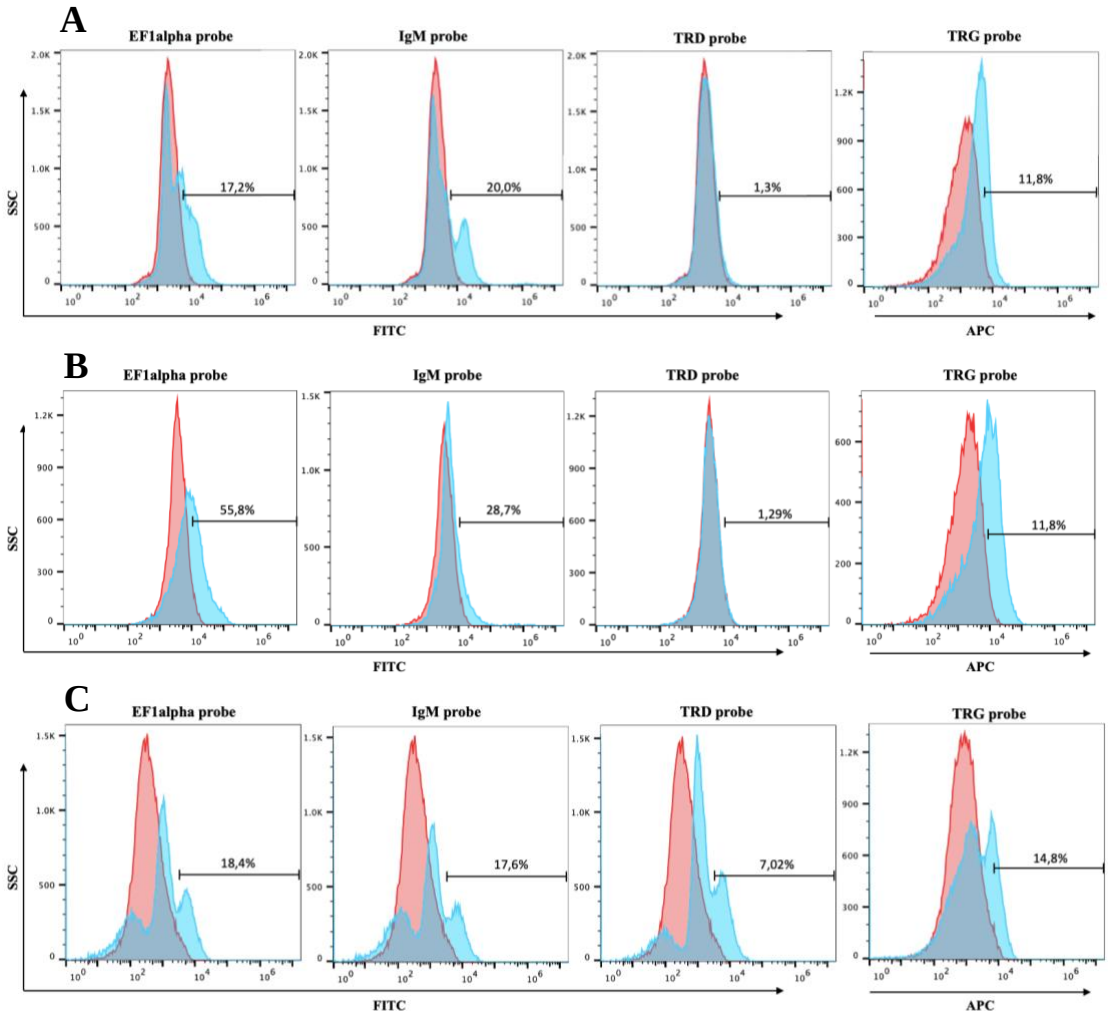

Figure 12: Flow cytometry analysis of SPLs, HKLs, and PBLS. Figure A shows the histogram for leukocytes from Gate 1 for (figure 11 A2,B2,C,D2). The red curve is the negative control, and the blue curve represent the leukocytes that have been stained with the respective probe. The black line is the range for FITC- and APC (for the TRG probes) positive leukocytes, and the percentage of stained leukocytes is shown over. **12A** shows the SPLs, **12B** the HKLs, and **12C** the PBLs.

Figure 13 shows the scatter plots of FITC and APC positive stained populations, and for SPLs (A) the IgM positive population are similar to the EF1α positive population in terms of scatter profiles. In spleen the populations stained positive for both Ef1a and IgM are predominantly small non-complex cells. A similar scatter profile was seen with the TRG probe. However, while there was no staining observed with the TRD probe for either SPLs or HKLs (B), staining was observed in PBLs. In HKLs, the IgM positive stained cells are small and less complex, while the TRG positive stained cells appeared slightly bigger and complex. Additionally, in PBLs (C), there was also clear positive stained population for the EF1α- and IgM probe. A large population of IgM-, EF1α-, and TRD positive stained cells was smaller and less complex, compared to TRG positive cells.

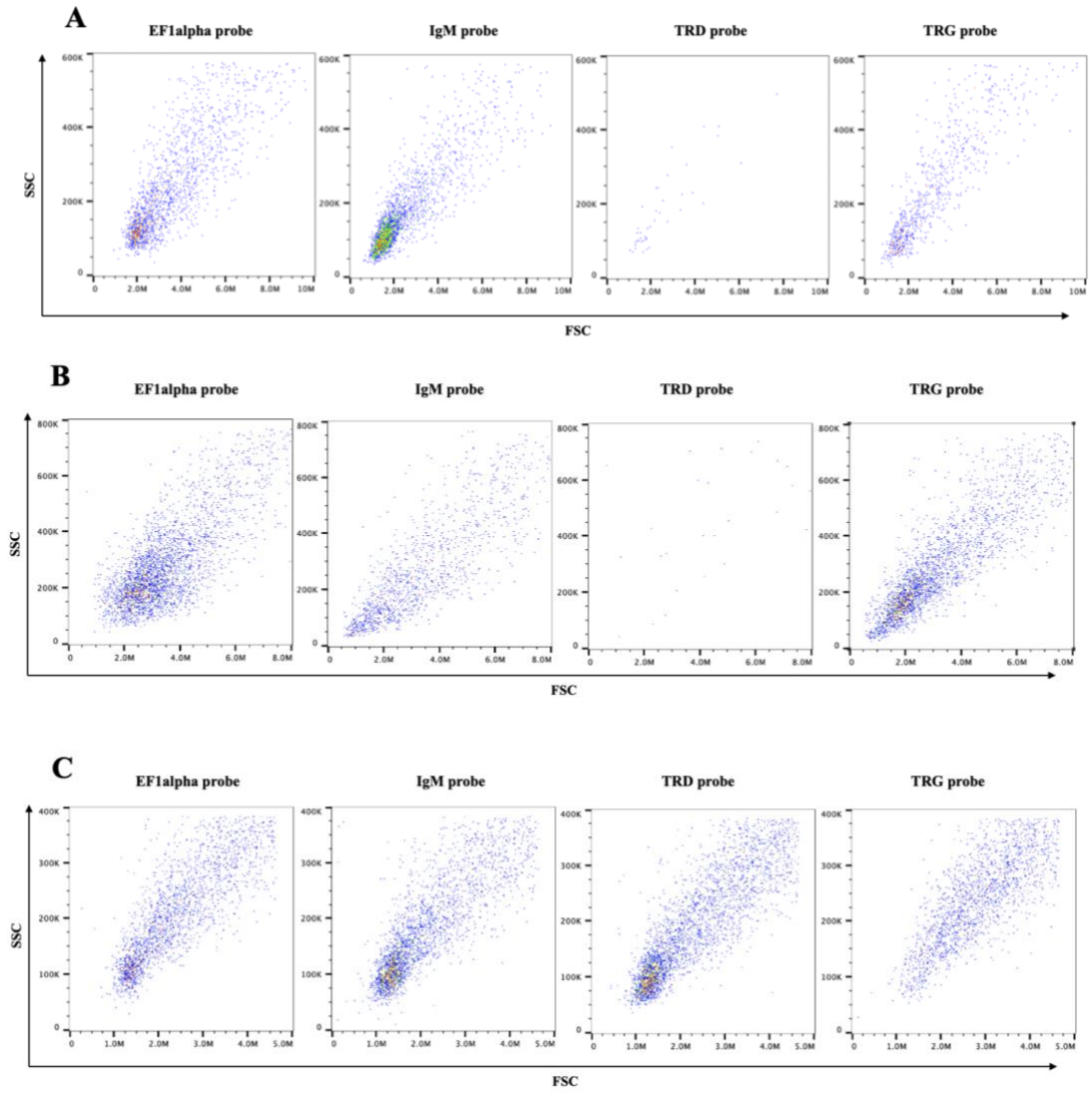

Figure 13: Pseudocolor plot for FITC- and APC-stained leukocytes. EF1α-, IgM- and TRD probes is stained with FITC, and the TRG- probe is stained with APC. **A** exhibit stained SPLs, **B** stained HKLs, **C** stained thymocytes, and **D** exhibit stained PBLs.

In total, HKLs from 4 different fish were analyzed (figure 14), resulting in an average of 15.5% IgM positive stained cells, 2% TRD positive stained cells, and 11.8% TRG positive stained cells. For SPLs, the average was observed to be 30.4% IgM, 3% TRD, and 14% TRG. PBLs had an average of 15% IgM, 9% TRD, and 14.5% TRG. Individual variations were observed, with IgM positive stained HKLs ranging from 5% to 28.7%, PBLs ranging from 14% to 17.6%, and SPLs ranging from 20% to 41%. Regarding TRD positive stained cells, in both HKLs and SPLs, the range was from 0% to 5%. However, for PBLs, TRD positive stained cells ranged from 5% to 13%. TRG positive cells in HKLs ranged from 5.27% to 19.2%, in PBLs from 13.7% to 14.08%, and in SPLs from 6.07% to 25.3%. While large variation was observed in percentage of positive staining cells, for all three experimental probes in HKLs and SPLs, less individual variation was observed in PBLs, albeit only two fish were tested from this particular tissue.

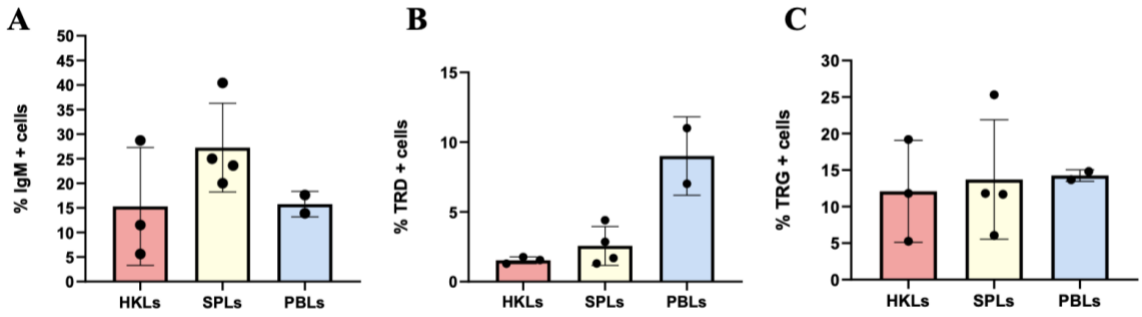

Figure 14: The results from all four rounds of PrimeFlow. Each dot represents the percentage of positive stained leukocytes. A illustrates the leukocytes positive for IgM, B for TRD, and C for TRG.

3.2 Relative expression of different TRGC-genes in Atlantic Salmon tissues

Previous in silico analysis have mapped the TRG locus in Atlantic salmon revealing the existence of seven unique TRGC genes (Herud, 2022). Among these seven TRGC genes, TRGC1, TRGC2_1, TRGC2_2, TRGC3 and TRGC5 have shown to be functionally expressed (Herud, 2022). To gain additional insight into the expression profiles and potential preferential TRGC usage, the relative expression of the TRGC genes in various lymphoid and mucosal tissues of six Atlantic salmon (Salmo salar) was examined by qPCR analysis. The goal was to determine which of the five functionally expressed TRGC genes exhibited the highest

expression levels, distinguishing between relative expression in mucosal and lymphoid tissues, and identifying the tissues with the highest expression. Due to TRGC2_1 and TRGC2_2 being very similar, with a nucleotide sequence identity of 97,6%, a common TRG2 primer was used to amplify both (Herud, 2022). TRGC2 exhibited markedly low expression across all tissues, with some samples displaying expression levels so low that they were undetermined. On the other hand, TRGC1, TRGC3, and TRGC5 commonly demonstrated the highest expression in the thymus (figure 15 F), standing out from other tissues. Moreover, while spleen, head kidney and gill showed high expression levels in TRGC1 and TRGC3, the highest amount of TRGC5 was expressed in middle kidney, pancreas and skin. In spleen, both TRGC1 and TRGC3, was expressed significantly higher than in liver and dorsal fin, and additionally TRGC3 expression was significantly higher in spleen than posterior kidney, intestine, heart and skin. Additionally, expression of TRGC3 and TRGC5 was significantly higher in pancreas than in liver, dorsal fin, heart, skin, and adipose fin. TRD expression was also highest expressed in spleen, head kidney, gill and pancreas, expression of all TRGC genes and TRD was expressed the lowest in muscle, liver, and dorsal fin.

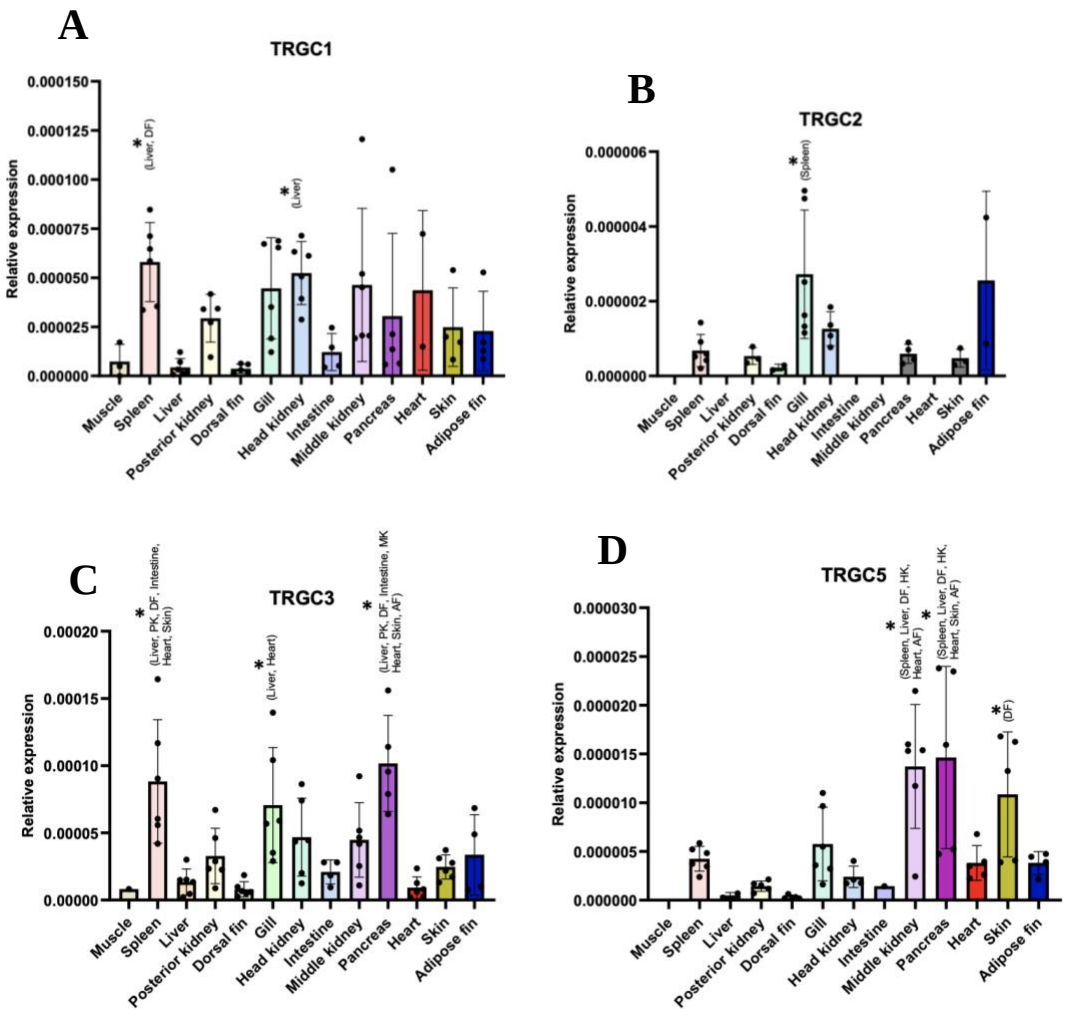

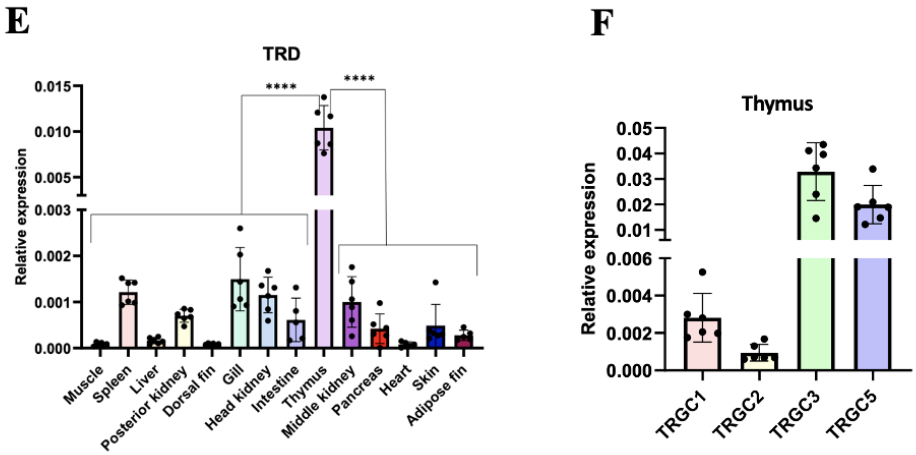

Figure 15: Relative expression levels of TRGC1, TRGC2, TRGC3, TRGC5, and TRD in mucosal and lymphoid tissue from six adult Atlantic salmon (*Salmo salar*). "*" illustrating significance based on one-way ANOVA.

3.3 Differential expression of TRGC genes in primary leukocytes

Next, quantitative polymerase chain reaction (qPCR) assays were used to investigate the functionality and expression levels of distinct TRGC and TRDC genes in freshly isolated leucocytes from spleen, head kidney, and peripheral blood (PBL). These samples were contrasted with cells who had been maintained in culture for up to 72hours. The expression levels were quantified using specific primers targeting each TRGC-region, and the relative expression levels were determined using the ΔCt method, with EF1α. Relative expression levels and standard deviations were calculated for each tissue type and primer set (TRGC1, TRGC2, TRGC3, and TRGC5). Figure 16 presents the basal expression patterns of TRGC1-, TRGC2, TRGC3-, and TRGC5 genes in PBLs, HKLs, and SPLs from six unvaccinated presmolt Atlantic salmons (*Salmo salar)*. The TRGC1 genes was generally expressed higher in SPLs compared to PBLs and HKLs, albeit with large individual variation. The SPLs cultured for 72 hours (Ct values: 30.6 – 36.6) exhibited higher expression compared to the SPLs cultured for 24 hours (Ct values: 33.1 – 38.4), and similar trends were observed for all the four primers. Expression levels of TRGC2 were consistently lower in all three tissues compared to TRGC1, TRGC3 and TRGC5. TRGC3 had the generally highest relative expression levels among all primers, with the highest expression in all three tissues. HKLs cultured for 72 hours (Ct values: 29.2 – 31.8) showed the highest expression levels of TRGC3 genes, and for the TRGC5 primer the SPLs

72h (Ct values: 29.5 – 33.4) showed the highest expression level. Overall SPLs had the highest expression of TRG genes, compared to HKLs and PBLs.

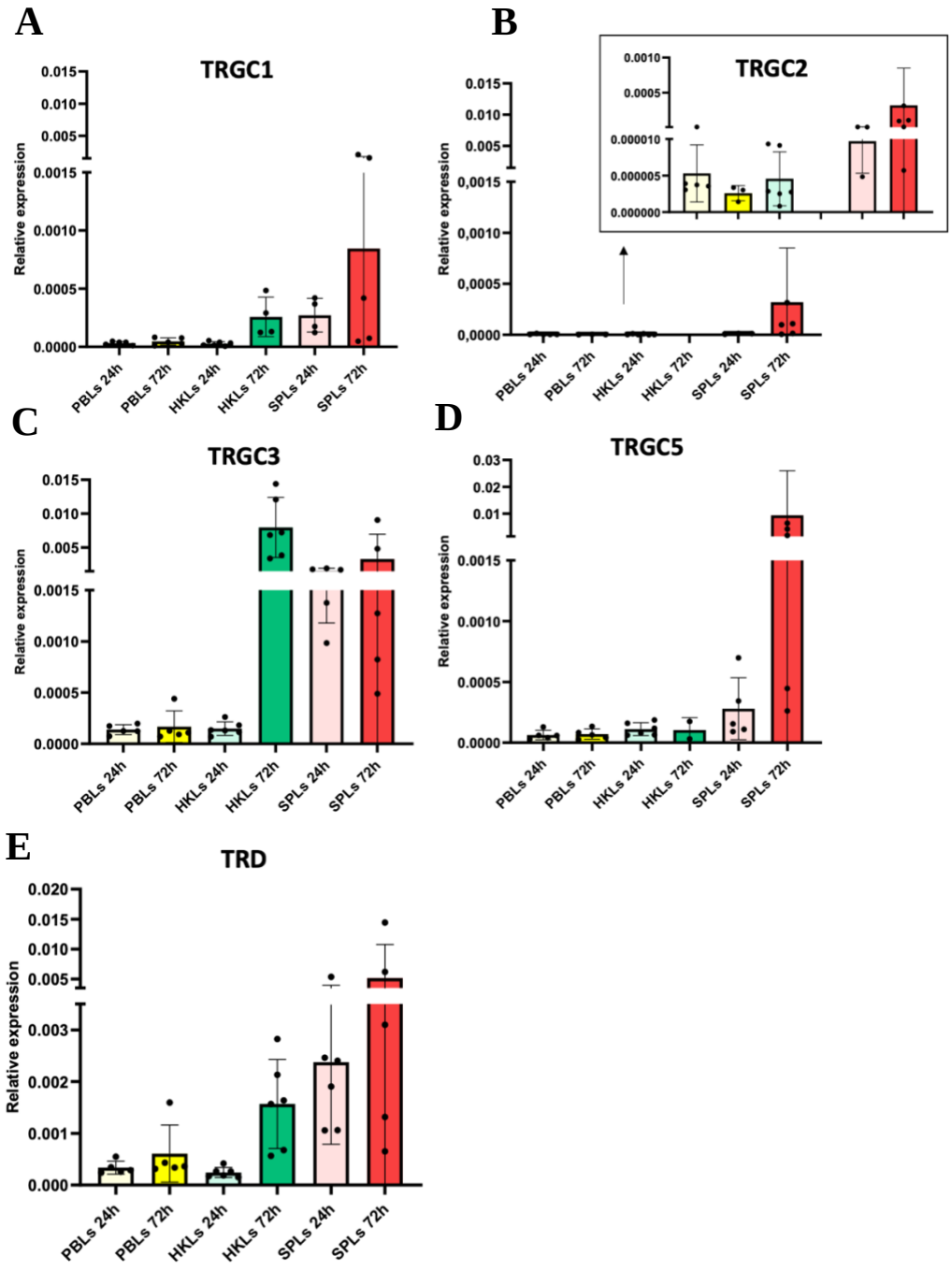

Figure 16: Basal expression of (A) TRGC1, (B) TRGC2, (C) TRGC3, and (D) TRGC5 in SPLs, HKLs and PBLs from six adult Atlanic salmon (*Salmo* salar). Notice that the y-axis scale for TRGC5 differ from the rest.

3.4 qPCR analysis of TRG-genes after stimulation with ConA

Investigating the increased expression of T cells is crucial for understanding immune activation and regulation. Con A is a lectin known for its ability to stimulate T cell proliferation (Nuñez Ortiz et al., 2014). In this study, we employed Con A stimulation on SPLs, HKLs, and PBLs from six unvaccinated presmolt Atlantic salmons at a 24 and 72-hour time point. Through qPCR analysis, we measured the fold change in expression of TRGC1, TRGC2, TRGC3 and TRGC5 to assess potential T cell proliferation and/or activation. This is presented in figure 17, and the bar graph illustrates the fold change relative to basal expression levels. The exact fold change values are presented in table 3 (see appendix).

The analysis of fold change values revealed upregulation for TRGC1 genes across the different leukocytes and time after Con A stimulation. In PBLs, upregulation was observed at both 24 hours and 72 hours post-stimulation, with fish 1, 2, 3, and 4 showing upregulation at 24 hours, and fish 2, 3, and 5 also exhibited upregulation at 72 hours. In SPLs, while no significant upregulation was detected at 24 hours post-stimulation, fish 3 and 5 displayed notable upregulation at 72 hours, with fold change values of 22,04 and 18,04 respectively. Similarly, HKLs showed only slight upregulation in fish 2 and 5 at 24 hours post-stimulation, with no significant upregulation observed at 72 hours post-stimulation across all fish. For the TRGC2 primer, there was a slight upregulation observed in PBLs for all fish except fish 5 at 24 hours post-stimulation, and for fish 3 and 6 at 72 hours, with relatively low fold change values averaging between 1 and 2. Upregulation was also noted in SPLs and HKLs at 24 hours, while HKLs at 72 hours showed undetermined results. Higher upregulation was observed in PBLs for the TRGC3 primer at both 24 hours and 72 hours compared to TRGC2 and TRGC1. In SPLs, the highest fold change was observed in fish 6 at 72 hours (45.7), and at 24 hours (5.8). In HKLs at 24 hours, there was upregulation in fold change for all fish, but none at 72 hours. For the TRGC5 primer, SPLs at 24 hours showed upregulation in fold change for all fish except fish 1 and 6, with only fish 3 and 6 showing upregulation at 72 hours. In PBLs, upregulation was observed for all at both 24 hours and 72 hours, except for fish 5 in both instances. Minimal upregulation was observed in HKLs at both 24 hours and 72 hours.

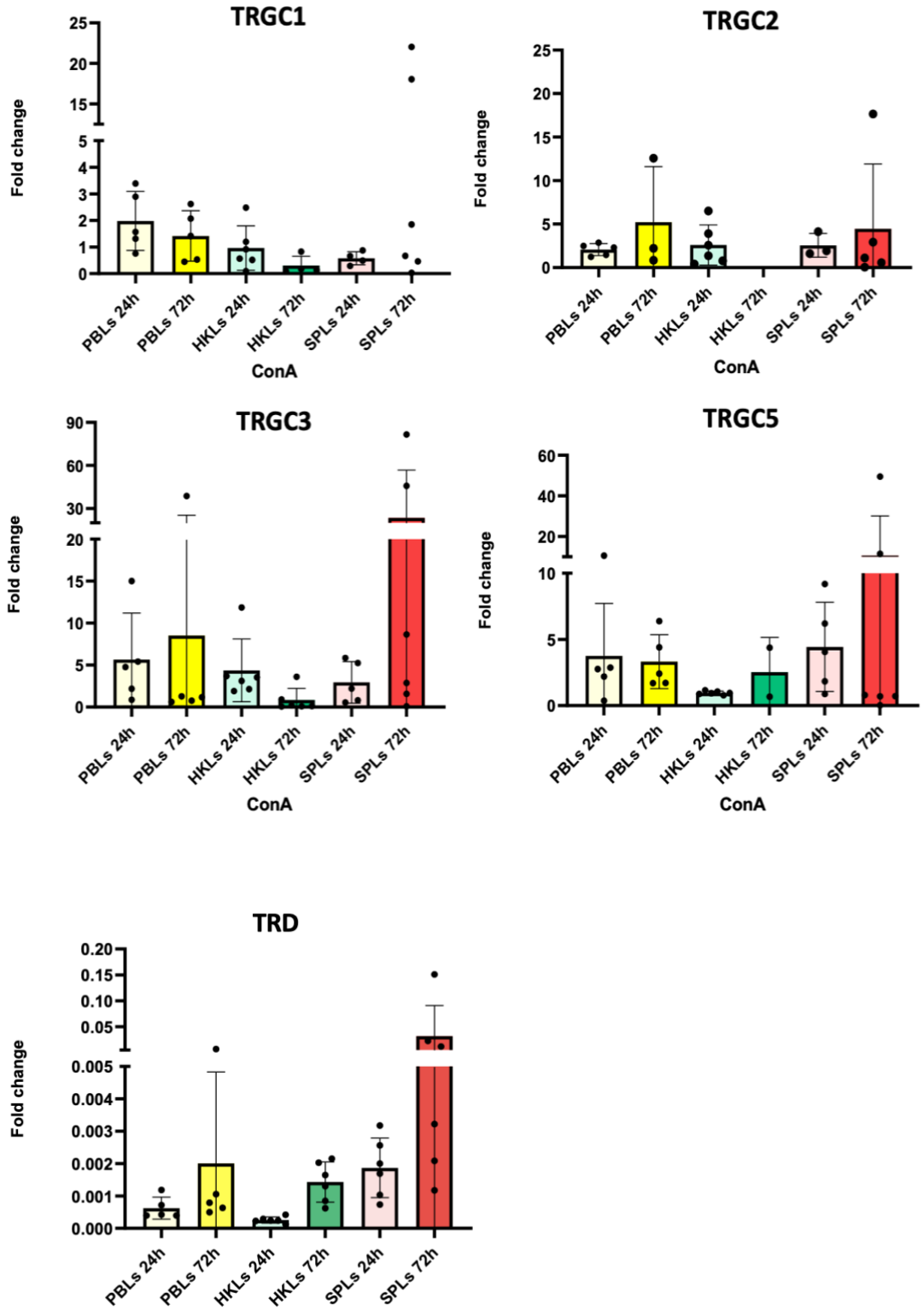

Figure 17: Fold change in (A) TRGC1, (B) TRGC2, (C) TRGC3, and (D) TRGC5 expression in SPLs, HKLs and PBLs after stimulation with Con A. Each bar represents the mean fold change, and error bars indicate the standard deviation.

3.5 RACE

In order to gain comprehensive and unbiased information about the V-J usage for each individual TRGC gene, RACE was employed to obtain more detailed information about the transcript structure. SMARTer RACE was chosen, as this method allows for amplification and sequencing of the full-length transcript.

RACE-ready cDNA was synthesized using RNA extracted from skin (S4, S5, and S6), gills (G4 and G6), and intestine (I4, I5, and I6). Two gene specific primers (GSP1 and GSP2), as well as two degenerate primers (degGSP1 and degGSP2), targeting two overlapping regions in the 3`-end of the constant region, was applied to amplify TRG from RACE ready cDNA. While no amplification was observed following RACE-ready reaction with GSP2 or degenerate GSP2, some amplification was detected with GSP1 (figure 19). A predominant band between 200 and 300 base pairs was observed across all tissues, albeit slightly weaker in gill 6 (G6). Degenerate GSP1 also showed some amplification at 250 base pairs, although clear bands were not observed for any primer. Additionally, smearing and primer dimer formation were noted for all four primers.

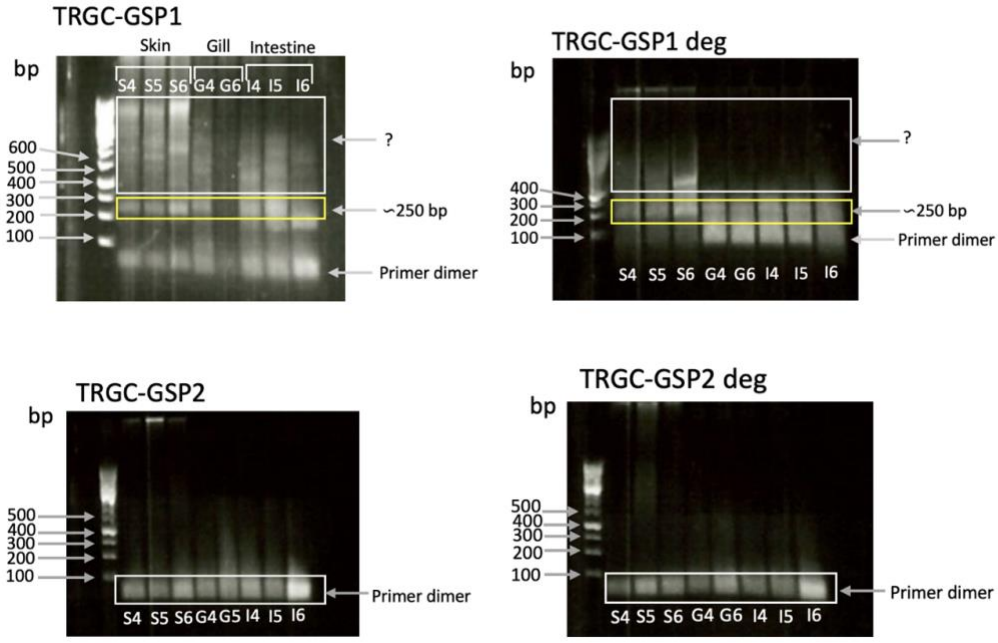

Figure 18: Gel electrophoresis results. A) Results from GSP1 and degGSP1, on RACE ready cDNA from skin (S4-S6), gill (G4, G6), and intestine (I4-I6). Diffuse band observed at 250 base pairs, marked with yellow box. (B)Results from GSP2 and degGSP2, no clear band observed. Observations below 100 base pairs, pointed at with grey arrows, are most likely primer dimer formation.

4 Discussion

γδ T cells in humans exhibit characteristics of both innate and adaptive immune functions, making sure the immune responses are both rapid and with a broad specificity. While numerous transcriptional analyses indicate that bony fish have γδ T cells, functional studies on fish γδ T cells are very limited. In this study, we have combined two molecular methods, PrimeFlow and qPCR, with the aim to study the tissue distribution of γδ-T cells in Atlantic salmon as well as the basal and inducible expression patterns of specific TRD and TRG genes. The results show that various TRG genes are not only differentially expressed in healthy fish but also differentially regulated in response to ConA stimulation in vitro. The PrimeFlow assay, that for the first time was tested on primary Atlantic salmon cells, showed detection of TRGC positive staining cells in head-kidney, spleen and PBLs

4.1 PrimeFlow: Advantages and disadvantages

This study demonstrates that PrimeFlow RNA assays can, in a slightly modified manner be used to detect mRNA in Atlantic salmon primary cells. Flow cytometry is a powerful method for the study of heterogeneous cell populations, and it can detect both cell-surface and intracellular proteins at single cell level. It can also be used to analyze large numbers of cells in a short time, as millions of cells can pass through the analytical checkpoint in less than a minute (Ferchen et al., 2023). However, this method is largely dependent on the availability of known and well characterized antibodies, a tool set which is largely lacking in fish research (Dixon et al., 2018). For research model species like mice, which are the classic model vertebrate organism, the repertoire of known antibodies is much greater than it is for fish. This limited repertoire of antibodies for fish is therefore restricting the use of traditional antibody staining in flow cytometry. In contrast, PrimeFlow offers the advantage of analyzing mRNA expression without the need for specific antibodies (Easthope, 2018; Lai et al., 2018). Cellular heterogeneity is present in most biological sample, which means that the protein level or gene expression will differ from cell to cell. Today, most of our understanding regarding gene expressions in fish is based on bulk population averages. qPCR is a widely used method for quantification of mRNA, due to it being highly sensitive, allows quantification of low-abundance transcripts as well as giving rapid results (Bustin et al., 2006). However, this type of method can mask small and rare sub-populations of cells. The qPCR-based approach also

limits the possibilities to pinpoint essential cell to cell differences. PrimeFlow analyzes millions of cells from specific sub-populations, allowing for the evaluation of transcriptional regulation and protein expression over time (Invitrogen, u.a). For instance, in this study, trough PrimeFlow, we were able to identify a small (1-2%) IgM high-intensity staining sub-population in SPLs. This population would have been indistinguishable using qPCR alone. Unlike qPCR which is restricted to the quantifiable detection of mRNA transcripts an added advantage to Prime flow is that RNA probes can be combined with specific antibodies. Thus, both mRNA and protein levels can be detected in the same cell (Invitrogen, u.a).

Although there are numerous advantages using PrimeFlow, the method also has its limitations. Firstly, a certain level of mRNA expression is required to achieve detection. Previous trials using probes designed to target non-classical MHC class I lineages genes which, based on qPCR analysis have a typical Ct value >27 in unstimulated cells did not show any positive staining cells (personal communication, Eva-Stina Edholm). This contrasts with qPCR, where genes with low expression (Ct-values 38 and 39), can still be detected. Second, enough cells that are robust enough to survive extended experimental manipulations involving fixation, permeabilization and signal amplification are required. Therefore, the type of cells picked for the assay must be evaluated, and the cells must be in excellent physiological condition at the start of the assay. Due to PrimeFlow not being tested on salmonid cells before, the method needed optimization. In the protocol, during fixation and permeabilization, incubation time is suggested to be 30 minutes at room temperature. However, we experienced leukocytes to have a better survival rate when fixed and incubated over night at 4°C. This may be because, in that way the leukocytes are exposed to less stress and they get to permeabilizated under more stable conditions. In the protocol, on day two, there was a total of four hours with incubation at 40°C. While mammalian cell culture are typically incubated at 37°C, due to this being normal body temperature, fish cell culture conditions are optimal between 15-20°C (Fernandez et al., 1993). The incubation temperature can therefore be a factor for fish cells not surviving amplification stages. During the study we tested SPLs, HKLs, PBLs and thymocytes on flow before and after permeabilization, before and after fixation, and before and after probe amplification. The results showed that overall, the cells had shrunk in size and a relatively large degree of mortality was observed. Based on scatter analysis SPLs had the least changes, and the best survival rate through the whole process, and both HKLs and PBLs also showed good results. All though the leukocytes were significantly smaller in size and lower in number after amplification compared

to after permeabilization, it was still possible to analyze the different populations. However, thymocytes did not survive the permeabilization and fixation steps.

Another challenge is that the probe designed for PrimeFlow must target a large portion of the sequence, which makes it difficult to have specific targets. In this study for instance, due to the high nucleotide similarity among the different Sasa-TRG constant region, probes specific for TRGC1, TRGC2, TRGC3 and TRGC 5 could not be designed. This is why there had to be a composite TRG probe, covering all the C-regions at once. In contrast, for qPCR analysis, we were able to design unique primers specific for each of the different TRGC genes. There was also made a TRD-probe, but this probe showed little to no positive staining. With the exception of PBLs from one fish, there might have been contamination between samples due to it being the only sample showing positive staining with the TRD probe. Compared to the qPCR data, TRD mRNA were detected in both spleen, thymus, peripheral blood and head kidney (Ct values ranging from 28,13- 35,55). The probe design could therefore not be optimal, or the target sequence may have been too short to be able to detect TRD. There is also a possibility that TRD expression is too low to be detected , and that we see TRG because the probe detects all TRG, which means the combined mRNA levels are higher.

4.1.1 Identification of high intense IgM mRNA expressing subpoulations using PrimeFlow

Previous studies, using anti-trout IgM mAb (anti-IgF1) and anti-IgG1-RPE, concluded with ∼23% IgM+ cells in naïve HKLs and SPLs after a flow cytometry analysis. Even though these antibodies originally were designed for trout IgM, the Atlantic salmon IgM molecule share amino acid features with rainbow trout IgM, and the antibodies are therefore cross-reactive with IgM from both species (Jenberie et al., 2020). In this study, flow cytometry analysis from PrimeFlow showed a frequency of 20% IgM+ cells in SPLs, 28,7% in HKLs and 17,6% PBLs from fish number 1. However, from the three next rounds with Primeflow the overall frequency of IgM+ cells ranged from 5-45%, which is both higher and lower than previously reported (Jenberie et al., 2020). Four independent studies with PrimeFlow were conducted using one individual of Atlantic salmon per round. The weight of fish ranged from 1250kg to 1330kg, which indicates a slight difference in size.

In addition, as we used different size fish, they are in different life stages, and all though all four fish were adults kept at seawater, that could have an impact. This might not only impact the IgM positive cells, but the total composition of cells which would impact the percentage. For instance, if a group of fish has the same number of IgM positive cells, but some have markedly more macrophages, the overall percentage of IgM positive cells would go down. In a previous study, the mRNA expression of IgM at different sizes of Atlantic salmon fry was tested, showing no expression at 0,15g size in contrast to an significant increase in 1,5g size for IgM (Gadan et al., 2013). The physiological condition of the fish is affecting the immune system, which might account for the variety in IgM+ mRNA expression. If the fish used in the experiment had some kind of infection or disease, it might be the reason for increased IgM+ B cells in the tissues. It is well known that fish infected with Pisciricettsia salmonis or SAV3, has elevated IgM expression (Jenberie et al., 2020; Van der Wal et al., 2021).

It was also observed a high intensity staining population with IgM+ B cells in SPLs, which were surprising. Due to using PrimeFlow instead of traditional antibody staining, all the measurements made are based upon mRNA. By using antibody staining with anti-IgM, staining of all surface expressed IgM protein will occur, which means there is a chance of detecting cells with an Fc-receptor that has taken up secreted IgM. Observations of these high intense populations are usually cells with Fc-receptors bound to IgM, and therefore not necessarily B-cells. For instance, macrophages bind IgM trough their Fc-receptor (Abbas et al., 2019). In this study, this high intense population stained with IgM+ is most likely B-cells due to only mRNA being stained. Based on these observation, it is possible that this population represents plasma cells, as they are larger than B cells and they secrete a large quantity of antibodies (Wu et al., 2022). Here it is notably that, if antibody staining was used, it is not unusual to observe more populations than expected, and there might be of other reasons. It could be due to multiple cell types expressing the same marker, but it could also result from antibodies binding non-specifically to dead cells. Another reason might be doublets of cells, which is when two or more cells stick together and are measured at the same time during flow cytometry (Nanocellect, 2022). These doublets will often show as a second population at approximately twice the fluorescence intensity, which is consistent with the results in this study.

4.1.2 EF1α expression

EF1α probe was used as a control for all the tissues, due to it being a common reference gene used for Atlantic salmon. EF1α is routinely used as the housekeeping control gene for normalization in qPCR, and this is based on several studies. A study conducted by Ingerslev et al. (2006), the expression level of the housekeeping genes EF1-α, RPS20 and Beta-Actin, were examined in different tissues and leukocytes form Atlantic salmon. This was performed to investigate the transcriptional stability within and between tissues, as well as finding the most suitable reference gene. They concluded with EF1a being the most stably expressed gene both between individuals and the different tissues/leukocytes. In another study, where the stability of six reference genes were examined in eight tissues of Atlantic salmon, to determine the most suitable genes to be used in qPCR, it was also concluded with EF1α being the most suitable (Olsvik et al., 2005).

However, in our PrimeFlow analysis the results showed variable binding intensity of the EF1α probe across cell populations, which indicates that there are populations with a high expression of EF1α, populations with low expression, and cells that do express EF1α mRNAs some cells did not stain above background levels. This is observed for all the tissues with variable grades of staining. One reason for this could be that some of the cells experienced RNA degradation during sample processing, storage or handling, which might have led to a too weak or no signal (Invitrogen, 2022). Another factor could be suboptimal permeabilization, which might lead to the probe not getting fully access to the intracellular targets. EF1α is typically expressed inside the cells, and suboptimal permeabilization can therefor result in reduced signal intensity or specificity (Invitrogen, 2022). As described previously the PrimeFlow protocol is not specifically designed for fish cells, and factors such as suboptimal incubator temperature, insufficient washing, incorrect diluents, or too rough handling might result in poor cell recovery. Due to stained populations, the problem is most likely not the probe design. Based on these results, additional reference gene that targets all cells should be used in addition to EF1α.

Thus, while EF1α is a suitable reference gene for Atlantic salmon in qPCR, however, it does not show the same response in Primeflow.

4.1.3 TRG expressing cells constitute a significant portion of leucocytes in HK, SPL and PBLs

It is challenging to investigate γδ T cells in fish. In this study, TRG -specific probes were utilized for the detection of TRG in SPLs, HKLs, and PBLs. PBLs showed ~14% staining with the TRG probe, which is higher than what is observed in humans (Kalyan & Kabelitz, 2013). As mentioned in the introduction, the γδ T cells in humans makes up 1-10% of all circulating T cells in the blood, and they are most abundant in the epithelia of tissues such as skin, small intestine, and the reproductive tract. In this study, the highest observation of TRG positive cells were observed in spleen, ranging from 6,07% to 25,3%. Compared to the basal expression study, qPCR also revealed a higher relative expression of TRG in SPLs than HKLs and PBLs. For the HKLs, TRG positive cells ranged from 5,27% to 19,2%, which also aligns with the qPCR results, showing a slightly lower relative expression for HKLs than SPLs. In Zebrafish, γδ T cells accounted for 7.7-20.5% of the total lymphocytes in spleen, head kidney, peripheral blood, skin, gill and intestine tissue (Wan et al., 2017). Therefore, our PrimeFlow results corresponds with both our qPCR results, and what that is observed in zebrafish. However, there is large variability in the TRG positive cell percentage among individuals. Even though the fish came from the same fish group, and had approximately the same size, there could be individual variations affecting the result. However, it is also important to note that as this is the first time this approach has been implemented in Atlantic salmon and a total of only four different experiments, with slight variation in each one, have been conducted. Thus, the optimal protocol needs to be repeated on multiple fish before any clear conclusions can be made with regards to the average number of TRG mRNA positive cells in different tissues.

4.2 Basal expression of TRGC genes

Atlantic salmon have 7 different TRGC genes (Herud, 2022; Yazawa et al., 2008), with five genes being functionally expressed (Herud, 2022). In contrast, zebrafish have 8 functional V segments, but only one TRGC gene (Wan et al., 2017). Herud (2022) compared the organization of the TCR loci across the Salmonidae family, revealing variation in TRGV, TRGJ and TRGC genes. Despite this variation, Salmonidae species share having >5 TRGC genes, distinguishing them from human and mice. Although humans and Atlantic salmon have almost the same number of V genes (12 in Atlantic salmon, 12-15 in human), Atlantic salmon have a more

complex organization due to several C genes and cassettes, resulting in greater diversity in corresponding protein structure (Yazawa et al., 2008).

TRGC genes typically consists of an immunoglobulin constant (Ig-C) region, transmembrane, cytoplasmic domain, and a connecting peptide region. However, both TRGC4 and TRGC6 is lacking connecting peptides. In addition, TRGC1 has one extra exon, which results in an extra-long connecting peptide. Due to the connecting peptide regions differing remarkably between the TRGC genes, Yazawa et al. (2008) suggested that this might affect the tridimensional structure of the receptor. In addition, this might lead to different TRGC sequences performing distinct cellular responses during TCR recognition of antigens. Herud (2022) also noted that either TRGC 4 or TRGC6 is functionally expressed, possibly due to their lack of connecting peptides.

In this study, the highest expression of all TRGC genes, across all tissues examined, was exhibited from the thymus. This was expected, due to it being a primary lymphoid organ where both T cell development and selection happens (Chilmonczyk, 1983). All TRGC genes were also expressed in spleen, head kidney, gill, skin, pancreas, and posterior kidney. Additionally, expression of TRGC1, TRGC3 and TRGC5 were observed in liver, heart, adipose- and dorsal fin. Yazawa et al. (2008) revealed that TRGC region mRNAs were mainly expressed in the kidney, skin, gut, gill, spleen, heart, liver and pyloric caeca, which aligns with characteristics observed in this study. Notably, all TRGC genes were expressed relatively high in the gills. γδ T cells in mammals are mainly localized in both epithelial and mucosal tissues, such as the intestine or skin, or in lymphoid organs, such as thymus or spleen (Yazawa et al., 2008). Due to the majority of γδ T cells reported in mammals are found in mucosal tissues, it is not unlikely to find γδ T cells in the gills. Gills are constantly exposed to the surrounding water, which also means continuous exposure to pathogens in the environment. Due to gas exchange in gills, they also have an extensive surface area which also increases the exposure to pathogens. This might be related to the high expression of TRGs in the tissue, but there is not enough research to make a conclusion.

An interesting observation was a markedly low TRGC2 expression across all tissues. As the primers used for TRGC1, TRGC2, TRGC3 and TRGC5 all showed good primer efficiency, ranging from 90-110%, this is most likely not due to variations in primer efficiency. However, it might indicate that TRGC2 is not as important in an immune response as the rest of the TRGC genes. Similar to TRGC1, TRGC3 and TRC5, TRGC2 belongs to a cassette with one J- and

three V-genes (figure 1), as well as a connecting peptide and both a constant- and transmembrane region. Due to the primer amplifying both TRGC2_1 and TRGC2_2, it is difficult to say whether it is TRGC2_1 or TRGC2_2 that is amplified and in which grade. Results from a study conducted by Herud (2022) allign with the TRGC2 observations made in this study. Based on having 97,6% nucleotide identity between TRGC2_1 and TRGC2_2, there might have occurred a genome duplication. Unfortunately, there is still lacking enough markers to determine the exact number of αβ and γδ T-cells in most fish.

The expression of TRGC1, TRGC2, TRGC3, and TRGC5 were also measured in SPLs, HKLs, and PBLs, after stimulation with Con A. Con A binds glycoprotein on the cell surface and induce T cell proliferation (Uen et al., 2013). Thus this approach enables us to elucidate which TRGC regions are predominantly expressed in different tissues in response to Con A stimulation providing indications to the roles of different T cell subtypes. TRGC3 responded the best to Con A, having the highest overall fold change for all tissues. Here it should be noted that, in the genome, the cassette encoding for TRGC3 do not have a TRGV gene connected to the respective cassette. However, we know that TRGC3 is expressed the highest out of all the constants regions, and it is therefore surprising that a "specific" TRGV region is missing. TRGC2_1 and TRGC_2 is located upstream from TRGC3, and due to TRGC2 being notably low expressed, TRGC3 might be using the V-genes connected to these cassettes to rearrange. If this theory is correct, this means that TRGC3 can potentially rearrange with 7 different TRGV-genes, which could explain the high expression of TRGC3 compared to TRGC1, TRGC2, and TRGC5. TRGC5 expression is also upregulated expression after Con A stimulation, and it has three V-genes in the cassette.

Table 2 (Appendix) also reveals that the overall highest fold change expression for all the TRGC in all tissues is observed in Fish 3. Individual variation, as describes earlier, might have affected the fold change as well. Out of all tissues, the highest fold change was observed in SPLs, and more specifically in SPLs after 72hours. There could be several reasons to why the fold change measurements are higher after 72 hours compared to 24 hours, and one explanation could be progressive activation or response. Con A binds to the cell surface, which trigger a cascade of events that eventually might lead to upregulation or proliferation of T cells. This process must go through gene transcription and protein syntheses to fully activate the T cells to proliferate, and this might start at a slower pace and then progressively go faster. A reason for why the highest fold change was observed after 72 hours, might therefor be a delayed activation process that shows a more substantial effect after 72 hours compared to 24 hours. Both V and

J genetic variation, as well as recombination between V and J genes, can affect the antigen recognition variation. Compared to other species such as mice, sheep, and humans, the Atlantic salmon TRGV segments do not appear to have as much genetic variation (Herzig et al., 2006; Yazawa et al., 2008). However, Atlantic salmon can potentially mix and match the V segments in unique ways, even though there are fewer segments. The way they do this is skipping over clusters, and this may be a method for more potential diversity for antigen recognition (Yazawa et al., 2008). This mixing and matching ability is also seen in cows, and it might help recognize a wider variety of pathogens. Unlike humans, who usually have a certain subtype (Vγ9/Vδ2), Atlantic salmon does not appear to show a specific preference for any combinations, however this conclusion is based on analysis of a limited number of cDNA sequences (Yazawa et al., 2008) and more targeted repertoire analysis need to be conducted before any conclusions can be made.

4.3 SMARTer RACE 5`/3`

Next, RACE was employed in an attempt to offer a comprehensive understanding of the TRG transcript diversity. To this end and with the aim to examine the different TRGC genes further and in more detail, deep sequencing of 5-RACE products was planned to show usage, functionality, combination and expression of the different TRG genes. By doing this, the total number of productive reads from each sample could be normalized to find the respective usage of TRGV and TRGJ genes, as well as seeing the TRGV-TRGJ combination across different individuals and tissues. In this way, the relative expression of both functional and nonfunctional sequences for all TRGV/TRGJ combinations, could help indicate whether it was a correlation between gene expression and relative position in the loci similar to what has been done for the TRA gene usage (Edholm et al., 2021). qPCR results showed highest fold increase in spleen with highest expression of TRGC3. As mentioned TRGC3 could possibly rearrange with 7 different V-regions, and by conducting RACE it would have been possible to determine which of TRGV regions that actually rearranged with TRGC3 and which was functional. Accordingly, four TRG reverse primers were designed. However, as both GSP1 and GSP2 resulted in a RACE cDNA product that was smeared (i.e the samples appeared as a diffuse band or just a continuous streak across the gel, instead of a distinct band). According to the SMARTer RACE 5´/3´ Kit User Manual, in most cases of smearing, the problem has occurred prior to the RACE reaction, and it might indicate contamination of the starting RNA. Often, degraded RNA or

poorly synthesized cDNA can result in smearing. To troubleshoot, the template quality was tested by using both old RACE ready cDNA (which have worked before), and new RACE ready cDNA from freshly isolated RNA. The result obtained from both the new and the old RACE ready cDNA was smeared, and this indicates that the problem is most likely not the quality of the cDNA template.

Using GSP1 we could see a weak band at 250 base pairs, however, the band was weak, and shorter than what would be expected for a full length rearranged TRG chain. In cases of insufficient target RNA, is that the primers can start interacting with each other. Additionally, primer dimer formation occurred for both GSP1 and GSP2, which is an unintended by-product that can occur during PCR. These primer dimers are short fragments of DNA, that are the result of the primers binding to each other instead of the target DNA. The problem with this is that they might start competing with the target RNA for resources such as DNA polymerase enzyme and nucleotides, which can result in hindering detection and quantification. As mentioned, the GSPs were supposed to target all C regions, and due to nucleotide variability, it was impossible to get a 100% specific primer. All though degenerate primers for both GSP1 and GSP2 were designed, similar results were observed. Poorly designed GSPs can cause several issues in PCR, such as non-specific amplification, formation of primer dimers and failed amplification of the target sequence. For further studies, the primer design will therefore need optimization.

5 Conclusion

In conclusion, this study demonstrates that an RNA-probe based detection method using PrimeFlow, a method previously not tested on salmonid cells, can be used to study and (based on variations in mRNA expression levels) distinguish among sub populations of Atlantic salmon immune leukocytes. PrimeFlow analysis must be conducted on multiple individuals, and the TRD probe design needs to be optimized before any main conclusion regarding the distribution of T cells in Atlantic salmon can be drawn. However, the results indicate that, based on TRG mRNA detection, γδ T cells are found in spleen, head-kindey and peripheral blood of healthy uninfected adult Atlantic salmon. The Prime Flow results showed highest expression of TRG- and IgM positive leukocytes in spleen, with notably 6,07- 25,03% APC (TRG) positive SPLs and 5-45% FITC (IgM) positive SPLs. It was also conducted expression studies, which is the first insight into differential usage of TRG genes. The basal expression TRG expression levels in spleen, head kidney, and peripheral blood substantiate the PrimeFlow results. Moreover, differential expression patterns of the different TRGC genes indicate that there is a specialization across different TRGC genes indicative of multiple subpopulations. Furthermore, the fold change of TRGC1, TRGC2, TRGC3, and TRGC5 in SPLs, HKLs and PBLs after 24- and 72 hours, measured in comparison to negative control samples, revealed highest upregulation in TRGC3. However, to fully understand the function, usage, and expression of the different TRGC genes in Atlantic Salmon, deep sequencing and repertoire analysis needs to be done. Collectively the findings of this study have laid the groundwork for obtaining a deeper understanding of the roles of γδT cells in Atlantic salmon, which will contribute to a deeper understanding of cell mediated immunity and thus the development of more effective virus vaccines for Atlantic salmon.

5.1 Future directions

For future experiments, the results from the PrimeFlow RNA assay should be verified on multiple individuals. In this study, the method was only conducted on four, >1kg, adult Atlantic salmon, and in only four tissues. For future studies, cells isolated from different tissues (i.e gill, intestine, skin) from Atlantic salmon, and fish at different life stages should also be tested. This will hopefully give more insight to the actual distribution of γδ T cells, and the percentage in each tissue. It can also provide information about how the amount of γδ T cells in Atlantic salmon changes through their life cycle. In the TRGC gene expression

study, SPLs, HKLs and PBLs were stimulated with the T cell mitogen Con A, which showed upregulation of some of the TRGC genes in the tissues. An idea could therefore be to conduct PrimeFlow on already stimulated cells, and then see if there is an increase in the number of TRG positive stained cells. While promising results were seen with the TRG probe, the TRD probe design needs optimization. Additionally, different combinations of probes could be conducted to see if the cells are double-positive. The distribution of conventional αβ T cells could also be tested with PrimeFlow, by designing probes for staining of TRA and TRB positive cells. If the results are promising using both TRG/TRD and TRA/TRB probes, an infection study with SAV3 would yield valuable insight into the distribution of T cells and provide information about if there is an upregulation/proliferation of T cells after being challenged with pathogens. Due to the EF1α not staining all populations, another reference gene (including EF1α) should also be tested. In addition, a live/dead staining and a doublet analysis should be conducted as part of the experimental setup. For the last future direction, due to RACE not being successful in this study, deep sequencing and repertoire analysis still remains to be undertaken. Therefore, the gene specific primer designs, as well as the procedure steps, should be optimized including optimization of incubation and annealing temperature during the amplification step should also be tested.

6 References

Abbas, A. K., Lichtman, A. H., & Pillai, S. (2019). *Basic immunology : functions and disorders of the immune system* (Sixth edition. ed.). Elsevier.

Ando, Y., Yasuoka, C., Mishima, T., Ikematsu, T., Uede, T., Matsunaga, T., & Inobe, M. (2014). Concanavalin A-mediated T cell proliferation is regulated by herpes virus entry mediator costimulatory molecule. *50*(4), 313-320. https://doi.org/10.1007/s11626-013-9705-2

Antonacci, R., Massari, S., Linguiti, G., Caputi Jambrenghi, A., Giannico, F., Lefranc, M.-P., & Ciccarese, S. (2020). Evolution of the T-Cell Receptor (TR) Loci in the Adaptive Immune Response: The Tale of the TRG Locus in Mammals. *Genes (Basel)*, *11*(6), 624. https://doi.org/10.3390/genes11060624

Barange, M., Bahri, T., Beveridge, M. C. M., Cochrane, K. L., Funge-Smith, S., & Poulain, F. (2018). Impacts of climate change
on fisheries and aquaculture. https://www.fao.org/3/i9705en/i9705en.pdf

Barraza, F., Montero, R., Wong-Benito, V., Valenzuela, H., Godoy-Guzmán, C., Guzmán, F., Köllner, B., Wang, T., Secombes, C. J., Maisey, K., & Imarai, M. (2020). Revisiting the Teleost Thymus: Current Knowledge and Future Perspectives. *10*(1), 8. https://doi.org/10.3390/biology10010008

Bela-ong, D. B., Thompson, K. D., Kim, H. J., Park, S. B., & Jung, T. S. (2023). CD4+ T lymphocyte responses to viruses and virus-relevant stimuli in teleost fish. *Fish & shellfish immunology*, *142*, 109007-109007. https://doi.org/10.1016/j.fsi.2023.109007

Berg, A., Bergh, Ø., Fjelldal, P. G., Hansen, T., Juell, J.-E., & Nerland, A. H. (2006). *Dyrevelferdsmessige konsekvenser av vaksinasjon av fisk - effekter og bivirkninger* (Fisken og havet, Issue. https://www.hi.no/resources/publikasjoner/fisken-og-havet/74729/nr.9_2006_dyrevelferdsmessige_konsekvenser_vaksinasjon_av_fisk_effekter_og_bivirkninger.pdf

Bernard, D., Six, A., Rigottier-Gois, L., Messiaen, S., Chilmonczyk, S., Quillet, E., Boudinot, P., & Benmansour, A. (2006). Phenotypic and Functional Similarity of Gut Intraepithelial and Systemic T Cells in a Teleost Fish. *Journal of Immunology*, *176*(7), 3942-3949. https://doi.org/10.4049/jimmunol.176.7.3942

Bjørgen, H., & Koppang, E. O. (2021). Anatomy of teleost fish immune structures and organs. *Immunogenetics*, *73*(1), 53-63. https://doi.org/10.1007/s00251-020-01196-0

Bjørgen, H., Løken, O. M., Aas, I. B., Fjelldal, P. G., Hansen, T., Austbø, L., & Koppang, E. O. (2019). Visualization of CCL19-like transcripts in the ILT, thymus and head kidney of Atlantic salmon (Salmo salar L.). *Fish Shellfish Immunol*, *93*, 763-765. https://doi.org/10.1016/j.fsi.2019.08.044

Bonilla, F., & Oettgen, H. (2010). Adaptive immunity. *J Allergy Clin Immunol*, *125*(2), 33-40. https://doi.org/10.1016/j.jaci.2009.09.017

Bonneville, M., O'Brien, R. L., & Born, W. K. (2010). Gammadelta T cell effector functions: a blend of innate programming and acquired plasticity. *Nature Reviews Immunology*, *10*(7), 467-478. https://doi.org/10.1038/nri2781

Bortoletti, M., Fonsatti, E., Leva, F., Maccatrozzo, L., Ballarin, C., Radaelli, G., Caberlotto, S., & Bertotto, D. (2023). Influence of Transportation on Stress Response and Cellular Oxidative Stress Markers in Juvenile Meagre (Argyrosomus regius). *13*(20), 3288. https://doi.org/10.3390/ani13203288

Boudinot, P., Boubekeur, S., & Benmansour, A. (2001). Rhabdovirus Infection Induces Public and Private T Cell Responses in Teleost Fish. *Journal of Immunology*, *167*(11), 6202-6209. https://doi.org/10.4049/jimmunol.167.11.6202

Bustin, S. A., Nolan, T., & Hands, R. E. (2006). Quantification of mRNA using real-time RT-PCR. *1*(3), 1559-1582. https://doi.org/10.1038/nprot.2006.236

Cao, J., Xu, H., Yu, Y., & Xu, Z. (2023). Regulatory roles of cytokines in T and B lymphocytes-mediated immunity in teleost fish. *Dev Comp Immunology*, *144*, 104621-104621. https://doi.org/10.1016/j.dci.2022.104621

Cascarano, M., Stavrakidis-Zachou, O., Mladineo, I., Thompson, K., Papandroulakis, N., & Katharios, P. (2021). Mediterranean Aquaculture in a Changing Climate: Temperature Effects on Pathogens and Diseases of Three Farmed Fish Species. *Pathogens*. https://doi.org/10.3390/pathogens10091205

Castro, R., Bernard, D., Lefranc, M. P., Six, A., Benmansour, A., & Boudinot, P. (2011). T cell diversity and TcR repertoires in teleost fish. *Fish Shellfish Immunol*, *31*(5), 644-654. https://doi.org/10.1016/j.fsi.2010.08.016

Cesta, M. F. (2006). Normal Structure, Function, and Histology of the Spleen. *Toxicol Pathology*, *34*(5), 455-465. https://doi.org/10.1080/01926230600867743

Chien, Y.-h., & Konigshofer, Y. (2007). Antigen recognition by γδ T cells. *Immunological reviews*, *215*(1), 46-58. https://doi.org/10.1111/j.1600-065X.2006.00470.x

Chilmonczyk, S. (1983). The thymus of the rainbow trout ([formula omitted]) light and electron microscopic study. *Dev Comp Immunol*, *7*(1), 59-68. https://doi.org/10.1016/0145-305X(83)90055-1

Ciccarese, S., Lanave, C., & Saccone, C. (1997). Evolution of T-cell receptor gamma and delta constant region and other T-cell-related proteins in the human-rodent-artiodactyl triplet. *Genetics*, *145*(2), 409-419. https://doi.org/10.1093/genetics/145.2.409

Clark, R. A. (2010). Skin-Resident T Cells: The Ups and Downs of On Site Immunity. *J Invest Dermatol*, *130*(2), 362-370. https://doi.org/10.1038/jid.2009.247

Conte, F. S. (2004). Stress and the welfare of cultured fish. *86*(3-4), 205-223. https://doi.org/https://doi.org/10.1016/j.applanim.2004.02.003

Cram, L. S. (2002). Flow cytometry, an overview: Advanced flow cytometry: Applications in Biomedical Research. *Methods in cell science*, *24*(1-3), 1-9.

Dadar, M., Dhama, K., Vakharia, V. N., Hoseinifar, S. H., Karthik, K., Tiwari, R., Khandia, R., Munjal, A., Salgado-Miranda, C., & Joshi, S. K. (2017). Advances in Aquaculture Vaccines Against Fish Pathogens: Global Status and Current Trends. *25*(3), 184-217. https://doi.org/https://doi.org/10.1080/23308249.2016.1261277

Dalum, A. S., Griffiths, D. J., Valen, E. C., Amthor, K. S., Austbø, L., Koppang, E. O., Press, C. M., & Kvellestad, A. (2016). Morphological and functional development of the interbranchial lymphoid tissue (ILT) in Atlantic salmon (Salmo salar L). *Fish Shellfish Immunol*, *58*, 153-164. https://doi.org/10.1016/j.fsi.2016.09.013

Díaz-Rosales, P., Bird, S., Wang, T. H., Fujiki, K., Davidson, W. S., Zou, J., & Secombes, C. J. (2009). Rainbow trout interleukin-2: Cloning, expression and bioactivity analysis. *Fish Shellfish Immunol*, *27*(3), 414-422. https://doi.org/10.1016/j.fsi.2009.06.008

Directorate-General for Maritime Affairs and Fisheries. (2021). *Overview of EU aquaculture (fish farming)*. Publication office of the European Union.

Dixon, B., Barreda, D. R., & Sunyer, J. O. (2018). Perspective on the Development and Validation of Ab Reagents to Fish Immune Proteins for the Correct Assessment of Immune Function. *Front Immunol*, *9*, 2957-2957. https://doi.org/10.3389/fimmu.2018.02957

Duchenne-Moutien, R. A., & Neetoo, H. (2021). Climate Change and Emerging Food Safety Issues: A Review. *84*(11), 1884-1897. https://doi.org/https://doi.org/10.4315/JFP-21-141

Easthope, E. (2018, 25 July, 2018). *Cutting-Edge Flow Cytometry Assays*. https://www.biocompare.com/Editorial-Articles/351905-Leading-Edge-Flow-Cytometry-Assays/

Edholm, E.-S., Fenton, C. G., Mondot, S., Paulssen, R. H., Lefranc, M.-P., Boudinot, P., & Magadan, S. (2021). Profiling the T Cell Receptor Alpha/Delta Locus in Salmonids. *Front Immunol*, *12*, 753960-753960. https://doi.org/10.3389/fimmu.2021.753960

Esteban, M. Á., Cuesta, A., Chaves-Pozo, E., & Meseguer, J. (2013). Influence of melatonin on the immune system of fish: a review. *14*(4), 7979-7999. https://doi.org/10.3390/ijms14047979

FAO. (2023). *GLOBEFISH Highlights – International markets for fisheries and aquaculture products*. FAO. Retrieved September, 2022 from

Fehling, H. J., Krotkova, A., Saint-Ruf, C., & von Boehmer, H. (1995). Crucial role of the pre-T-cell receptor α gene in development of ap but not γδ T cells. *Nature (London)*, *375*(6534), 795-798. https://doi.org/10.1038/375795a0

Ferchen, K., Salomonis, N., & Grimes, H. L. (2023). pyInfinityFlow: optimized imputation and analysis of high-dimensional flow cytometry data for millions of cells. *Bioinformatics*, *39*(5). https://doi.org/10.1093/bioinformatics/btad287

Fernandez, R. D., Yoshimizu, M., Ezura, Y., & Kimura, T. (1993). Comparative Growth Response of Fish Cell Lines in Different Media, Temperatures, and Sodium Chloride Concentrations. *Fish Pathology*, *28*(1), 27-34. https://doi.org/10.3147/jsfp.28.27

Flajnik, M. F. (2018). A cold-blooded view of adaptive immunity. *Nat Rev Immunol*, *18*(7), 438-453. https://doi.org/10.1038/s41577-018-0003-9

Gadan, K., Sandtrø, A., Marjara, I. S., Santi, N., Munang'andu, H. M., & Evensen, Ø. (2013). Stress-induced reversion to virulence of infectious pancreatic necrosis virus in naïve fry of Atlantic salmon (Salmo salar L.). *8*(2), 54656-54656. https://doi.org/10.1371/journal.pone.0054656

Ganusov, V. V., & De Boer, R. J. (2007). Do most lymphocytes in humans really reside in the gut? *Trends in immunology*, *28*(12), 514-518. https://doi.org/10.1016/j.it.2007.08.009

Gentry, R. R., Lester, S. E., Kappel, C. V., White, C., Bell, T. W., Stevens, J., & Gaines, S. D. (2017). Offshore aquaculture: Spatial planning principles for sustainable development. *7*(2), 733-743. https://doi.org/10.1002/ece3.2637

Gudding, R., & Goodrich, T. (2014). The History of Fish Vaccination. *Fish Vaccination*, *1*. https://doi.org/https://doi.org/10.1002/9781118806913.ch1

Hansen, J. D., & Strassburger, P. (2000). Description of an ectothermic TCR coreceptor, CD8 alpha, in rainbow trout. *Journal of Immunology*, *164*(6), 3132-3139. https://doi.org/10.4049/jimmunol.164.6.3132

Haugarvoll, E., Bjerkås, I., Nowak, B. F., Hordvik, I., & Koppang, E. O. (2008). Identification and characterization of a novel intraepithelial lymphoid tissue in the gills of Atlantic salmon. *Journal Anatomy*, *213*(2), 202-209. https://doi.org/10.1111/j.1469-7580.2008.00943.x

Hayday, A. C. (2009). Gammadelta T cells and the lymphoid stress-surveillance response. *Immunity*, *31*(2), 184-196. https://doi.org/10.1016/j.immuni.2009.08.006

Heath, W. R. (1998). T Lymphocytes. *Encyclopedia of Immunology*, 2341-2343. https://doi.org/10.1006/rwei.1999.0588

Herud, M. J. (2022). *?? T-celler i atlantisk laks: Innsyn i ?? T-cellers roller i antivirale responser mot Piscine Orthoreovirus (PRV) oppnådd gjennom genomiske og molekylære analy* Universitetet i Tromsø]. Tromsø.

Herzig, C., Blumerman, S., Lefranc, M.-P., & Baldwin, C. (2006). Bovine T cell receptor gamma variable and constant genes: combinatorial usage by circulating γδ T cells.

Immunogenetics (New York), *58*(2-3), 138-151. https://doi.org/10.1007/s00251-006-0097-2

Hordvik, I., Torvund, J., Moore, L., & Endresen, C. (2004). Structure and organization of the T cell receptor alpha chain genes in Atlantic salmon. *Mol Immunol*, *41*(5), 553-559. https://doi.org/10.1016/j.molimm.2004.03.006

Ingerslev, H.-C., Pettersen, E. F., Jakobsen, R. A., Petersen, C. B., & Wergeland, H. I. (2006). Expression profiling and validation of reference gene candidates in immune relevant tissues and cells from Atlantic salmon (Salmo salar L.). *43*(8), 1194-1201. https://doi.org/10.1016/j.molimm.2005.07.009

Invitrogen. (2022). PrimeFlow RNA Assay Kit In T. F. Scientific (Ed.).

Invitrogen. (u.a). *PrimeFlow RNA Assay*. ThermoFisher Scientific. https://assets.thermofisher.com/TFS-Assets/BID/brochures/primeflow-rna-assays-brochure.pdf

Janeway, C. A., & Medzhitov, R. (2002). INNATE IMMUNE RECOGNITION. *Annu Rev Immunol*, *20*(1), 197-216. https://doi.org/10.1146/annurev.immunol.20.083001.084359

Janeway, C. A., Murphy, K., Mowat, A., & Weaver, C. T. (2001). *T-cell receptor gene rearrangement* (5th ed., Vol. Immunobiology: The Immune System in Health and Disease). Garland Science.

Jenberie, S., Peñaranda, M. M. D., Thim, H. L., Styrvold, M. B., Strandskog, G., Jørgensen, J. B., & Jensen, I. (2020). Salmonid Alphavirus Subtype 3 Induces Prolonged Local B Cell Responses in Atlantic Salmon (Salmo salar) After Intraperitoneal Infection. *11*, 1682-1682. https://doi.org/10.3389/fimmu.2020.01682

Johnsen, P. F. F., Rognsås, L. L., Erraia, J., Grønvik, O., Fjose, S., Blomgren, A., Fjelldal, Ø., Robertsen, R., Iversen, A., & Nyrud, T. (2022). *RINGVIRKNINGER AV SJØMATNÆRINGEN I 2021*. https://www.menon.no/the-economic-impact-of-the-norwegian-seafood-industry/?lang=en

Joshi, C. J., Ke, W., Drangowska-Way, A., O'Rourke, E. J., & Lewis, N. E. (2022). What are housekeeping genes? *PLoS computational biology*, *18*(7), e1010295-e1010295. https://doi.org/10.1371/journal.pcbi.1010295

Kalyan, S., & Kabelitz, D. (2013). Defining the nature of human γδ T cells: a biographical sketch of the highly empathetic. *10*(1), 21-29. https://doi.org/10.1038/cmi.2012.44

Khan, M., Khan, S., & K., M. (2011). Aquaculture as a food production system: A review. *Biology and Medicine*, *3*(291-302).

Klein, L., Kyewski, B., Allen, P. M., & Hogquist, K. A. (2014). Positive and negative selection of the T cell repertoire: what thymocytes see (and don't see). *Nature reviews. Immunology*, *14*(6), 377-391. https://doi.org/10.1038/nri3667

Klesius, P. H., & Pridgeon, J. W. (2014). Vaccination against Enteric Septicemia of Catfish. *Fish Vaccination*, *18*. https://doi.org/10.1002/9781118806913

Koppang, E. O., Fischer, U., Moore, L., Tranulis, M. A., Dijkstra, J. M., Köllner, B., Aune, L., Jirillo, E., & Hordvik, I. (2010). Salmonid T cells assemble in the thymus, spleen and in novel interbranchial lymphoid tissue. *J Anat*, *217*(6), 728-739. https://doi.org/10.1111/j.1469-7580.2010.01305.x

Koppang, E. O., Hordvik, I., Bjerkås, I., Torvund, J., Aune, L., Thevarajan, J., & Endresen, C. (2003). Production of rabbit antisera against recombinant MHC class II β chain and identification of immunoreactive cells in Atlantic salmon (Salmo salar). *Fish Shellfish Immunol*, *14*(2), 115-132. https://doi.org/10.1006/fsim.2002.0424

Kozarewa, I., Armisen, J., Gardner, A., Stlatko, B., & Hendrickson, C. L. (2015). Overview of Target Enrichment Strategies. *Curr Protoc Mol Biol*, *112*. https://doi.org/10.1002/0471142727.mb0721s112

Krangel, M. S. (2009). Mechanics of T cell receptor gene rearrangement. *Curr Opin Immunol*, *21*(2), 133-139. https://doi.org/10.1016/j.coi.2009.03.009

Kumar, B. V., Connors, T. J., & Farber, D. L. (2018). Human T Cell Development, Localization, and Function throughout Life. *Immunity*, *48*(2), 202-213. https://doi.org/10.1016/j.immuni.2018.01.007

Kurath, G. (2008). Biotechnology and DNA vaccines for aquatic animals. *27*(0253-1933), 175-196. https://doi.org/10.20506/rst.27.1.1793

Lai, C., Stepniak, D., Sias, L., & Funatake, C. (2018). A sensitive flow cytometric method for multi-parametric analysis of microRNA, messenger RNA and protein in single cells. *134-135*, 136-148. https://doi.org/10.1016/j.ymeth.2017.12.016

Lawand, M., Déchanet-Merville, J., & Dieu-Nosjean, M.-C. (2017). Key Features of Gamma-Delta T-Cell Subsets in Human Diseases and Their Immunotherapeutic Implications. *Front Immunol*, *8*, 761-761. https://doi.org/10.3389/fimmu.2017.00761

Laydon, D. J., Bangham, C. R. M., & Asquith, B. (2015). Estimating T-cell repertoire diversity: limitations of classical estimators and a new approach. *Philos Trans R Soc Lond B Biol Sci*, *370*(1675), 20140291-20140291. https://doi.org/10.1098/rstb.2014.0291

Lefranc, M.-P. (2014). Immunoglobulin and T Cell Receptor Genes: IMGT(®) and the Birth and Rise of Immunoinformatics. *Front Immunol*, *5*, 22-22. https://doi.org/10.3389/fimmu.2014.00022

Legemiddelverket. (2017, 28, June 2017). Legemiddelnytt. *Norsk veterinærtidsskrift*, *6*(03325741), 76. https://nvt.vetnett.no/asset/Utgaver/2017/06/nvt-2017-06.pdf

Lewis, S. M., Williams, A., & Eisenbarth, S. C. (2019). Structure-function of the immune system in the spleen. *Sci Immunol*, *4*. https://doi.org/10.1126/sciimmunol.aau6085

Liang, C., Sheng, X., Tang, X., Xing, J., Chi, H., & Zhan, W. (2022). Structural characteristics and mucosal immune response of the interbranchial lymphoid tissue in the gills of flounder (Paralichthys olivaceus). *Fish Shellfish Immunol*, *123*, 388-398. https://doi.org/10.1016/j.fsi.2022.03.022

Løken, O. M., Bjørgen, H., Hordvik, I., & Koppang, E. O. (2020). A teleost structural analogue to the avian bursa of Fabricius. *Journal of Anatomy*, *236*(5), 798-808. https://doi.org/10.1111/joa.13147

Ma, J., Bruce, T. J., Jones, E. M., & Cain, K. D. (2019). A Review of Fish Vaccine Development Strategies: Conventional Methods and Modern Biotechnological Approaches. *Microorganisms*, *7*(11), 569. https://doi.org/10.3390/microorganisms7110569

Maniar, A., Zhang, X., Lin, W., Gastman, B. R., Pauza, C. D., Strome, S. E., & Chapoval, A. I. (2010). Human γδ T lymphocytes induce robust NK cell–mediated antitumor cytotoxicity through CD137 engagement. *Blood*, *116*(10), 1726-1733. https://doi.org/10.1182/blood-2009-07-234211

Meridian Bioscience. *Random Hexamer Primers*. https://www.bioline.com/random-hexamer-primers.html

Miccoli, A., Manni, M., Picchietti, S., & Scapigliati, G. (2021). State-of-the-Art Vaccine Research for Aquaculture Use: The Case of Three Economically Relevant Fish Species. *Vaccines (Basel)*, *9*(2), 140. https://doi.org/10.3390/vaccines9020140

Munang'andua, H. M., Fredriksenb, B. N., Mutoloki, S., Brudesethc, B., Kuo, T.-Y., Marjaraa, I. S., Dalmo, R. A., & Evensen, Ø. (2012). Comparison of vaccine efficacy for different antigen delivery systems for

infectious pancreatic necrosis virus vaccines in Atlantic salmon (Salmo salar L.) in a cohabitation challenge model. *Vaccine*, *30*, 4007-4016. https://doi.org/http://dx.doi.org/10.1016/j.vaccine.2012.04.039

Murphy, K., Janeway, C. A., Mowat, A., & Weaver, C. T. (2012). *Janeway's immunobiology* (8th ed., Vol. 10-21). Garland Science.

Nanocellect. (2022). *How to Identify and Remove Doublets in Flow Cytometry*. Biomedical, Inc. Retrieved 01. December from https://nanocellect.com/blog/how-to-identify-and-remove-doublets-in-flow-cytometry/

Nardocci, G., Navarro, C., Cortés PP, & Imarai M, M. M., Valenzuela B, Jara P, Acuña-Castillo C, Fernández R. (2014). Neuroendocrine mechanisms for immune system regulation during stress in fish. *Fish Shellfish Immunol*, *531-8*. https://doi.org/10.1016/j.fsi.2014.08.001

Netea, M. G., Schlitzer, A., Placek, K., Joosten, L. A. B., & Schultze, J. L. (2019). Innate and Adaptive Immune Memory: an Evolutionary Continuum in the Host's Response to Pathogens. *Cell Host Microbe*, *25*(1), 13-26. https://doi.org/10.1016/j.chom.2018.12.006

Norwegian seafood council. (2024, 4 January, 2024). *Record exports of Norwegian seafood in 2023 due to price growth and weak krone*. https://en.seafood.no/news-and-media/news-archive/record-exports-of-norwegian-seafood-in-2023-due-to-price-growth-and-weak-krone/

Nuñez Ortiz, N., Gerdol, M., Stocchi, V., Marozzi, C., Randelli, E., Bernini, C., Buonocore, F., Picchietti, S., Papeschi, C., Sood, N., Pallavicini, A., & Scapigliati, G. (2014). T cell transcripts and T cell activities in the gills of the teleost fish sea bass (Dicentrarchus labrax). *47*(2), 309-318. https://doi.org/10.1016/j.dci.2014.07.015

Office of Aquaculture. (2020, 15 September, 2022). *Aquaculture Supports a Sustainable Earth*. NOOA Fisheries.

Olsvik, P. A., Lie, K. K., Jordal, A.-E. O., Nilsen, T. O., & Hordvik, I. (2005). Evaluation of potential reference genes in real-time RT-PCR studies of Atlantic salmon. *BMC Mol Biol*, *6*(1), 21-21. https://doi.org/10.1186/1471-2199-6-21

Parker, M. E., & Ciofani, M. (2020). Regulation of γδ T Cell Effector Diversification in the Thymus. *Front Immunol*, *11*, 42-42. https://doi.org/10.3389/fimmu.2020.00042

Pasquale, A. D., Preiss, S., Da Silva, F. T., & Garçon, N. (2015). Vaccine Adjuvants: from 1920 to 2015 and Beyond. *Vaccines (Basel)*, 320-343. https://doi.org/10.3390/vaccines3020320

Paw, J. N., & Thia-Eng, C. (1991). Climate changes and sea level rise: Implications on coastal area utilization and management in South-east Asia. *Ocean and shoreline management*, *15*(3), 205-232. https://doi.org/10.1016/0951-8312(91)90043-2

Petro, K., Okino, S., Kong, M., & Wang, Y. (2015). Evaluation of Bias Associated with High Multiplex Target-Specific Pre-Amplification. *The FASEB journal*, *29*(S1). https://doi.org/10.1096/fasebj.29.1_supplement.709.3

PHARMAQ. (2020). *ALPHA JECT micro 7 ILA*. Felleskatalogen. https://www.felleskatalogen.no/medisin-vet/alpha-ject-micro-7-ila-pharmaq-663201

Picchietti, S., Guerra, L., Bertoni, F., Randelli, E., Belardinelli, M. C., Buonocore, F., Fausto, A. M., Rombout, J. H., Scapigliati, G., & Abelli, L. (2011). Intestinal T cells of Dicentrarchus labrax (L.): Gene expression and functional studies. *Fish Shellfish Immunol*, *30*(2), 609-617. https://doi.org/10.1016/j.fsi.2010.12.006

Regjeringen. (2009). *Dyrevelferdsloven*. https://www.regjeringen.no/no/dokumenter/dyrevelferdsloven/id571188/

Rodríguez, A., Rodríguez, M., Luque, M. I., Justesen, A. F., & Córdoba, J. J. (2011). Quantification of ochratoxin A-producing molds in food products by SYBR Green and TaqMan real-time PCR methods. *149*(3), 226-235. https://doi.org/10.1016/j.ijfoodmicro.2011.06.019

Rosati, E., Dowds, C. M., Liaskou, E., Henriksen, E. K. K., Karlsen, T. H., & Franke, A. (2017). Overview of methodologies for T-cell receptor repertoire analysis. *BMC Biotechnol*, *17*(1), 61-61. https://doi.org/10.1186/s12896-017-0379-9

Røsaeg, M. V., Thorarinsson, R., & Aunsmo, A. (2021). Effect of vaccines against pancreas disease in farmed Atlantic salmon. *J Fish Dis*, 1911-1924. https://doi.org/10.1111/jfd.13505

Seafish. (2023). *Value and importance of aquaculture*. Retrieved 26, January 2024 from https://www.seafish.org/insight-and-research/aquaculture-data-and-insight/value-and-importance-of-aquaculture/

Secombes, C. (2008). Will advances in fish immunology change vaccination strategies? *Fish Shellfish Immunol*, *25*(4), 409-416. https://doi.org/10.1016/j.fsi.2008.05.001

Sievers, M., Korsøen, Ø., Warren-Myers, F., Oppedal, F., Macaulay, G., Folkedal, O., & Dempster, T. (2021). Submerged cage aquaculture of marine fish: A review of the biological challenges and opportunities. *14*(1), 106-119. https://doi.org/https://doi.org/10.1111/raq.12587

Sigma-Aldrich. (2012). *DNase I*. https://www.sigmaaldrich.com/deepweb/assets/sigmaaldrich/product/documents/708/494/ampd1bul.pdf

Somamoto, T., Nakanishi, T., & Nakao, M. (2013). Identification of anti-viral cytotoxic effector cells in the ginbuna crucian carp,

Carassius auratus langsdorfii. *Developmental and Comparative Immunology*, *39*, 370-377. https://doi.org/http://dx.doi.org/10.1016/j.dci.2012.11.001

Sommerset, I., Wiik-Nielsen, J., Moldal, T., Oliveira, V. H., SVendsen, J. C., Haukaas, A., & Bruun, E. (2024). Fiskehelserapporten 2023. (8a). (12 March, 2024)

Sommerset, I., Wiik-Nielsen, J., Oliveira, V. H. S., Moldal, T., Bornø, G., Haukaas, A., & Brun, E. (2023). *Fiskehelserapporten 2022* (Veterinærinstituttets rapportserie nr. 5a).

Sowder, J. T., Chen, C. L. H., Ager, L. L., Chan, M. M., & Cooper, M. D. (1988). A large subpopulation of avian T cells express a homologue of the mammalian Tγ/δ receptor. *J Exp Med*, *167*(2), 315-322. https://doi.org/10.1084/jem.167.2.315

Tafalla, C., Leal, E., Yamaguchi, T., & Fischer, U. (2016). T cell immunity in the teleost digestive tract. *Dev Comp Immunology*, *64*, 167-177. https://doi.org/10.1016/j.dci.2016.02.019

Takara. (2024). *cDNA amplification kits for 5' and 3' RACE*. Takara Bio Europe. https://www.takarabio.com/products/mrna-and-cdna-synthesis/race-kits/smarter-5-race-and-3-race

Thermo Fisher Scientific. (2024). *Why does the immune repertoire matter?* . https://www.thermofisher.com/no/en/home/life-science/sequencing/sequencing-learning-center/next-generation-sequencing-information/immuno-oncology-research/why-immune-repertoire-matters.html

Tlaxca, J. L., Ellis, S., & Remmele Jr, R. L. (2015). Live attenuated and inactivated viral vaccine formulation and nasal delivery: potential and challenges. *Adv Drug Deliv Rev*, 56-78. https://doi.org/10.1016/j.addr.2014.10.002

Uen, Y.-H., Lin, K.-Y., Sun, D.-P., Liao, C.-C., Hsieh, M.-S., Huang, Y.-K., Chen, Y.-W., Huang, P.-H., Chen, W.-J., Tai, C.-C., Lee, K.-W., Chen, Y.-C., & Lin, C.-Y. (2013). Comparative proteomics, network analysis and post-translational modification identification reveal differential profiles of plasma Con A-bound glycoprotein biomarkers in gastric cancer. *83*, 197-213. https://doi.org/10.1016/j.jprot.2013.03.007

Van der Wal, Y. A., Jenberie, S., Nordli, H., Greiner-Tollersrud, L., Kool, J., Jensen, I., & Jørgensen, J. B. (2021). The importance of the Atlantic salmon peritoneal cavity B cell response: Local IgM secreting cells are predominant upon Piscirickettsia salmonis

infection. *Dev Comp Immunol*, *123*, 104125-104125. https://doi.org/10.1016/j.dci.2021.104125

Vantourout, P., & Hayday, A. (2013). Six-of-the-best: unique contributions of γδ T cells to immunology. *Nature Review Immunology*, *13*(2), 88-100. https://doi.org/10.1038/nri3384

Vinitnantharat, S., Gravningen, K., & Greger, E. (2007). Fish Vaccines. *Advances in Veterinary Medicine*, *41*(1999), 539-550. https://doi.org/10.1016/S0065-3519(99)80040-8

Wan, F., Hu, C.-B., Ma, J.-X., Gao, K., Xiang, L.-X., & Shao, J.-Z. (2017). Characterization of γδ T Cells from Zebrafish Provides Insights into Their Important Role in Adaptive Humoral Immunity. *Front Immunol*, *7*, 675-675. https://doi.org/10.3389/fimmu.2016.00675

World Food Programme. (2024). *Help end world hunger*. https://www.wfp.org/support-us/stories/donate-now?utm_source=google&utm_medium=cpc&utm_campaign=12117193110&utm_content=154247927512&gad_source=1&gclid=Cj0KCQjwlZixBhCoARIsAIC745Auqf8Wt4ew7O7mMB1K_2iCcEPtVR0A6kksWhFnrBG04ddAwKwtgUgaAjPpEALw_wcB&gclsrc=aw.ds

Wu, L., Yang, Y., Gao, A., Li, J., & Ye, J. (2022). Teleost fish IgM+ plasma-like cells possess IgM-secreting, phagocytic, and antigen-presenting capacities. *Frontiers in immunology*, *13*, 1016974-1016974. https://doi.org/10.3389/fimmu.2022.1016974

Yamaguchi, T., Takizawa, F., Furihata, M., Soto-Lampe, V., Dijkstra, J. M., & Fischer, U. (2019). Teleost cytotoxic T cells. *Fish & Shellfish Immunology*, *95*, 422-439. https://doi.org/https://doi.org/10.1016/j.fsi.2019.10.041

Yazawa, R., Cooper, G. A., Beetz-Sargent, M., Robb, A., McKinnel, L., Davidson, W. S., & Koop, B. F. (2008). Functional adaptive diversity of the Atlantic salmon T-cell receptor gamma locus. *Mol Immunol*, *45*(8), 2150-2157. https://doi.org/10.1016/j.molimm.2007.12.007

Aas, I. B., Austbø, L., König, M., Syed, M., Falk, K., Hordvik, I., & Koppang, E. O. (2014). Transcriptional characterization of the T cell population within the salmonid interbranchial lymphoid tissue. *J Immunol*, *193*(7), 3463-3469. https://doi.org/10.4049/jimmunol.1400797

7 Appendix

Table 2: Fold change in PBLs, HKLs, and SPLs after ConA stimulation. Compared to basal expression after 24- and 72 hours.

TRGC1	PBLs 24h	PBLs 72h	HKLs 24h	HKLs 72h	SPLs 24h	SPLs 72h
F1	1,32	0,53	0,92	0,83	0,49	0,92
F2	2,9	2,07	2,48			2,48
F3	1,57	2,62	0,52		0,88	0,52
F4	3,39	0,45	0,57	0,13	0,29	0,57
F5			1,2	0,18		1,2
F6	0,76	1,42	0,09	0,09	0,66	0,09
TRGC2	PBLs 24h	PBLs 72h	HKLs 24h	HKLs 72h	SPLs 24h	SPLs 72h
F1	2,3	0,85	0,78			0,57
F2	1,25		3,91			2,92
F3	2,49	2,22	0,41			17,65
F4	1,46		1,37		1,62	1,11
F5			2,57		4,13	0,06
F6	2,86	12,57	6,51		1,94	95,8
TRGC3	PBLs 24h	PBLs 72h	HKLs 24h	HKLs 72h	SPLs 24h	SPLs 72h
F1	2,2	1,17	11,85	0,92		8,66
F2	5,42	1,28	2,14	3,62	2,2	1,59
F3	4,78	0,76	1,91	0,08	5,85	81,61
F4	15,01	0,61	3,55	0,21	0,82	2,88
F5			3,69	0,09	5,25	0,09
F6	0,86	38,75	3,11	0,13	0,55	45,78
TRGC5	PBLs 24h	PBLs 72h	HKLs 24h	HKLs 72h	SPLs 24h	SPLs 72h
F1	2,76	2,42	0,95	0,68		0,7
F2	2,19	1,71	1,06	4,38	9,2	0,79
F3	2,87	4,4	1,16		6,21	49,54
F4	10,62	1,7	0,87		4,07	0,71
F5			0,94		1,83	0,02
F6	0,37	6,38	0,78		0,88	11,5

Table 3. Kits that were used with producer and catalog number.

Kit	Producer	Catalog number
SMARTer RACE 5'/3' Kit Components	Takara	634860
PrimeFlow™ RNA Assay Kit	Thermo Fisher Scientific	88-18005-210
TaqMan Reverse Transcription Reagents	Termo Fischer Scientific	N8080234
RNeasy Mini Kit	Quiagen	74106

Table 4. Chemicals and reagents that were used with producer and catalog number.

Chemicals and reagents	Producer	Catalog number
50mM EDTA	Thermo Fisher Scientific	
10X RT Buffer	Thermo Fisher Scientific	N8989234
1 kb DNA Ladder	Invitrogen	N10787-018
6X Tritrack Loading Dye	Thermo Scientific	R1161
dNTP mix 10 nM	Thermo Fisher Scientific	N8080234
Ethanol	Sigma-Aldrich	
Fast SYBR Green Master Mix	Applied Biosystems	4385612
$MgCl_2$ solution	Thermo Fisher Scientific	N9090234
Multiscribe Reverse Transcriptase	Thermo Fisher Scientific	4311235
Random Hexamer	Thermo Fisher Scientific	N8080127
RNase Inhibitor	Thermo Fisher Scientific	N8080119
DNase I RNase-free	Thermo Scientific	EN0521
10X reaction buffer with $MgCl_2$	Thermo Scientific	B43
PrimeFlow® RNA Fixation Buffer 1A	Thermo Fisher Scientific	00-18100
PrimeFlow® RNA Fixation Buffer 1B	Thermo Fisher Scientific	00-18200
PrimeFlow® RNA Permeabilization Buffer (10X)	Thermo Fisher Scientific	00-18300
PrimeFlow® RNA Fixation Buffer 2	Thermo Fisher Scientific	00-18400
PrimeFlow® RNA Wash Buffer	Thermo Fisher Scientific	00-19180
PrimeFlow® RNA Target Probe Diluent	Thermo Fisher Scientific	00-19185
PrimeFlow® RNA PreAmp Mix	Thermo Fisher Scientific	00-16000
PrimeFlow® RNA Amp mix	Thermo Fisher Scientific	00-16001
PrimeFlow® RNA Label Probe Diluent	Thermo Fisher Scientific	00-19183

PrimeFlow® RNA Storage Buffer	Thermo Fisher Scientific	00-19178
PrimeFlow® RNase Inhibitors (100X)	Thermo Fisher Scientific	00-16002
PrimeFlow® RNA Compensation kit	Thermo Fisher Scientific	88-17009
PrimeFlow® RNA Label Probes	Thermo Fisher Scientific	00-16003

Table 5. Reagents and volume used in cDNA synthesis.

Reagents (cDNA synthesis)	**Volume per reaction**
50mM EDTA	1 μl
10X RT Buffer	2 μl
dNTP mix 10 nM	4 μl
$MgCl_2$ solution	1,4 μl
Multiscribe Reverse Transcriptase	1 μl
RNase Inhibitor	1 μl
Random Hexamer	1 μl
DNase treated RNA	9,6 μl
Total	20 μl

Table 6. Reagents and volume used in qPCR analysis.

Solution for qPCR reaction	**Volume per reaction**
Mix with forward and reverse primer	2,5 μl
Fast SYBR Green Master Mix	5 μl
cDNA	2,5
Total	10 μl

Table 7. Reagents used in PrimeFlow analysis.

Reagents (PrimeFlow)	**Volume per reaction**
PrimeFlow® RNA Fixation Buffer 1A	500 μl
PrimeFlow® RNA Fixation Buffer 1B	500 μl
PrimeFlow® RNA Permeabilization Buffer (10X)	300 μl
PrimeFlow® RNase Inhibitors (100X)	30 μl

ddH2O	2,7 ml
PrimeFlow® RNA Fixation Buffer 2	125 μl
PrimeFlow® RNA Wash Buffer	875 μl
Target probe	5 μl
PrimeFlow® RNA Target Probe Diluent	95 μl
PrimeFlow® RNA PreAmp Mix	100 μl
PrimeFlow® RNA Amp mix	100 μl
PrimeFlow® RNA Label Probe Diluent	100 μl
PrimeFlow® RNA Label Probe	1 μl
Flow cyt stain buffer	2 ml
PrimeFlow® RNA Wash Buffer	8 ml
Total	15,5 ml

Table 8. Reagents and volume used in first-strand cDNA-synthesis.

Buffer mix reagents	**Volume per reaction**
5X First-Strand Buffer	4 μl
Dithiothreitol (DTT) (100nM)	0,5 μl
dNTP mix (20nm)	1 μl
Total	5,5 μl
RNA	1 -10 μl
5`RACE CDS Primer A	1 μl
MilliQ water	0-9 μl
SMARTer II A Oligonucleotide	1 μl
RACE ready cDNA Master mix	
Buffer mix	5,5 μl
RNase Inhibitor (40 U/μl)	0,5 μl
SMARTScribe Reverse Transcriptase (100 U)	2 μl
Total	20 μl

Table 9. Reagents and volume used in the RACE reaction.

Reagents in RACE reaction	**Volume per reaction**
Master mix	
PCR-grade H2O	93 μl
2X SeqAmp Buffer	150 μl
SeqAmp DNA Polymerase	6 μl

Total	249 μl
PCR-solution	
5`RACE ready cDNA	2,5 μl
10x UPM	5 μl
5`GSP (Gene specific primer)	1 μl
Master mix	41,5 μl
Total	50 μl

Table 10. Primers used in relative expression, Con A studies, and RACE.

Primer	**Sequence**
TRGC1 Forward	TTGGGCACTCAAGATGTTGACATA
TRGC1 Reverse	TGGATCCTCATAGGTAACGTGCAG
TRGC2 Forward	GGCCCTCAAGATGTTAACATACC
TRGC2 Reverse	GGACTTTAATGAATCGTTGGTAAC
TRGC3 Forward	GGCCCTCAAGATGTTTACATGCTA
TRGC3 Reverse	CTGTGTGTCATTTCTGAACGAACA
TRGC5 Forward	GTCTGTTCTGTGGAGCATGAATGG
TRGC5 Reverse	CTGCAGAGTCAGTGGCTCCTGCGT
Elongation Factor 1 alpha Forward	CCCCTCCAGGACGTTTACA
Elongation Factor 1 alpha Reverse	CACACGGCCCACAGGTACA
TRD Forward	AGCGTTGTGAGATGGATGG
TRD Reverse	AGTTGTAGCCGTGETGTTATAG
TRGCGSP1	GATTACGCCAAGCTTTGTCTCCAGCCAAACATAGCAGGGTG
degTRGCGSP1	GATTACGCCAAGCTTTGTCTCYAGCCARACATAGCAGGGTG
TRGCGSP2	GATTACGCCAAGCTTCTGGGTAGACCGTCACTTTGGGTTT
degTRGCGSP1	GATTACGCCAAGCTTCTGRGTASACCGTCACTTTGGGTTT
TRDGSP2	GATTACGCCAAGCTTCACTCTTGTGTAGTGGGGTGAGGATG
UnivTRGC	TGTCTCCAGCCAAACATAGCAGGGTG

Sasa_**TRGC1**
KPKVTVYSVSKPEPNRKTTLLCLARDMFPDLVKISWKVMDKNGRTMEVPKAEMEELEQREEGRTTSMIIIDKE
KTYRNKYICSVEHKLGTQDVDIPK

Sasa_TRGC2_1
KPKVTVYPASKPEPNRKTTLLCLARDMFPDLVKISWKMVDENGQTVEVPKAEREELEQREEGRTTSMIIIDKD
KTYRNKYSCSVEHEGGPQDVNIPE

Sasa_TCRG2_2
NPKVTVYPASKPEPNRKTTLLCLARDMFPDLVKISWKMVDKNGRTVEVPKAEREELEQREEGRTTSMIIIDKD
KTYSNKYSCSVEHEGGPQDVDIPE

Sasa_**TRGC3**
KPKVTVYSESNPESNVNTLLCLAGDMFPDLVKISWKMEDENGRAVEVPKAEGEQLEQREEGQTTSMIITDKEK
IYRNKYICSVEHEGGPQDVYMLK

Sasa_**TRGC5**
KPKVTVYPASNSESNGKTTLLCLARDMFPDLVKISWKIEDANGRRMEVSKAETEQLEQREEGQTTSMIIIDKE
KTYRNKYVCSVEHEWGAQQFDIPK

Sasa_TRGC4
KPKVTVYPASNPESNGKTTLICLARDMFPDLVKISWKMEDEYGQTVEVSKAETEQLEQREEGQTTSMIIIDKE
NAYKNKYRCYVEHEGDPQDVDMLK

Sasa_TRGC6
KPKVTMYLAFKPELNGKTTLLCLARDMFPDLVKISWKMEDENGRTVEVPKAEMEQLEQREEGQTTSMIIMYQG
K-ADAKYICSVEHEAGPEEADTPK

(Sasa_TRGC2_1 & Sasa_TCRG2_2 =41,
=PKVTVYPASKPEPNRKTTLLCLARDMFPDLVKISWKMVD)

(Sasa_TRGC2_1 & Sasa_TCRG2_2 =32,=TVEVPKAEREELEQREEGRTTSMIIIDKDKTY)

(Sasa_**TRGC1**, *Sasa_TRGC2_1*, *Sasa_TCRG2_2*, Sasa_**TRGC5**, *Sasa_TRGC4*,
Sasa_TRGC6, *=21* KTTLLCLARDMFPDLVKISWK)

(Sasa_**TRGC5**, *Sasa_TRGC4*, *=25 ESNGKTTLICLARDMFPDLVKISWK)*

(Sasa_**TRGC5**, *Sasa_TRGC4*, *=27* EVSKAETEQLEQREEGQTTSMIIIDKE)

(Sasa_**TRGC1 &** *Sasa_TRGC2_1*, =28 =SKPEPNRKTTLLCLARDMFPDLVKISWK)
EVPKAEREELEQREEGRTTSMIIIDKDKTYRNKYSCSVEH

Figure 20. TRGC amino acids used in PrimeFlow RNA Assay probe design.

>Sasa_TCRG2_2

aaccccaaagtgacggtctacccagcgtccaaacctgagccaaataggaaaaccaccctgctatgtttggctagagacatgtttccagacttggtcaa
gatttcatggaagatggtggataaaaatggccgaacagtagaggtacccaaagcagagagggaagagctggagcagagggaggaaggacggacgacca
gtatgatcatcattgataaagacaagacatacagcaacaaatacagctgttctgtggaacatgaaggggccctcaagatgttgacataccagaagat
gaaccaactgaagcttctccaaccaccatggctgcaccaaccactctgcaggttaccaacgattcattcaagtccatatgcggtctgaacttggcctc
tctggtttacacagtgatgatagtgaagagcatggtgtactgctatgggctctctttcctgctgcactacaggaacatgggttgtagacccaaaacct
gtagacaaattcattga

>SALSAL_TRG_C1

AAACCCAAAGTGACGGTCTACTCAGTGTCCAAACCTGAGCCGAACAGGAAAACCACCCTGCTATGTCTGGCTAGAGACATGTTTCCAGACTTGGTCAA
GATTTCATGGAAGGTGATGGATAAAAACGGCCGAACAATGGAGGTGCCCAAAGCAGAGATGGAAGAGCTGGAGCAGAGAGAGGAAGGGCGGACGACAA
GTATGATCATCATTGATAAAGAGAAGACGTACAGGAACAAATACATATGTTCTGTGGAGCATAAA**TTGGGCACTCAAGATGTTGACATA**CCAAAAGAG
GAACCAACTGAAGCTCCTCCAACCA**CCATGGCTGCACCAACCACTCTGCACGTTACCTATGAGGATCCA**ACTGAAGCTCCTCCATCCACAAAGGCTGC
ACCAACTGCTCTGCAGGCTACAAACGATTCCTTCCAGTCAACATGCAGTCTCAACCTGGCCTCTCTGGTTTACACAGTGATGATAGTGAAGAGCATGG
TGTACTGCTGTGCGCTCTCTCTCCTGCTGCACAAAAGGAACCTGGGAAGTAGACCCAGCACCAGTAGACCCATACATTGA

>SALSAL_TRG_C2

AAACCCAAAGTGACGGTCTACCCAGCGTCCAAACCTGAGCCAAATAGGAAAACCACCCTGCTATGTCTGGCTAGAGACATGTTTCCAGACTTGGTCAA
GATTTCATGGAAGATGGTGGATGAAAATGGCCAAACAGTAGAGGTACCCAAAGCAGAGAGGGAAGAGCTGGAACAGAGGGAGGAAGGACGGACGACCA
GTATGATCATCATTGATAAAGACAAGACATACAGGAACAAATACAGCTGTTCTGTGGAGCATGAAGGG**GGCCCTCAAGATGTTAACATACCA**GAAGAG
GAACCAACTGAAGCTTCTCCAACCACCATGGCTTCACCAACCACTCTGCAG**GTTACCAACGATTCATTAAAGTCC**ATATGCAGTCTGAACTTGGCCTC
TCTGGTTTACACAGTGATGATAGTGAAGAGCATGGTGTACTGCTATGGGCTCTCTTTCCTGCTGCACTACAGGAACATGGGTTGTAGACCCAAAACCT
GTAGACAAATTCATTGA

>SALSAL_TRG_C3

AAACCCAAAGTGACGGTCTACTCAGAGTCCAACCCTGAGTCGAATGTGAACACCCTGCTATGTCTGGCTGGAGACATGTTTCCAGACTTGGTCAAGAT
CTCATGGAAGATGGAGGATGAAAACGGCAGAGCAGTCGAGGTGCCTAAAGCAGAGGGGGAACAACTGGAGCAGAGGGAGGAAGGACAGACGACCAGTA
TGATCATCACTGATAAAGAGAAGATTTACAGGAACAAATACATCTGTTCTGTGGAGCATGAAGGG**GGCCCTCAAGATGTTTACATGCTA**AAAGATCAA
CCAACTGAAGCTCCGCCAACCACCGTGGCTGCACCAACC**TGTTCGTTCAGAAATGACACACAG**CAGTCACAGTCTCTACATCTTACCGATGATTCCTT
CCAGTCAACGTTTAGTCTGAACCTGGCCTCTATCCTTTACACAGTGATGATAGTGAAGAGCATGGTGTACTGCTGTGGGCTCTCTATCCTGCTGCACC
ACAGGAGCTTGGGAAGAGGACCCAGCACCTGTAGACACATTTATTGA

>SALSAL_TRG_C4

AAACCCAAAGTGACGGTCTACCCAGCGTCCAACCCTGAGTCGAATGGGAAGACCACCCTGATATGTCTGGCTAGAGACATGTTTCCAGACTTGGTCAA
GATCTCATGGAAGATGGAGGATGAATACGGCCAAACAGTGGAGGTGTCCAAAGCAGAGACGGAACAGCTAGAGCAGAGGGAGGAAGGACAGACGACCA
GTATGATCATCAT**TGATAAAGAGAATGCGTACAAGAA**CAAATACAGATGTTATGTGGAGCATGAAGGGGACCCTCAAGATGTTGACAT**GCTAAAAGAT**
CCCTTCTCCTTCATGTGCAGTCTGAACCTGGCCTCTTTGGTTTATACAGTGATGATAGTGAAGAGCATGGTGTACTGCTGTGGGCTCTCTCTCCTGCT
GCACCACAGGAAC**ATGGGGAAGTGGACACAACACCTG**TAG

>SALSAL_TRG_C5

AAACCCAAAGTGACGGTGTACCCAGCGTCCAACTCTGAGTCGAATGGGAAGACCACCCTGCTATGTCTGGCTAGAGACATGTTTCCAGACTTGGTCAA
GATCTCATGGAAGATTGAGGATGCAAACGGCAGAAGAATGGAGGTGTCCAAAGCAGAGACGGAACAGCTGGAGCAGAGGGAGGAAGGACAGACAACCA
GTATGATCATCATTGATAAAGAGAAGACGTACAGGAACAAATAC**GTCTGTTCTGTGGAGCATGAATGG**GGCGCTCAACAATTTGACATTCCAAAAGAT
ACTCCACCAACCTGCCCGTTCAGAAATGA**CACGCAGGAGCCACTG****ACTCTGCAG**TTTACCGAAGATTCCTTCCAGTCAACGTGCAGTCTGAACCTGGC
CTCTGTGGTTTACACAGTGATGATCGTGAAGAGCATGGTGTACTGCTGTGGGCTCTCTCTCCTGCTGCACCACAGGATTCTAGGAAGAGGACCCAGCA
CCTGA

>SALSAL_TRG_C6

AAACCCAAAGTGACCATGTACCTGGCGTTCAAACCTGAGCTGAATGGGAAGACCACCCTGCTATGTCTGGCTAGAGACATGTTTCCAGACTTAGTCAA
GATCTCATGGAAGATGGAGGATGAAAACGGCCGAACCGTGGAGGTGCCCAAAGCAGAGATGGAACAGCTGGAGCAGAGGGAGGAAGGACAGACGACCA
GTATGATCATCAT**GTATCAAGGAAAGGCAGATGCCA**AATACATCTGTTCGGTGGAGCATGAAGCGGGCCCTGAAGAAGCTGA**CACACCAAAAG**CAACC
TTCCAGTCCATGTGCAGTCTGCGTCTGGCCTCTCTGGTTTACACAGTGATGATAGCGAAGAGTATGTTGTACTGCTGTGGGCTCTCTCTCCTGCTGCA
CCACAGGAACATGGGAAATAGCCCCCCTACCTGA

Figure 21. TRGC nucleotide sequences used in probe design. Color coordinating is used to map out which parts in the different TRGC nucleotide seqences that are identical, and where they differ from each other.